ChemComm

HIGHLIGHT

View Article Online
View Journal | View Issue

Cite this: *Chem. Commun.*, 2026, **62**, 3662

Targeted photodynamic therapy for pancreatic cancer: recent innovations from fundamentals to *in vivo* and clinical applications (2020–2025)

Souleymane Sarr,†[a] Jérémy Godard,†[b] Emmanuel Valzer,†[c] Elodie Czuba,†[de] Samir Acherar,[a] Muriel Barberi-Heyob,[f] Mireille Blanchard-Desce,[g] Emmanuel Boleslawski,[h] Frédérique Brégier,[i] Anne-Laure Bulin,[j] Hélène Burckel,[de] Joël Daouk,[f] Anabela da Silva,[k] Jonathan Daniel,[g] Nadira Delhem,[l] Anne-Sophie Dewalle,[l] Céline Frochot,†*[m] Gilles Gasser,[n] Valérie Heitz,[c] Nicolas Jonckheere,[o] Gilles Lemercier,[bp] Serge Mordon,[q] Georges Noël,[de] Anthony Novell,[r] Jean-Luc Ravanat,[s] Gaël Roth[t] and Vincent Sol†*[i]

Photodynamic therapy (PDT) is a clinically-approved medical modality to treat different types of localised conditions such as cancer, infections or skin conditions. Pancreatic cancer (PC) is a deadly cancer displaying a dramatic overall prognosis that has barely improved in decades as the majority of PC patients are diagnosed at a locally advanced or metastatic stage and cannot benefit of surgical resection which is the only curative treatment, the overall 5-year survival rate remains extremely low. Thus, finding new therapies for non-metastatic PC to improve local control as a bridge to surgical resection and improve survival outcomes remains a huge challenge. In this context, PDT could be an interesting option. This review will focus on the use of PDT with targeted photosensitisers or nanoparticles to treat PC in recent studies (2020–2025) from *in vitro* to *in vivo* experiments and clinical applications.

Received 30th September 2025,
Accepted 19th December 2025

DOI: 10.1039/d5cc05629b

rsc.li/chemcomm

[a] *Université de Lorraine, CNRS, LCPM, F-54000 Nancy, France*
[b] *Université Paris Cité, CNRS, ITODYS, UMR 7086, 75013 Paris, France*
[c] *Laboratoire LSAMM, UMR 7177, Institut de Chimie de Strasbourg, CNRS/UMR 7177, Université de Strasbourg, 4 rue Blaise Pascal, 67000 Strasbourg, France*
[d] *Institut de Cancérologie Strasbourg Europe (ICANS), UNICANCER, Radiobiology Laboratory, Paul Strauss Comprehensive, Cancer Center, 67000 Strasbourg, France*
[e] *Cube, UMR7357, Equipe Imagerie Multimodale Intégrative en Santé, Université de Strasbourg, France*
[f] *Université de Lorraine, CNRS, CRAN, F-54505 Vandœuvre-lès-Nancy, France*
[g] *Université de Bordeaux, CNRS, INP-Bordeaux, ISM, UMR 5255, 33405 Talence, France*
[h] *CHU Lille – Hôpital Claude Huriez, France*
[i] *Univ. Limoges, LABCiS UR 22722, F-87000 Limoges, France. E-mail: vincent.sol@unilim.fr*
[j] *Université Grenoble Alpes, INSERM U1209, CNRS UMR 5309, Institut pour l'Avancée des Biosciences, Équipe Thérapies ciblées, Diagnostic précoce et Imagerie du cancer, 38000 Grenoble, France*
[k] *Aix Marseille Univ, CNRS, Centrale Med, Institut Fresnel, Marseille, France*
[l] *Univ Lille, INSERM, CHU Lille, U1189-ONCOTHAI-Assisted Laser Therapy and Immunotherapy for Oncology, Lille F-59000, France*
[m] *Université de Lorraine, CNRS, LRGP, F-54000 Nancy, France. E-mail: celine.frochot@univ-lorraine.fr*
[n] *Chimie ParisTech, CNRS, Institute of Chemistry for Life and Health Sciences, Laboratory for Inorganic Chemistry, PSL University, 75005 Paris, France*
[o] *Université de Lille, CNRS, INSERM, CHU Lille, UMR 9020-U1277-CANTHER-Cancer Heterogeneity Plasticity and Resistance to Therapies, Lille, France*
[p] *Université de Reims Champagne-Ardenne URCA, France*
[q] *Hemerion Therapeutics, Villeneuve d'Ascq, France*
[r] *Université Paris-Saclay, CNRS, Inserm, CEA, BioMaps, SHFJ, Orsay*
[s] *Univ. Grenoble Alpes, CEA, CNRS, Grenoble INP, IRIG, SyMMES UMR 5819, Grenoble, France*
[t] *Université Grenoble Alpes/Hepato-Gastroenterology and Digestive Oncology Department, CHU Grenoble Alpes/Institute for Advanced Biosciences, CNRS UMR 5309-INSERM U1209, 38043 Grenoble, France*
† Contributed equally.

Introduction

Photodynamic therapy (PDT) is a clinically-approved medical modality used to treat different types of localised conditions such as cancer, infections or skin conditions (*e.g.*, actinic keratosis, removal of port wine stains). It involves the use of a photosensitiser (PS) that is generally administered intravenously, although some topical applications are sometimes employed. Once the PS has reached its desired target (*e.g.*, tumour), a physician illuminates the area of interest with a

Souleymane Sarr is currently a second-year PhD student at the LRGP, University of Lorraine (Nancy), under the supervision of Dr S. Acherar and Dr C. Frochot. He obtained a Master's degree in Chemistry from the University of Clermont Auvergne in 2023. He then worked as a Research Engineer in Organic Synthesis at the Institute of Chemistry of Clermont-Ferrand (2023–2024), under the supervision of Prof. C. Taillefumier and Dr O. Roy. His PhD research focuses on the design of new peptidic vectors for the photodynamic therapy of pancreatic cancer.

Dr Jérémy Godard earned his PhD in organic synthesis in 2020 from the LABCiS laboratory (Limoges University, France). He then served at the same institute as a non-tenured teaching and research fellow before joining the ITODyS laboratory (Paris-Cité University, France) as a postdoctoral researcher in 2023. His research mainly focuses on the synthesis of photosensitizers (phenalenones, porphyrins, ruthenium complexes, etc.) bearing targeting units for antimicrobial and anticancerous photodynamic therapy.

Emmanuel Valzer obtained his Bachelor's degree from the University of Besançon (2011), and moved to the University of Birmingham, England, as an Erasmus student. After a four-year industrial experience in Liverpool, he completed his Master's at the University of Strasbourg. In 2022, he received his PhD at the University of Bordeaux working with Prof. S. Quideau and Prof. L. Pouységu on hypervalent iodine chemistry. He then carried out a postdoctoral stay in total synthesis with Dr N. Girard at the faculty of pharmacy of Strasbourg. He is currently a postdoctoral researcher with Prof. V. Heitz, developing photosensitizers for photodynamic therapy.

Samir Acherar is Associate Professor (HDR) in Organic Chemistry at Université de Lorraine (France). His research focuses on the design, synthesis and conformational analysis of peptides, pseudopeptides and foldamers, as well as on solid-phase peptide synthesis of targeting agents for biomedical applications. His work lies at the interface of organic chemistry and chemical biology, addressing drug delivery, photodynamic therapy, and theranostic and radiotheranostic approaches. These strategies are applied to cancer, neurodegenerative and cerebrovascular diseases. He has co-authored more than 70 peer-reviewed publications in international journals.

Muriel Barberi-Heyob is professor of cell biology at Lorraine University and co-director of CRAN (UMR 7039 CNRS, Nancy). Her research focuses on photodynamic therapy (PDT), radiotherapy, X-ray–induced PDT, within the field of nanomedicine in oncology, and more recently on internal radiotherapy. Her major contributions include the development of innovative technologies designed to reach, localize, and treat not only the central tumor mass but, critically, the infiltrative peripheral regions of high-grade brain tumors, including glioblastoma. Her current research explores multifunctional nanoparticles for radiotherapy and internal radiotherapy through Euronanomed-, ANR-, and INCa-funded projects.

Mireille Blanchard-Desce is a senior researcher at CNRS. She graduated from the Ecole Normale Supérieure in Paris and defended her PhD in Molecular Electronics under the supervision of Pr. Jean Marie Lehn in 1989. After a postdoc in biophysics, she worked in the department of Chemistry at Ecole Normale Supérieure, then moved to the University of Rennes in 2000 and later to the University of Bordeaux in 2011. Her current research focusses on molecular-based photonics and nanophotonics with applications in various fields, especially life sciences (bioimaging, therapy). She has authored over 300 peer-reviewed publications.

Frédérique Bregier completed her PhD in bioinorganic chemistry in 2009 under the supervision of Prof. Martin Bröring at Philipps-Universität Marburg. She then carried out four postdoctoral fellowships at the University of Burgundy, the University of Limoges and the University of Rouen Normandy. She became an assistant professor at the University of Limoges in 2015. Her research focuses on the hemisynthesis and synthesis of new compounds for applications in anticancer or antimicrobial photodynamic therapy. She has co-authored 46 research articles, 2 patents, and has co-supervised three doctoral theses.

Anne-Laure Bulin has been a researcher at the National Institute for Health and Medical Research (Inserm) since 2019, working at the Institute for Advanced Biosciences, University Grenoble Alpes. She earned her PhD in Physics from the University of Lyon (2014), then worked at Wellman Center for Photomedicine, Harvard Medical School, studying photodynamic therapy combined with radiotherapy. In 2018, she joined the Synchrotron Radiation for Biomedicine team in Grenoble, focusing on improving synchrotron radiotherapy using nanoscintillators. Supported by an ERC Starting Grant, her current research investigates the radiotherapeutic

light device at a specific wavelength absorbed by the PS. This illumination excites the PS which first reaches an excited singlet state and then, after intersystem coupling (ISC), a triplet state. Because of their long lifetime, triplet excited state promotes ROS. In the chemical reaction pathways occurring and leading to biological damages during PDT treatments, three mechanisms are admitted; they are known as Type I electron transfer, Type II direct energy transfer to $^3O_2$, and Type III

Hélène Burckel is a radiobiology researcher and Deputy Director of the Radiobiology Laboratory at the Strauss Institute in Strasbourg, affiliated with the University of Strasbourg (ICube UMR7357). Her work focuses on improving radiotherapy through radiosensitization strategies and modulation of the tumor microenvironment, proton and FLASH irradiation and innovative combinations with immunotherapy and cryotherapy. She has coordinated and obtained multiple grants in glioblastoma, pancreatic and colorectal cancers. She also serves as deputy treasurer of the French Radiation Biology Society and co-organizes its scientific meetings.

Joël Daouk is a medical physicist specialized in nuclear medicine and photodynamic therapy. He spent ten years in the nuclear medicine department of Amiens university hospital where he designed PET/CT image reconstruction algorithms et conducted various clinical trials on hepatic and lung cancer. His current works integrate translational both biological, physical and numerical studies to bring original insight concerning interactions between biological tissues and several origins of radiation, notably in presence of nanoparticles. The main applications of these translational studies are brain tumors, notably glioblastoma.

Anabela Da Silva is a senior researcher at CNRS (French National Research Center). She holds a PhD in Optics and Photonics (P. & M. Curie U., Paris, France). After a post-doc at Harvard Medical School/Mass. General Hospital, she got a researcher position at CEA-LETI (Grenoble, France). Her main research field is Diffuse Optics for biomedical applications with a special focus on Diffuse Optical Tomography, polarization gating imaging and PhotoAcoustic imaging.

Nadira Delhem is a Professor of Cell Biology and Immunology at the University of Lille and Director of the INSERM U1189 research unit (ONCOTHAI). She trained in life and health sciences and completed postdoctoral fellowships in France and at the NIH (USA). Her research focuses on immuno-oncology, virus-induced cancers, and innovative therapies including Immunotherapy and laser-based and photodynamic approaches. She has authored over 120 peer-reviewed publications, holds five patents, supervised numerous PhD students, is an active leader in national and international scientific networks and serves as scientific director in several clinical and translational research studies.

Anne-Sophie Dewalle is a research engineer expert in scientific computing at the INSERM U1189 unit "Laser assisted therapies and immunotherapies for oncology (ONCOTHAI)". She is the leader of the Physico-PDT team of the unit. Her research activity is focused on light-based therapies and more particularly on photodynamic therapy and laser-induced interstitial thermal therapy. Her contribution ranges from preclinical studies (development of dedicated illumination devices; dosimetry; modeling of the therapeutic effects) to clinical trials (development of treatment planning systems; administration of therapies at the patient's bedside). She has authored over 40 peer-reviewed publications.

Céline Frochot is a senior researcher at CNRS. She was graduated from the Ecole Nationale Supérieure des Industries Chimiques (ENSIC, Nancy) and received her PhD degree in 1997. She spent two years in Amsterdam developing light-driven rotor molecules. In 2000, she became a CNRS researcher. Her interest is to develop novel photo-activable compounds for nanomedicine and photodynamic therapy. Particularly, the main field of her research in LRGP (UMR 7274 CNRS-UL) concerns synthesis and photophysical properties of targeted photosensitizers or nanoparticles designed for photodynamic therapy applications. She has authored over 190 peer-reviewed publications/reviews/book chapters.

Gilles Gasser started his independent career at the University of Zurich (Switzerland) in 2010 before moving to Chimie ParisTech, PSL University in 2016 to take a PSL Chair of Excellence. Gilles was the recipient of several fellowships and awards including the Alfred Werner Award from the Swiss Chemical Society, an ERC Consolidator Grant and Proof of Concept, the European BioInorganic Chemistry (EuroBIC), the Coordination Chemistry Prize from the French Chemical Society (Senior Level) and recently the Seqens Prize from the French Academy of Sciences for outstanding work in medicinal chemistry.

Valérie Heitz is a Professor of Chemistry at the University of Strasbourg. She completed her PhD under the supervision of J.-P. Sauvage in 1992, working in the field of artificial photosynthesis. After postdoctoral work in photophysics, she joined the University of Strasbourg and has led the Laboratoire de Synthèse des Assemblages Moléculaires Multifonctionnels (LSAMM) since 2010. Her research focuses on the design and synthesis of functional supramolecular systems, including stimuli-responsive systems, allosteric receptors, and interlocked molecules. In addition, she conducts research in chemical biology, particularly on near-infrared photosensitizers for anticancer and antimicrobial photodynamic therapy and on porphyrin-conjugates for theranostic applications.

mechanism, involving radical species in the absence of dioxygen. Depending on the conditions, one of these reactions can strongly predominate, but two, even three of them can take place simultaneously. In the Type I reaction, and after light excitation, the ^{3}PS* captures an electron from a reducing molecule (R) located in its vicinity (typically NADH, NADPH, ascorbate, amino-acids, unsaturated lipids or the tripeptide gluthatione). This induces an electron transfer from the PS$^{\bullet-}$ to O_2 producing the superoxide anion radical ($O_2^{\bullet-}$). After the subsequent reduction, this leads to the generation of other cytotoxic reactive oxygen species (ROS) including hydrogen peroxide (H_2O_2) and finally the very cytotoxic hydroxyl radical (HO$^\bullet$), (Fig. 1). In the Type II mechanism, a direct energy transfer occurs from the ^{3}PS* photo-excited state to the triplet ground state molecular oxygen ($^3O_2$, sufficiently high in concentration for optimization of this direct interaction), that is converted to singlet oxygen ($^1O_2$). This ROS will then participate to the light induced targeted cellular damages.

Nicolas Jonckheere leads the Chemoresistance and therapeutic targeting in pancreatic cancers (PancResT) team in CRC Lille (Inserm U1366). He has worked for 25 years on the MUC4 roles and cellular mechanisms in pancreatic cancer. His work is aiming to propose MUC4 and its membrane partners such as ErbB2 oncoreceptor or ion channel TRPM7 as therapeutic targets in pancreatic cancer by combining complementary research using in vitro, in vivo (preclinical transgenic mouse models) and ex vivo. Since 2021, he also initiated an emerging project about chemoresistance and classifications of pancreatic neuroendocrine tumors.

Gilles Lemercier obtained his PhD in coordination chemistry in Toulouse (France) in 1994 and was in postdoctoral positions at EPFL Lausanne and Geneva Univ. (Switzerland) until 1998; then he got an Associate Professor position at ENS-Lyon (France), working on nonlinear optics properties (SHG, 2PA) of organic molecules and coordination complexes. In 2008, he became Professor at University of Reims Champagne-Ardenne (France). He is now developing his research at ITODYS Laboratory (Paris Cité) mainly related to the synthesis and study of new Ru(II) based photosensitizers for antimicrobial and anticancer activities in Photodynamic Therapy.

Professor Serge Mordon is a biomedical researcher internationally recognized for his work in photomedicine and therapeutic laser technologies. He has held senior research positions at INSERM (French National Institute of Health and Medical Research), where he contributed extensively to translational research at the interface of physics, engineering, and clinical medicine. His work spans photodynamic therapy, fluorescence imaging, and innovative light-based medical devices, with numerous scientific publications and patents. In recognition of his international scientific leadership, he was appointed Finland Distinguished Professor, strengthening academic collaboration between France and Finland in biomedical innovation.

Anthony Novell has been a Research Director at CNRS and leads the ''Methodological and Technical Development in Biomedical Engineering'' team at the BioMaps laboratory in Orsay. His research focuses on therapeutic ultrasound and drug delivery for treating brain disorders, spanning fundamental physics to clinical translation. Since joining CNRS in 2018, he has supervised over 35 students and authored 63 peer-reviewed publications and 5 patents. Notably, he developed ultra-rapid ultrasound dose control and robot-assisted whole-brain treatment strategies. These innovations led to the co-founding of TheraSonic in December 2023 to develop clinical BBB-opening devices.

Jean-Luc Ravanat, is research director at CEA Grenoble, UMR-5819. He has a background in biochemistry and organic chemistry. His work focuses on DNA damage and repair, mostly induced by ionizing and non-ionizing (photosensitization) radiations. In particular he developed highly sensitive and specific analytical methods to measure DNA lesions at the cellular level, with a particular focus on oxidative DNA modifications. During the last two decades his competences has been used in numerous research projects focused on improving radiotherapy through radiosensitization strategies.

Gaël Roth is a professor in gastrointestinal oncology specialized in biliary tract and pancreatic cancer at Grenoble Alpes Universitary Hospital. He is member of number of scientific societies in oncology. He is leading the French PRODIGE biliary tract cancer study group and is president of the French Association for the Study of Biliary Tract Cancers (ACABi). He is actively participating to clinical research and leads several multicentric clinical trials from phase 1 to 3 in liver, pancreatic and biliary cancers with 2 ongoing trials in locally advanced pancreatic cancers. He is actively contributing to the development of national clinical practice guidelines, and has authored or co-authored more than 50 peer-reviewed scientific publications.

Vincent Sol is a Professor of Organic chemistry at the University of Limoges. He obtained his PhD in 1997 under supervision of Pr P. Krausz and joined the Laboratoire de Chimie des Subtances Naturelles (LCSN) in 1998. After a research position at the University of Hull (Pr G. MacKenzie) in 2009–2010, he led the LCSN from 2011 to 2023. His research focuses on the design, synthesis or hemisynthesis of tetrapyrrolic macrocycle for anticancer and antimicrobial photodynamic therapy. In addition, he conducts research on chemistry of natural polysaccharide for biological application as biomaterial, nanoparticles or hydrogel.

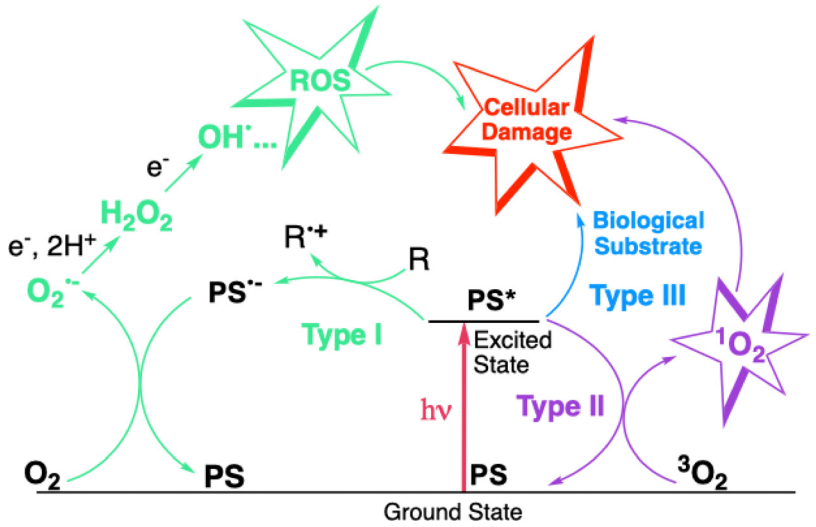

Fig. 1 Scheme of the photochemical and photophysical mechanisms leading to reactive species production during PDT.

In addition to the above-mentioned Type I and Type II mechanisms, Claudio H. Sibata and coll.,[1] proposed the introduction of a Type III photochemical pathway, following which the radical anion $PS^{\bullet -}$ and/or other radicals formed in absence of oxygen could also lead to a PDT effect and also may include damages to DNA. This mechanism avoids the dioxygen necessity and may be of significant clinical relevance especially for hypoxic deep-seated tumour. The resulting ROS produced in this case, encompass $O_2^{\bullet -}$, H_2O_2, $HO^{\bullet}$, and $^1O_2$. The last two being the most reactive and cytotoxic species and therefore those with the shortest diffusion distance (around 2 nm for $HO^{\bullet}$ and 10^{-9} s for its half-lifetime, 10–100 nm diffusion distance for $^1O_2$ in water); the less reactive hydrogen peroxide (lifetime millisecond to second) can diffuse over distances of 1–10 μm, which can also be of interest for treatment purposes. As a (photo-)catalyst, one PS molecule can generate thousands of $^1O_2$ molecules in a Type II mechanism, depending notably on its $^1O_2$ formation quantum yield, the surrounding environment, and also the respective occurrence of Type I, Type II and Type III mechanisms.

The high specificity of this treatment guaranteed by the selective accumulation of the PS and/or the localized light delivery, leading to cell death in a very localised manner,[2] is undoubtedly one of the main advantages of PDT over other medical techniques as it generally leads to minimal side-effects.

Importantly, depending on the medical conditions targeted with PDT, different types of combinations PSs/wavelength excitation are used. For example, for actinic keratosis, daylight PDT (*e.g.*, sunlight) can actually be employed. On the contrary, for brain cancer, PSs that absorb towards the deep-red or even the near-Infrared (NIR) will be used to leverage the deeper penetration of these longer-wavelength photons.

Pancreatic cancer (PC) is a deadly cancer causing 511 000 deaths per year worldwide in 2022 (GLOBOCAN) mostly caused by a late diagnosis and a lack of efficient therapies. PC displays a dramatic overall prognosis that has hardly improved within the past decades as the majority of PC patients are diagnosed at a late stage. At presentation the majority of patients present locally advanced or metastatic disease and cannot benefit from surgical resection which currently remains the only curative treatment option. Consequently, the overall 5-year survival rate remains extremely low (<11%). Major risk factors of PC are age, preventable behaviours (tobacco, alcohol), obesity and low physical activity. Diabetes mellitus is also thought to be both a risk factor and a consequence of early-stage pancreatic cancer.

A major characteristic of PC is the intense desmoplastic reaction surrounding the malignant cells leading to a highly hypoxic rich microenvironment composed of stromal extracellular matrix (ECM) secretion (collagen, fibronectin, laminin) and heterogeneous cellular composition (*e.g.* tumour cells, pancreatic stellate cells, cancer associated fibroblasts, infiltrated immune cells, endothelial cells and neuronal cells).[3] Beside the intra-tumoural heterogeneity, PC also harbours a high inter-patient diversity. Genomic studies showed recurrent mutations/deletions of key oncogenes and tumour suppressor genes, such as KRAS (>90%), TP53, SMAD4, or CDKN2A (50–80%). Moreover, molecular classification based on gene expression showed different subtypes of pancreatic cancer independently of tumour purity with consensual subtypes designated as classical *vs.* basal-like cancers.[4] Occurrence of basal-like region in the tumour is associated with reduced overall survival. It was proposed that classical tumours evolve to intermediate phenotype and finally to classical[5] subtypes. An additional immunogenic subgroup, enriched with stromal immune cell populations, has been also described. Differential expression of several genes (*e.g.* MUC1, mesothelin) were described in PDAC and could represent attractive candidates for novel therapeutic targets or tumour markers.[6] Aberrant signalling pathways are largely described with the notable alterations of hallmarks pathways such as epithelial-to-mesenchymal transition (EMT), apoptosis, survival mTOR pathway, cell cycle, and tyrosine kinase receptors (*e.g.* Epidermal Growth Factor

Receptor –EGFR– family, TGF-b pathway, HGFR) pathways.[3,4] These aberrant pathways are common drivers of carcinogenesis and are commonly used for targeted therapies.

To date, the only intent-to-cure strategy for PDAC is a combination of surgery with systemic therapy, which is only possible in a non-metastatic setting. Indeed, PDAC can be either treated by up-front surgery followed by adjuvant chemotherapy if considered as resectable (10–15% of patients at diagnosis) with a resection rate of 80%,[7] or by induction of a systemic therapy with the triplet Folfirinox, followed by surgery in borderline with a resection rate around 50–60%.[8,9] Due to a very high relapse rate even in resectable diseases, many trials are intending to prove the benefit of a pre-operative therapy to better select patients for surgery, improve resection rate and relapse-free survival.[10,11] In locally advanced settings, resection rate is only 10–15% based on prospective data and systemic treatment must be systematically performed.[10,11] Chemoradiation therapy after Folfirinox is also an option but suffers from low evidence and recent controversial results regarding its ability to efficiently control this disease.[12]

Nanomedicines could improve the accumulation of the drug into the tumour. To leverage these properties, there are currently two FDA approved nanoparticles (NPs): Onivyde (liposomal irinotecan) and Abraxane (nab-paclitaxel) that lead to an improvement in overall survival of only 2 months.[13–15]

Thus, finding new therapies for non-metastatic PDAC to improve local control as a bridge to surgical resection and improve survival outcomes remains a major challenge.[16–21] In this context, photodynamic therapy (PDT) represents an interesting and potentially valuable option. PDT employs photosensitizers that, upon activation by specific wavelengths of light, generate reactive oxygen species (ROS) and induce localized tumor cell death.[22] This selective mechanism limits off-target toxicity compared with systemic chemotherapy. In addition to direct cytotoxicity, PDT can disrupt the tumor vasculature, induce ischemic necrosis, modify the tumor microenvironment, and promote immunological cell death, thereby complementing other modalities such as chemotherapy, radiation therapy, and immunotherapy.[23–25] Preclinical and clinical studies indicate that PDT can improve local tumor control and symptom management, particularly in patients with obstructive jaundice or pain in biliary tract cancers.[26] The therapeutic potential of PDT—especially in combination with systemic treatments—is further supported by ongoing work on targeted photosensitizers, advanced light-delivery technologies, and nanoparticle-based approaches.[27] This review focuses on these targeted PSs and nanomedicine strategies evaluated in pancreatic cancer from 2000 to 2025, spanning *in vitro* studies, *in vivo* models, and clinical applications.[28–34]

Photodynamic therapy

Active targeted treatment. Direct Active targeting aims to improve cancer treatment efficiency by attaching PSs or their NP carriers to specific ligands (*e.g.*, antibodies, peptides, aptamers) that selectively recognize and bind to receptors overexpressed on the surface of cancer cells. This targeted interaction helps PSs to internalize into cancer cells through receptor-mediated endocytosis, which boosts their uptake and enhances their therapeutic impact.[35] In PDAC, several key receptors and tumour-associated markers have been identified as suitable targets, including epidermal growth factor receptor (EGFR), urokinase-type plasminogen activator receptor (uPAR), folate receptor alpha (FRα), CD44, mucins (MUC1, MUC4), carbohydrate antigen CA19-9, and mesothelin.[36] One example is the use of cetuximab-linked photoimmunoconjugates targeting EGFR, which have shown effective internalization by tumour cells and strong phototoxic effects. Similarly, gold nanoclusters activated by cathepsin E and functionalized with the U11 peptide to target uPAR have shown promising specificity.[36] Another recent development involves the use of nanobodies directed against midkine (*i.e.*, a protein frequently overexpressed in the PDAC microenvironment) to guide PSs more selectively.[37]

Indirect active targeting, also known as vascular targeting, shifts the focus from cancer cells to the abnormal blood vessels that support tumour growth. Instead of directly targeting tumour cells, this strategy uses ligands that bind to receptors highly expressed on the endothelial cells of newly forming (angiogenic) blood vessels. Through PDT, this allows for the selective disruption of the tumour's blood supply.[38] Damaging these vessels can trigger a cascade of effects, including reduced oxygen levels (hypoxia), cell death (necrosis), and a bystander effect that amplifies the overall impact on the tumour. Some of the main molecular targets in this approach include VEGF receptors, integrins like $\alpha_v\beta_3$, neuropilin-1, somatostatin receptors (particularly SSTR2), and tissue factor (TF).[39]

Recently, Deng *et al.*[40] proposed a novel approach which exploits the overexpression of the polyamine transport system (PTS) in cancer cells. The PS derivative N3 is synthetised from spermine and BODIPY-2I (Fig. 2A). This compound demonstrated encouraging results in a series of biological tests. At a concentration of 80 nM, N3 reduced the viability of PANC-1 cells by 98% and BxPC-3 cells by 75% after excitation with light of 550 $\pm$ 50 nm wavelength, 6.5 mW cm^{-2} for 15 or 30 min. *In vivo* experiment on models CDX Mouse Models demonstrated that administration of N3 at a dose of 2.23 mg kg^{-1}, followed by illumination (2 h after injection, 2 min of illumination (532 nm, 1.25 mW cm^{-2})) induced a significant reduction in tumour volume, with complete disappearance of the tumours in some animals after two weeks (Fig. 2B).

Van Lith's team[41] targeted cancer-associated fibroblast (CAF), which account for up to 90% of the tumour mass in PDAC. These cells, which express fibroblast activating factor (FAP), play a key role in tumour progression and resistance to treatment. To do so, the authors developed an anti-FAP monoclonal antibody (28H1), to which they added the phthalocyanine IRDye700DX and the diethylenetriaminepentaacetic acid (DTPA) chelator (Fig. 3A). As a negative control, DP47GS an isotype control of 28H1 with no known binding specificity and no affinity for murine or human FAP, was also used. *In vitro* tests carried out on FAP+ fibroblast cells (NIH-3T3) confirmed the existence of light (50 J cm^{-2}, 690 nm, 290 mW cm^{-2}) and

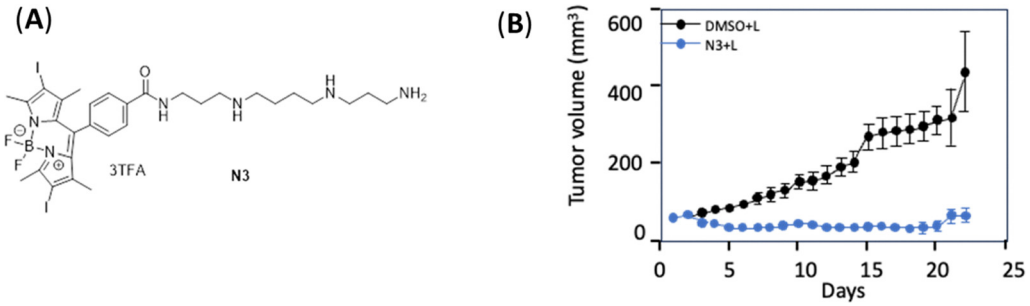

Fig. 2 (A) Chemical structure of N3. (B) The PDT effect of N3 in a CDX mouse model. The tumours on mice in the N3 group (tumour-bearing mice treated with N3 and excited every 2 days in the first 7 days) and DMSO group (tumour-bearing mice treated with DMSO and excited every 2 days in the first 7 days).

protein dose-dependent cell death, which was observed exclusively in the presence of the 28H1-700DX antibody-conjugated PS. In an *in vivo* study in two mouse models of pancreatic cancer (PDAC299 and CKP), the targeted antibody accumulated significantly in areas with high levels of CAF, inducing local apoptosis as evidenced by degradation of the pro-apoptotic protein Caspase-3. No damage to healthy tissue was observed, underlining the specificity and safety of PDT. Fig. 3B presents the tumour-to-blood ratio of ^{111}In-labeled 28H1-700DX or DP47GS-700DX at 24 h post-injection.

Hasan's group[42] developed photoimmune nanoconjugates (TR-PINs) with three ligands: cetuximab (anti-EGFR mAb), holotransferrin (natural ligand for TfR), and trastuzumab (anti-HER-2 mAb), that can target three receptors overexpressed in the tumours: epidermal growth factor receptor, EGFR, transferrin receptor TfR and human epidermal growth factor receptor 2 HER2. TR-PINs carried a lipid-anchored derivative of the PS benzoporphyrin derivative (BPD-PC). Triple targeting of receptors resulted in a 41-fold increase in binding to MIA PaCa-2 cells compared with non-targeted NHPs. In three-dimensional tumour models, TR-PINs efficiently destroyed tumour spheroids and markedly reduced cell viability using 690 nm light excitation and a fluence of 40 J cm^{-2} delivered at an irradiance of 150 mW cm^{-2}. This methodical approach facilitates the treatment of different cell subpopulations within a tumour, thereby reducing the risk of resistance.

Ferino *et al.*[43] examined an innovative approach targeting cancers associated with RAS (for rat sarcoma protein) gene mutations (notably KRAS and NRAS), by exploiting the G-quadruplex (G4) structures present in their messenger RNAs. They developed tetracationic pyridinium porphyrins modified with 12-carbon alkyl chains, capable of binding specifically to these G4 structures in the target RNAs. They demonstrated that, under light excitation (660 nm, 7.2 J cm^{-2}), these compounds produce ROS in PANC-1 cells. Analyses by flow cytometry and confocal microscopy confirmed the presence of the targeted RNA in the cells. In PANC-1, PDT led tp a reduction in KRAS/NRAS expression, a decline in metabolic activity and the induction of apoptosis *via* the activation of caspases 3, 7 and PARP-1. The tumour growth after injection of alkyl porphyrin 2b (3 mg kg^{-1}) and TMPyP2 (30 mg kg^{-1}) and excitation at 660 nm (193 J cm^{-2}) showed a statistical reduction with TMPyP2 (Fig. 4).

Acedo team's[44] developed an entirely organic PS, based on a BODIPY dye, designed for image-guided PDT (ig-PDT) of cancer. When tested on MIAPaCa-2, PANC-1 and H6c7 cells, this

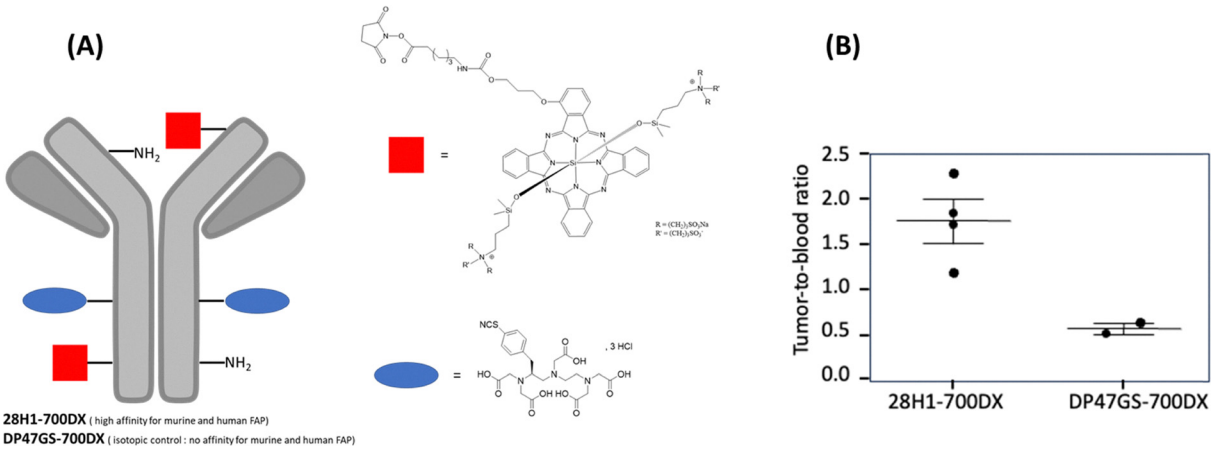

Fig. 3 (A) Structure of two antibodies 28H1-700DX and DP47GS-700DX. (B) Tumour-to-blood ratio of ^{111}In-labeled 28H1-700DX or DP47GS-700DX at 24 h post-injection of ^{11}In-labeled 28H1-700DX or DP47GS-700DX.

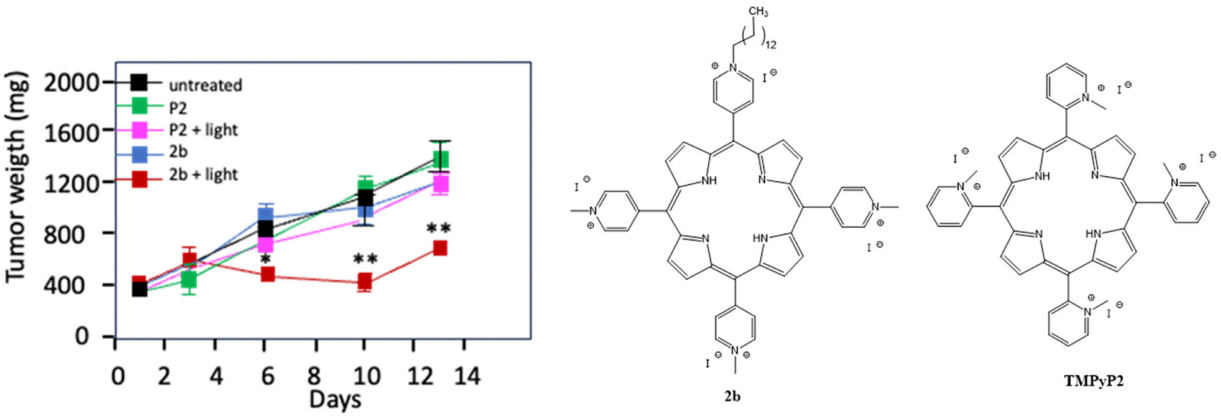

Fig. 4 Tumour growth after injection of alkyl porphyrin 2b (3 mg kg^{-1}) and P2 (TMPyP2) (30 mg kg^{-1}) after excitation at 660 nm (193 J cm^{-2}). *$p < 0.05$, **$p < 0.01$.

BODIPY showed selective accumulation in mitochondria and induced apoptosis after illumination (525 nm, 5.73 mW cm^{-2}). *In vitro* assays revealed a significantly higher ROS production in MIAPaCa-2 cells (92%) compared to PANC-1 cells (14%) at a concentration of 1 μM of BODIPY. Increasing the concentration to 2.5 μM resulted in further increasing the ROS production in both lines, reaching 89% for MIAPaCa-2 and 64% for PANC-1.

Zhu *et al.*[45] targeted ferroptosis, a form of iron-dependent cell death. They developed two enantiomeric iridium(III) complexes containing a phenylquinazolinone-derived ligand, designated as *Δ*-IrPPQ and *Λ*-IrPPQ. The study aimed to selectively inhibit metallothionein-1 (MT1), a protein that plays a key role in regulating ferroptosis. The results showed that the Λ-IrPPQ complex effectively induces ferroptosis in PANC-1 cancer cells. This is achieved by increasing ROS production, lipid peroxidation, glutathione depletion, and FSP1 inactivation. The superior efficacy of the *Λ*-IrPPQ ($IC_{50irrad}$ = 2.7 μM) complex compared with the *Δ*-IrPPQ ($IC_{50irrad}$ > 50 μM) complex is explained by its greater affinity for MT1, as revealed by proteomic analyses and molecular simulations. The study emphasises the significance of chirality when designing targeted metal therapies and proposes a new approach to overcoming resistance to standard treatments for PDAC.

Kuroda *et al.*[46] reported the coupling of IRDye700DX to a recombinant lectin rBC2LCN, that targets fucosylated glycans (H type-3 motif) expressed in pancreatic cancer, called rBC2-IR700. Panc-1 cells were illuminated (NIR light, 50 mW cm^{-2}) after 3 h incubation of rBC2-IR700 (1 μg mL^{-1}) and more than 80% of cell death could be observed at 32 J cm^{-2} whereas no cell death was observed in SUIT-2 cells. Subcutaneous Capan-1 xenograft mice were illuminated (NIR light, 100 J cm^{-2}) 6 h after rBC2-IR700 injection (20 μg) leading to a significant growth inhibition which is not the case for mice that receive only light or PS.

Luo *et al.*[47] synthesized FAPα activatable PS by coupling N-terminal blocked FAPα-sensitive dipeptides to methylene blue as a PS. This compound has no photoactivity but the fluorescence and $^1O_2$ formation will be restored after the action of FAPα. After incubation in MIA PaCa-2 cells and illumination at 633 nm (100 mW cm^{-2}, 5 min) the cell viability decreased to 42%. Unfortunately, the authors failed to establish a MIA PaCa-2 tumour xenografted module.

The parameters of all the studies dealing with targeted PDT to treat PDAC are summarized in Table 1.

Passive targeted treatment. After discussing active targeting approaches, which rely on the specific recognition of tumour or stromal cells receptors, it is relevant to consider so-called passive strategies. These are mainly based on the enhanced permeability and retention (EPR) effect and provide an alternative means to improve the accumulation of photosensitisers within pancreatic tumours. NPs are versatile structures investigated as drug-delivery systems, allowing to use this EPR effect of solid tumours. Thus, biocompatible NPs with particle size in the range of 10–100 nm can accumulate in tumours due the permeability of their blood vessels and their poor lymphatic drainage.[53] In the context of PDT, liposomes, polymeric and inorganic NPs have been reported.[54] They act as carriers for the PS, circumvent the hydrophobic issue encountered with many PSs, increasing their stability against enzymatic degradation, improving their biodistribution and increasing their delivery inside the tumour.[55] Ideally, a high loading of the PS inside the NPs must be achieved while avoiding aggregation that compromises their phototoxicity. Other benefits of nanocarriers include the possibility of a concomitant encapsulation of oxygen supplier to circumvent the hypoxia limitation often in pancreatic tumours. More generally, the capacity of NPs to co-load various drugs and pro-drugs is promising since combined therapies are nowadays considered essential to overcome the poor prognosis of pancreatic cancer (*vide infra*). A recent review focusing on nanotechnology as a means of overcoming the limitation of PDT in treating PC has been published.[56] Therefore, publications between 2020 and 2025 on passive treatment will not be discussed here, but the PDT protocols used are summarized in Table 2.

Active and passive targeted treatment. Targeted NPs are highly pertinent in PDT for several diseases, including for cancer, and more specifically for PC, because they can enhance selectivity, they improve therapeutic efficacy, and reduce side effects.[54,80]

Table 1 Reference, targeting method, PS used, light excitation conditions, *in vitro* and *in vivo* conditions for active targeted PDT to treat PDAC

	Targeting method		PS			*In vitro* and *in vivo*	
Ref.	Type	Specificities	Nature	ROS produced (QY)	Light excitation conditions	Cell lines used	Animal model used
45	Active	Phenylquinazolinone-derived ancillary ligand to target FSP1	IrPPQ	$^1O_2$ and $O_2^{\bullet -}$ (43.3 to 49.7%)	380–390 nm 30 mW cm^{-2} 10 min	HT-1080, SK-MEL-28, PANC-1	—
48	Active	HSP90 inhibitor	IGC & 17-DMAG	(46%)	808 nm 1 mW cm^{-2} 5 min	Panc02	Male C57BL/6 mice
41	Active	Fibroblast activation protein (FAP)	IRDye700DX (silica phthalocyanine derivative) conjugated with the chelating acid (DTPA) DTPA-700DX-MB	$^1O_2$	690 nm 60 J cm^{-2}	3T3, 3T3-FAP et PDAC299	Female C57BL/6 mice
49	Active	FAP 28H1	IRDye700DX (700DX)	$^1O_2$	690 nm, 50 J cm^{-2} 290 mW cm^{-2}	3T3-FAP, PETR4906, PDAC299	Female C57/BL6 mice
42	Active	HER-2, TfR, EGFR	TR-PINs benzoporphyrine (BPD-PC)	$^1O_2$	690 nm 150 mW cm^{-2}	MIA PaCa-2, A431, SCC-9, T47D, CHO-WT	—
43	Active	KRAS quadruplex d' ARN 5′-UTR (RG4) (UTR-1, UTR-C, utr-z) NRAS	The derivatives of TMPyP4 (2a–d) obtained by replacing the methyl group with an alkyl chain of 12, 14, 16, and 18 carbons	$^1O_2$	660 ± 5 nm 7.2 J cm^{-2}	Panc-1 MIA PaCa-2	—
50	Active		UCNP@PMVEMA-THPC NPs	$^1O_2$	980 nm	Capan-2, PANC-01, PA-TU-8902.	Outbred nude female mice (Hsd: athymic Nude-Fox n1nu)
51	Active	GLUT receptor	Porphyrin-based MOF, HfMOF-PFP-Ni. Chlorine-based MOF (HfMOF-PFC-Ni)	$^1O_2$	White LED light 100 mW cm^{-2} 30 min	MDA-MB-231, MIA-PaCa 2, HeLa	—
52	Active	EGFR	Multi-photoactivable inhibitor liposomes (TPMILs) Benzoporphyrin PS (DBP)	$^1O_2$ (5%)	690 nm 40 J cm^{-2}, 100 mW m^{-2} or 20 J cm^{-1}	MIA PaCa-2 PCAF	Male athymic Swiss nude mice
44	Active	The mitochondria	BODIPY (Bore dipyrromethene)	$^1O_2$ (4%)	525 nm 5.73 mW cm^{-2}	MIA PaCa-2, PANC-1, H6c7	—
40	Active	PTS (Polyamine Transport System)	BODIPY-2I	$^1O_2$	550 ± 50 nm, 6,5 p m^{-2}	PANC-1, BxPC-3, hTERT-HPNE	Nude mice
46	Active	Fucosylated glycan	IRDye700DX	—	NIR light *In vitro*: 50 mW cm^{-2} 1–32 J cm^{-1} *In vivo*: 100 J cm^{-1}	Capan-1 (+) SUIT-2 (−)	Female BALB/c nude mice and CB17/Icr-scid/SCID mice
47	Active	Fibroblast activation protein α (FAPα)	Methylene blue	$^1O_2$	633 nm 100 mW cm^{-2} 5 min	MIA CaPa-2	5–6 weeks old female nu/nu athymic nude mice

Table 2 Reference, PS used, light excitation conditions, *in vitro* and *in vivo* conditions for passive targeted PDT to treat PDAC

Ref.	Photosensitiser	ROS produced (QY)	Light excitation conditions	Cell lines used	Animal model used
57	Ce6	$^1O_2$	660 nm 50 mW cm^{-2} 5 J cm^{-2}	AsPC-1, MIA, PaCa-2, B16F10, Panc02	Mice C57BL6 and dog
58	Porphyrins loaded with $PMLABe_{73}$ based NPs	ROS	790 nm	MCF-7, MDA-MB-231, Capan-1	—
59	MHI-I2 (1)	$^1O_2$	780 nm (1)	U87-MG	Male CD-1 mice male hairless athymic nu/nu mice
	QuatCy-I 2 (2)		750 nm (2) 3.8 mW cm^{-2}		C57BL/6 mice
60	TMPyP4	$^1O_2$, $O_2^{\bullet-}$	490 nm	A549, PANC, MIHA	—
61	NPs PPA@AgND-ALA		635 nm 50 mW cm^{-2}	4T1	Mice
50	UCNP@PMVEMA conjugate with *m*THPC	$^1O_2$	650 nm, 980 nm, 0.5 W cm^{-2}	Capan-2, PANC-01	Mice
62	Verteporfin		—	PANC-1, BxPC3	—
63	PET-ONCO (^{124}I-l PS) Chlorophyll-a coupled with a radionuclide ^{124}I		665 nm	Panc-1, Colon26, 4 T1, GL261, U87, UMUC3	Mice BALB/c and BALB/c rats
64	HPPH NPs HMON-Au@Cu-TA	$^{\bullet}OH$	671 nm 0.1 W cm^{-2}	BxPC-3	Nude mice
65	Triplet anthracene derivative	Type I and II	White light 15 mW cm^{-2}, various intervals	CT-26, HCT116, Pan02	BALB/c female white mice CT-26
66	Ce6-curcumine	$^1O_2$	660 nm 50 mW cm^{-2} 5 J cm^{-2}	AsPC-1, MIA-PaCa-2, PANC-1	Mice C57BL/6 and mice ICR
67	NP BTz-IC	Type I	808 nm	Pan02	Mice C57/BL6
25	Benzoporphyrine derivative encapsulated in liposomes	$^1O_2$	690 nm 100 mW cm^{-2}	PANC-1	—
68	UCNP/RB, Ce6-PEG containing rose bengal (RB) and Ce6	$^1O_2$	1550 nm	Panc-1	NOD SCID mice
69	N*b*B (BODIPY-naphtholimine-BF_2)	$^1O_2$	White light 9.34 mW cm^{-2}	MIA PaCa-2, PANC-1	—
70	*m*THPC		980 nm 40 mW cm^{-2} 30 min	Capan-2, PANC-1, PA-TU-8902	Nude female mice Capan-2
71	Verteporfin	Type I or II	690 nm 20 J cm^{-2} 17.86 mW cm^{-2}	CT1BA5	Male mice C57BL/6 CT1BA5
72	Bremachlorin		662 nm 116 mW cm^{-2} 116 J cm^{-2}	PDAC (2838c3)	BALB/c nude mice PDAC clone type 2838c3
73	Photofrin Ce6		630 nm 300 mW cm^{-2} 100 J cm^{-2} Mini-LED 630 nm 8.5 mW cm^{-2}	MIA PaCa-2 and BxPC-3	Male nude mice BALB/c
74	BPD	$^1O_2$	685 nm 5 mW cm^{-2}	MIA PaCa-2	Mice
75	Cationic alkylated porphyrins: free form or grafted onto the surface of POPC liposomes	$^1O_2$ —	Metal halide lamp 8 mW cm^{-2} 15 min 7.2 J cm^{-2}	Panc-1, BxPC-3, MIAPaCa-2	—

Table 2 (*continued*)

Ref.	Photosensitiser	ROS produced (QY)	Light excitation conditions	Cell lines used	Animal model used
76	Protoporphyrin IX (PpIX) 5-ALA	Type I and II	635 nm 40 J cm^{-2} 135 mW cm^{-2}	PANC 1 PancOR	—
77	5-ALA	$^1O_2$	630 nm	CAL-27, CAPAN-2	—
78	UCNPs co-encapsulated MnO_2, PSMA and riboflavin	$^1O_2$	980 nm 10 min 0.5 W cm^{-2}	Panc02, HEK293	—
79	Methylene blue	—	633 nm 6 min 4.5 J cm^{-2} 11.3 mW cm^{-2}	AsPC-1, BxPC-3, MiaPaCa-2, Panc-1	—

More specifically they bare relevance:

(1) to add an active targeting to the so-called passive one; as NPs can also be functionalized with ligands such as peptides[81,82] or antibodies to specifically bind to surface cell proteins (*e.g.* aptamers, peptides, and other polymers,[83]) and tumour-associated markers (*e.g.* integrins, EGFR[84]) improving the targeting of the PS delivery and, very often, the related internalization.

(2) to minimize non-specific accumulation of the PS. Decorated NPs prevent systemic (photo-) toxicity and destruction of healthy tissues upon light irradiation; a recent review in the domain has been published.[85]

(3) to possibly increase of the hydrophilicity of the PS when embedded by grafting or encapsulation to NP; this can also be at the origin of an increased stability and circulation time of the NP.

(4) the use of oxygen-absorbing materials for the NPs, in order to elaborate an oxygen self-sufficient PDT nanoplatform for treating hypoxic tumour microenvironment (TME); an example in this domain is the use of perfluorocarbon NPs.[86–88]

(5) a time and spatially-controlled release of the PS, for example in the TME upon stimulus like pH, redox potential or using an enzyme responsive edifice.[89]

(6) the capability offered to deliver several and different agents; this can be PS but also drugs for more classical therapy, or imaging agents (magnetic contrast agents for MRI, or optical probes). It paves the way to multifunctionality and theranostics, combining therapy and imaging or combining PDT with other therapies.

The strategy developed by Hafiz *et al.*[90] consists of gallium-indium alloy (EGaIn) NPs, which are more commonly referred to as EGaP. These NPs were functionalised with hyaluronic acid (HA) to target tumour cells overexpressing CD44 receptors, and integrated benzoporphyrin derivative (BPD). *In vitro* studies demonstrated effective internalisation of EGaPs in cancer cells (AsPC-1, pancreatic cancer cells derived from ascites) and MIA PaCa-2 cells as well as high production of ROS after light illumination (690 nm, 50 mW cm^{-2}, 0–1 J cm^{-2}). Upon illumination, BPD and free EGaP exhibited mild, dose-sensitive cell killing in MIA-PaCa-2 and AsPC-1 cells (690 nm, 50 mW cm^{-2}, 0, 1, 2.5, 5, and 10 J cm^{-2}). PDT experiments were conducted on AsPC-1 pancreatic cancer tumours in nude mice (690 nm, 75 mW cm^{-2}, 200 J cm^{-2}). Significant tumour regression was observed, associated with tumour necrosis that was significantly higher than that achieved with conventional BPD formulations (Fig. 5).

Shapoval *et al.*[50] used up-conversion NPs (UCNPs) doped with Fe^{2+}, Yb^{3+} and Er^{3+} ions, and conjugated with temoporfin *m*THPC as a PS. The UCNPs, stabilised by a copolymer poly(methyl-vinyl ether-*alt*-maleic acid) (PMVEMA) coating, exhibit enhanced emission in the red spectrum due to Fe^{2+} co-doping, thus optimising *m*THPC excitation.

In vitro PDT experiments (20 h, excitation at 980 nm by a Coherent 170 fs pulsed Chameleon laser with a power of 40 mW for 30 min) on Capan-2, PANC-1 and PA-TU-8902 cell lines, demonstrated that nanoconjugates exhibited potent cellular phototoxicity following effective cellular internalisation. *In vivo* trials on athymic nude mice confirmed the therapeutic

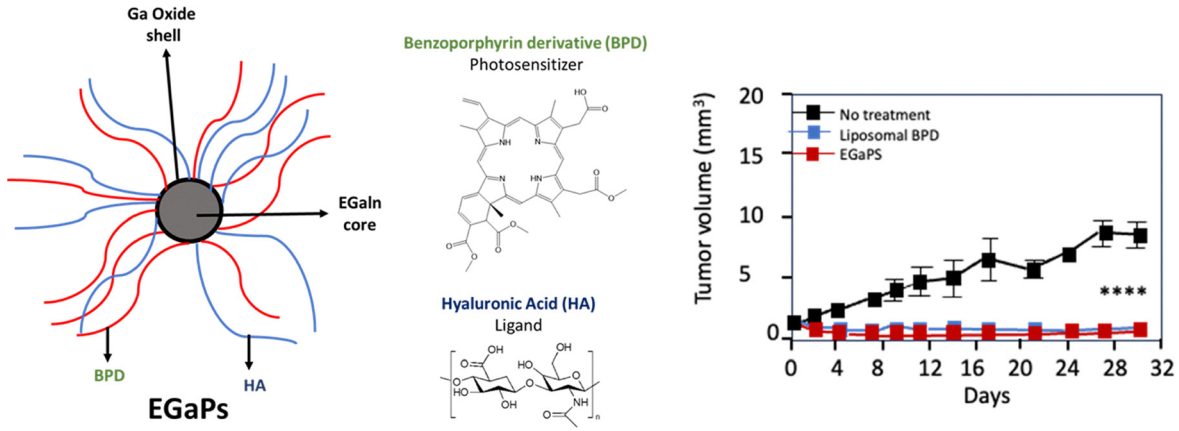

Fig. 5 Schematic representation of EGaPs and *in vivo* treatment efficacy of EGaPs in AsPC-1 tumour model: normalized tumour volume of mice treated with EGaPs and traditionally used liposomal formulation of BPD.

efficacy of the treatment, with marked tumour necrosis after intra tumour injection and NIR exposure, with no significant side effects. A statistically significant reduction in Capan-2 human pancreatic tumour growth rate was achieved after PDT, with a tumour volume of 0.35 cm^3 on day 30 compared with a volume range of 0.45 to 0.47 cm^3 in the two control groups. (Fig. 6).

Sakamaki *et al.*[51] used an organometallic structure (MOF) bioconjugated to a chlorin as a PS. The MOF is composed of hafnium metal centers, which offer optimal stability and porosity for encapsulating the chlorin. The surface of the NPs was modified with maltotriose, a sugar known for its ability to specifically target GLUT receptors in cancer cells, thereby enhancing the accumulation of MOF in tumours. *In vitro* assays demonstrated significantly higher cell toxicity of chlorin-conjugated MOF MA-HfMOF-PFC-Ni-Zn (20 μg mL^{-1}) on MIA PaCa-2, compared to porphyrin-based MOF MA-HfMOF-PFP-Ni-Zn (80 μg mL^{-1}) after excitation with white LED light (100 mW cm^{-2}, 30 min). In addition, no toxicity was observed in the absence of irradiation, underlining the safety of the system. The effective internalisation of NPs into tumour cells was confirmed by imaging studies.

Zhao *et al.*[91] examined a different approach, using a π-extended porphyrins (rTPA), for near-infrared excitation, incorporated in a mitochondrial-targeting career (MITO-Porter) to facilitate active targeting of mitochondria. These PSs showed selective accumulation in the mitochondria of cancer cells, as confirmed by co-localisation analyses with mitochondrial markers. It is to be noted that all rTPA derivatives in MITO-Porter (rTPA@MPs) including rTPA-NH_2@MP and rTPA-OH@MP, demonstrated significant anticancer properties on PCI-55 cells. In fact, rTPA-NH_2@MP demonstrated optimal antitumour efficacy, as illustrated in Fig. 7. When exposed to light (700 nm, 80 mW cm^{-2}, 5 min), rTPA-NH_2 efficiently generates $^1O_2$ with a quantum yield (Φ_Δ) of 23%, inducing a particular form of apoptosis through mitochondrial oxidative stress. In the absence of light, PS cytotoxicity remains low, ensuring photosensitive selectivity. This research highlights the therapeutic potential of π-extended porphyrins in the targeted treatment of deep and resistant cancers.

Tao *at al.*[92] designed a sequence activated nanotheranostic TCM-U118&Cy@P for human pancreatic cancer with multifunctionality such as both passive and active targeting, pH sensitivity and near-infrared fluorescence. This fluorescent

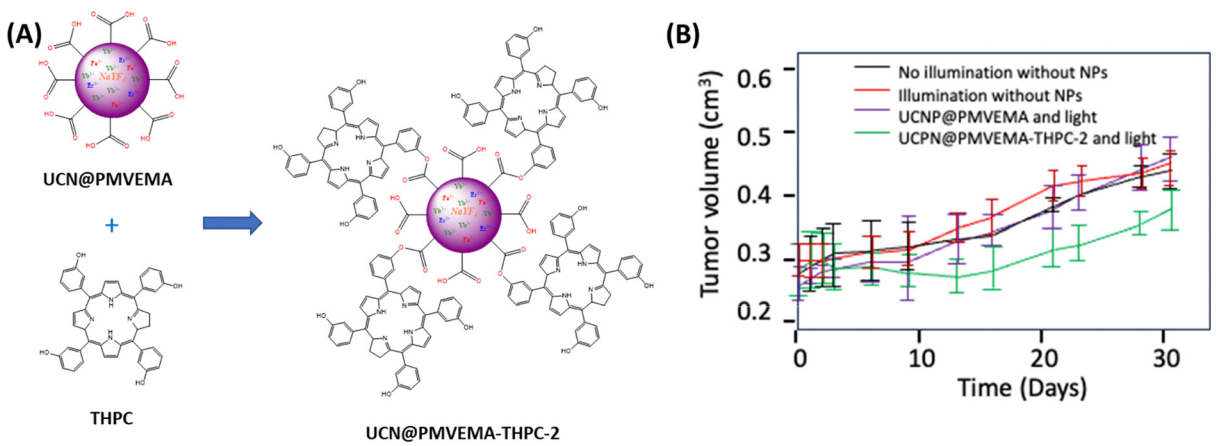

Fig. 6 (A) Structure of UCN@PMVEMA and UCN@PMVEMA-THPC-2. (B) *In vivo* PDT with UCN@PMVEMA-THPC-2. Tumour growth (n = 4). Illumination was performed at 980 nm laser 10 min after administration. Statistical significance between UCN@PMVEMA-THPC-2 and other three groups $p < 0.05$.

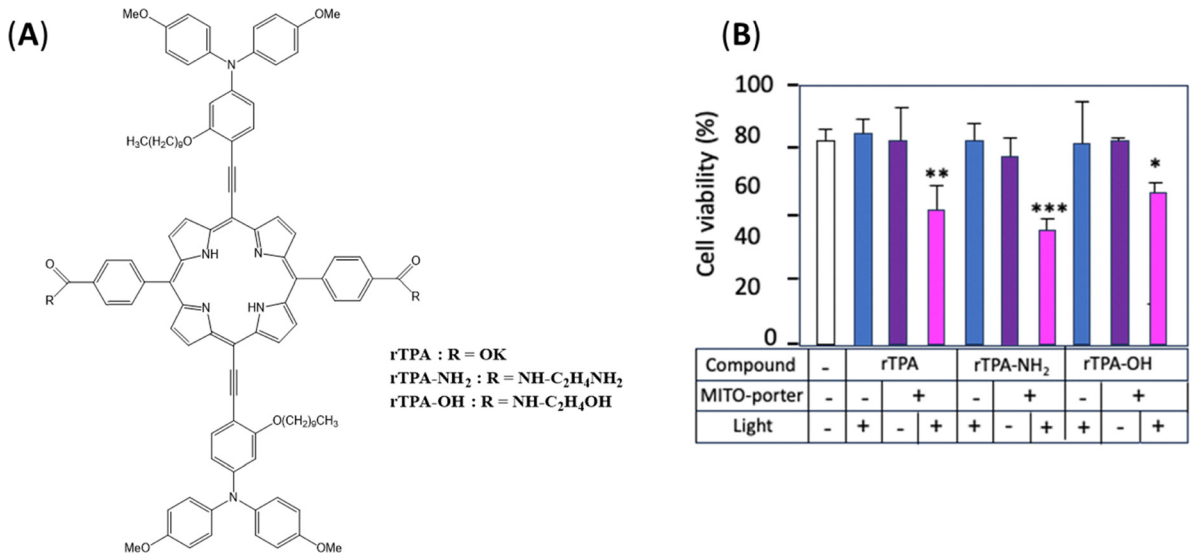

Fig. 7 (A) Chemical structures of rTPA derivatives (B) phototoxicity of PCI-55 cells for 0.25 μM of rTPA, rTPA-NH_2 and RTPA-OH with or without microporteur. Data are means +/− S.D. (n = 3–4) *p < 0.05, **p < 0.01, ***p < 0.001 compared with the negative control.

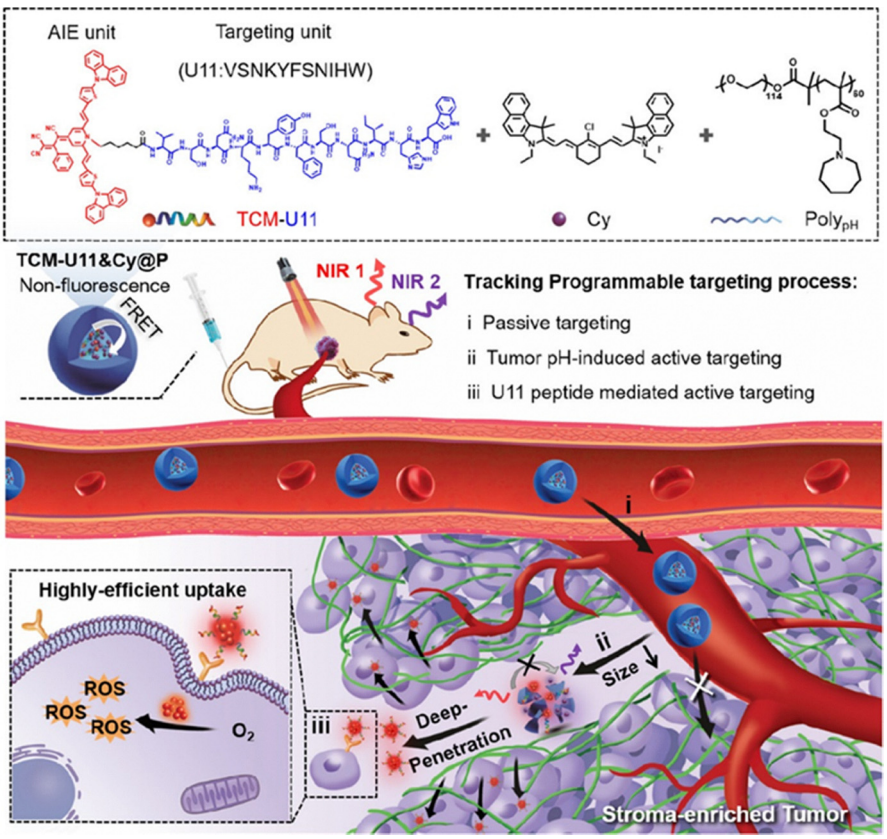

Fig. 8 Schematic illustration of sequence-activated fluorescent nanotheranostics for programmable targeting of the pancreatic tumour.[92]

nanotheranostic agent is featuring three components: (i) a diblock copolymer serving as carrier sensitive to acidic pH, (ii) a non-fluorescent tricyano-methylene-pyridine dye with aggregation-induced emission (AIE) properties acting both as a Förster resonance energy transfer (FRET) donor and as a photosensitiser, covalently bonded to U11 peptide (TCM-U11) for targeting PDAC cells and (iii) a NIR emitting cyanine (Cy) as a FRET acceptor (Fig. 8). *In vitro* (3D Panc-1 spheroid) and

in vivo evaluation showed that TCM-U118&Cy@P possessed potent for tumour targeting, deep delivery and phototoxicity. Moreover, this nanotheranostic agent successfully mapped human clinical specimens with high resolution.

Yan *et al.*[93] synthetised a novel drug delivery system with chlorin Ce6 as a PS for the treatment of the rare pancreatic disease, neuroendocrine neoplasm (pNENs). Thus, the hydrophilic octreotide (OCT), which is an FDA-approved cyclooctapeptide analogue of natural somatostatin and able to target selectively somatostatin receptor (SSTrs), and the hydrophobic Ce6 were covalently coupled through a specific ROS/GSH-labile linker (Fig. 9A). The resulting conjugate can self-assemble into OCT-Ce6 NPs (OCNPs) in water. *In vitro* evaluation with QGP-1 (pancreatic neuroendocrine) and HPNE (Human normal pancreatic) tumour cell lines, showed that OCNPs is able to produce $^1O_2$ after illumination. Besides, OCNPs was also able to block cells from entering S/G2 phase to lead to apoptosis and necrosis. *In vivo* assays on QGP-1 tumour-bearing nude mouse model, showed that OCNPs could specifically accumulate in tumour tissues and inhibit tumour growth when illuminated (660 nm, 100 mW cm^{-2} for 15 min) (Fig. 9B and C) without toxicity and side effects on major organs.

Work published by Dai *et al.*[94] developed a supramolecular NP (T-NP$_{Ce6\text{-}L\text{-}N}$) in order to solve multiple innate challenges of conventional PDT. This nanocomplex integrated photosensitiser: Ce6 with luminol and nitric oxide (NO) for chemoluminescence resonance energy transfer (CRET)-activated PDT. *In vitro* evaluation on L3.6 pl cancer cell line, showed selective targeting of pancreatic cancer cells with minimal cytotoxicity on normal cells. *In vivo* experiments evaluated on L3.6 pl tumour bearing nude mice, showed tumour suppression (on subcutaneous, large, deep seated orthotopic and metastatic tumours).

Ozge *et al.*[95] synthesized Zn phthalocyanine-loaded mesoporous silica NPs coupled with a radiolabeled cetuximab antibody (^{131}I radionuclide). *In vivo* PDT studies were performed on AsPC-1 bearing nude mice. PDT was performed with 685 nm red light, 100 J cm^{-2} with different concentrations of ZnPc containing MSNP5 (5–20 μM). It was shown that necrosis in tumour tissue was higher in the PDT group than the control group.

The details of all the studies published between 2020 and 2025 dealing with both active and passive targeted PDT to treat PDAC are collected in Table 3.

PDT coupled to other therapies

Immunotherapy. Hypoxia is a defining feature of pancreatic ductal adenocarcinoma (PDAC) and plays a pivotal role in shaping an immunosuppressive tumor microenvironment

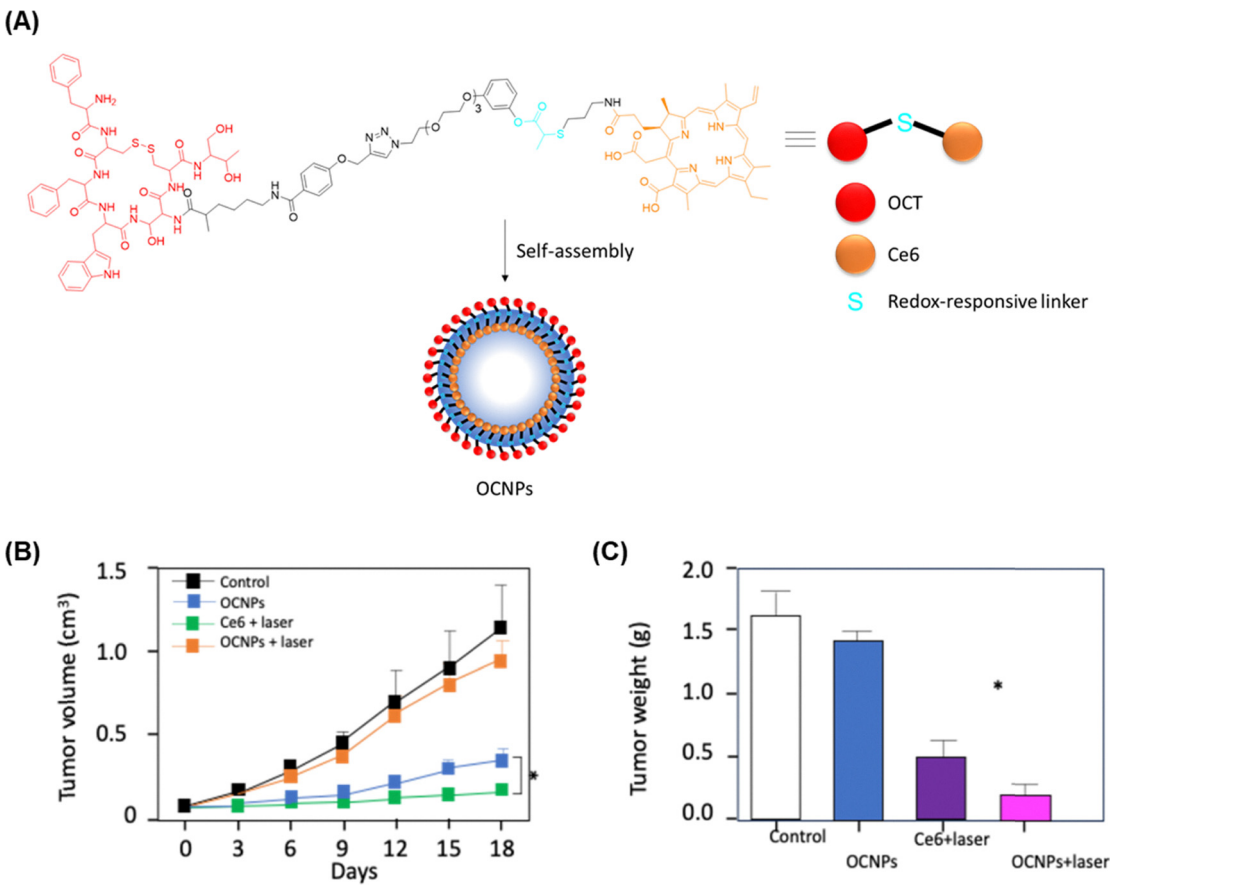

Fig. 9 (A) Chemical structure of OCNPs. *In vivo* anti-pNENs effect of OCNPs: (B) curves of changes in tumour volumes in different groups during treatment, (C) average tumour weight in different treatment groups after 18 days of treatment.

Table 3 Reference, targeting method, PS used, light excitation conditions, *in vitro* and *in vivo* conditions for both active and passive targeted PDT to treat PDAC

	Targeting method		PS				
Ref.	Type	Specificities	Nature	ROS produced (QY)	Light excitation conditions	Cell lines used	Animal model used
92	Both	uPAR EPR	NPs TCM-U11&Cy@P Cyanine (Cy)		NIR 1 NIR 2	PANC-1	Male BALB/cA nude mice
93	Both	Active (SSTR-targeting) passive (ROS/GSH sensitive + EPR effect)	Ce6 NP	$^1O_2$	660 nm 100 mW cm^{-2} 2 min	HPNE, QCP-1, BALB/c	Mice
94	Both	Host–guest interactions between β-CD and benzimidazole (BM)	CRET from Luminol activating Ce6		Self activated (with H_2O_2 and Fe^{3+})	L3.6 Pl	BALB/c nude mice and C57BL/6
91	Both	MITO-Porter	rTPA	$^1O_2$ (23%)	700 nm 80 mW cm^{-2} 5 min	PCI55	—
95	Both	EGFR	NPs (MSNP5) containing Zinc Phthalocyanine (ZnPc)		685 nm 100 J cm^{-2}	MIA PaCa-2, AsPC-1, PANC-1	Male nude mice
90	both	CD44 receptors	EGaP NPs containing benzoporphyrin (BPD)		690 nm 75 mW cm^{-2}	MIA PaCa-2, AsPC-1	Mice
51	Both	GLUT receptors	MOF coupled to a chlorin		White LED 100 mW cm^{-2}, 30 min	MIA-PaCa-2	Mice

(TME). Through stabilization of hypoxia-inducible factors (HIFs), metabolic reprogramming, and modulation of immune signaling, hypoxia suppresses effector immune cells while promoting regulatory and suppressive cell populations. This immunosuppressive milieu limits the efficacy of conventional immunotherapies in PDAC. Recent studies highlight that light-activated immunomodulation—particularly photodynamic therapy (PDT) and reactive oxygen species (ROS)-based photoimmunotherapy—can counteract hypoxia-driven immunosuppression. These approaches induce immunogenic cell death, promote macrophage repolarization, and enhance T-cell activation, thereby improving the responsiveness of pancreatic tumors to immunotherapy.

Tumor hypoxia, typically defined as oxygen partial pressure below 10 mmHg, arises from the rapid proliferation and aberrant vasculature characteristic of most solid tumors, including PDAC. This oxygen deprivation profoundly alters tumor and immune cell behavior. Hypoxia stabilizes HIF-1α and HIF-2α, which translocate to the nucleus and bind hypoxia-responsive elements (HREs) to regulate transcription of genes controlling metabolism, angiogenesis, and immune escape.[96] Through these mechanisms, hypoxia upregulates immune checkpoint ligands such as PD-L1, CD47, and HLA-G, directly impairing cytotoxic lymphocyte recognition.[96,97]

The effects of hypoxia on immune effector cells are multifaceted. Low oxygen levels inhibit cytotoxic T lymphocyte (CTL) and natural killer (NK) cell proliferation, reduce cytokine secretion (*e.g.*, IFN-γ, IL-2), and downregulate activating receptors such as NKG2D.[98] Metabolic stress under hypoxia—driven by increased glycolysis, lactate accumulation, and extracellular acidification—further suppresses T-cell activation and promotes exhaustion.[98,99] Lactate accumulation also facilitates M2-type macrophage polarization *via* histone lactylation, while adenosine generated through HIF-1-induced CD39/CD73 expression activates A2A receptors on T cells, leading to cAMP-mediated inhibition of effector function.[99] These metabolic shifts transform the TME into a niche that is hostile to cytotoxic immune cells yet favorable to suppressive phenotypes.

Concurrently, hypoxia enhances recruitment and activation of immunosuppressive populations such as regulatory T cells (Tregs), myeloid-derived suppressor cells (MDSCs), and M2-type tumor-associated macrophages (TAMs). Elevated expression of chemokines including CXCL12/SDF-1α and CCL28, along with increased secretion of VEGF, IL-10, and TGF-β, drives accumulation of these cells in hypoxic tumor zones.[98,100] Within PDAC, TAMs exposed to hypoxia undergo M2 polarization, secreting anti-inflammatory cytokines that blunt anti-tumor immunity.[97,100] Gene-expression profiling of PDAC tissues confirms that tumors with high hypoxia signatures exhibit lower $CD8^+$ T-cell infiltration and enrichment of suppressive macrophages[101] The combination of these factors renders PDAC a profoundly "cold" tumor, resistant to checkpoint blockade and other immunotherapies.

Among the strategies to overcome this barrier, photodynamic therapy (PDT) and light-activated immunomodulation have shown significant promise. PDT uses a photosensitizer, light, and molecular oxygen to generate ROS, inducing tumor

cell death through apoptosis, necrosis, or pyroptosis. Importantly, PDT provokes immunogenic cell death (ICD), releasing damage-associated molecular patterns (DAMPs) such as calreticulin, HMGB1, and ATP that stimulate dendritic cell maturation and antigen presentation, thereby enhancing T-cell priming.[102] In pancreatic cancer models, PDT-induced pyroptosis has been shown to trigger M1 macrophage polarization, dendritic cell activation, and $CD8^+$ T-cell infiltration, resulting in both local and systemic anti-tumor effects.[103]

However, the classical type II PDT mechanism depends on molecular oxygen to produce singlet oxygen ($^1O_2$), and thus its efficacy diminishes in hypoxic TMEs. To address this limitation, new type I photosensitizers capable of generating radicals independently of oxygen have been developed. For example, TPA-DCR nanoparticles induce ROS *via* a type I mechanism and can repolarize macrophages from M2 to M1 phenotype even under hypoxic conditions, thereby enhancing T-cell infiltration.[104] Similarly, a multifunctional nanoplatform combining M1-macrophage membranes, a type I photosensitizer, and anti-PD-L1 siRNA (M1@PAP) successfully remodeled the PDAC microenvironment, reduced immunosuppression, and improved response to checkpoint blockade.[105] These findings underscore that ROS can act a both cytotoxic and immunostimulatory signals, promoting macrophage re-education and dendritic cell activation.

In PDAC and other hypoxic tumors, ROS-mediated immune activation also stimulates nitric oxide (NO) release, improving vascular perfusion and immune cell infiltration. Consequently, light-activated immunotherapies can break the feedback loop of hypoxia-driven immunosuppression by remodeling the microenvironment at multiple levels—metabolic, vascular, and immunologic. Moreover, combining PDT with checkpoint blockade or adoptive cell therapy has yielded synergistic responses. By increasing tumor antigen release and immune infiltration, PDT ''primes'' tumors to respond more effectively to immunotherapies that would otherwise fail in PDAC. Supporting this, metabolic reprogramming through PIM3 inhibition was recently shown to reverse hypoxia-induced CAR-T cell dysfunction in solid tumor models, reinforcing the importance of targeting the hypoxic niche.[106]

In summary, hypoxia acts as a central architect of immune evasion in pancreatic cancer through HIF-dependent transcriptional reprogramming, metabolic adaptation, and promotion of immunosuppressive cell networks. Overcoming these barriers requires both molecular and physical strategies capable of restoring immune competence. Light-activated therapies such as PDT and novel ROS-based photoimmunotherapies provide a powerful approach to reprogram the hypoxic TME by inducing immunogenic cell death, restoring macrophage balance, and facilitating T-cell recruitment. Collectively, these advances hold great potential to convert pancreatic cancer from an immune-deserted malignancy into one responsive to immunotherapy, paving the way toward more durable and effective treatment outcomes.

Several mechanisms underlie the immune stimulation (Table 4):

Table 4 PDT activates immune response using several mechanisms

Mechanism	Immunological role
ROS-induced ICD	Releases DAMPs and tumour antigens ↔ DC uptake & T cell priming
Local inflammation	Cytokine-rich milieu recruits innate immune cells
Innate cells (neutrophils, macrophages, NK)	Execute tumour control and enhance antigen processing
Adaptive immunity	Tumour-specific $CD8^+$ T cell responses target residual/metastatic tumour

DAMPs: damage-associated molecular patterns.Several variables modulate the effectiveness of PDT-induced immune activation: PS localization and concentration, light fluence rate, and oxygen availability affect ICD and ROS generation. Functional immune competence of the patient or host is essential for downstream response.[107]

ROS generated during PDT cause tumour cells to undergo for instance, apoptosis or necrosis, exposing and releasing DAMPs such as calreticulin (CRT), heat-shock proteins (HSPs), HMGB1, and extracellular ATP. These signals promote dendritic cell (DC) maturation, antigen uptake, and cross-presentation of tumour antigens to naïve T cells in lymph nodes, ultimately activating $CD8^+$ cytotoxic T lymphocytes.[90,91]

PDT induces oxidative damage to tumour cells and vasculature, leading to infiltration by neutrophils, mast cells, monocytes/macrophages, and NK cells.[92] Activated transcription factors such as NF-κB and AP-1 drive the expression of pro-inflammatory cytokines (*e.g.* IL-1β, IL-2, IL-6, TNF-α, G-CSF) and stress proteins, further amplifying immune activation.[93] IL-1β plays a pivotal role, as its neutralization impairs PDT efficacy, whereas blockade of anti-inflammatory signals (*e.g.* IL-10, TGF-β) enhances the antitumour effect.

Neutrophils, which rapidly infiltrate after PDT, orchestrate much of the early immune response; their depletion reduces therapeutic efficacy. Macrophages and monocytes release TNF-α and nitric oxide, augmenting tumouricidal activity, while NK cells contribute to the control of distant lesions. Inactivation or depletion of these cell populations markedly diminishes systemic efficacy.[94]

The antigen-rich inflammatory environment generated by PDT enables DC-mediated antigen presentation and T-cell priming, resulting in tumour-specific $CD8^+$ T cells capable of eliminating residual disease and metastases.[94,95] Preclinical studies confirm that intact lymphoid immunity is required for durable cures: PDT loses efficacy in immunodeficient mice but is restored upon lymphocyte reconstitution.

PDT is approved for various solid tumours (*e.g.* skin, oesophageal, bladder, lung), offering localized cytotoxicity plus immune activation. Combining PDT with immunotherapies such as checkpoint inhibitors (*e.g.* anti-PD-1/PD-L1) can lift tumour-induced immune suppression and potentiate long-lasting responses. Several clinical trials are underway in settings like non-small-cell lung cancer and mesothelioma. Additional strategies include combining PDT with DC vaccines, cytokine adjuvants, or other immune-modulating agents to further amplify the antitumour immune response.[108]

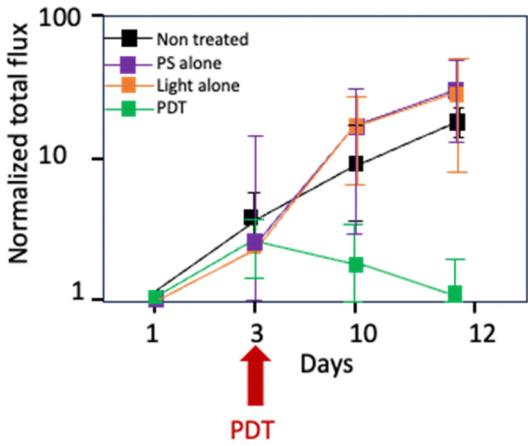

Fig. 10 *In vivo* evaluation of PDT efficiency in a humanized severe combined immunodeficiency mouse (MIA PaCa-2 Luc SC xenographed), n = 3, PDT is performed on day 3.

In conclusion, PDT is compelling from an immunology standpoint because it creates a powerful bridge from tumour destruction to sustained systemic immunity. The combination of ICD, acute innate activation, and generation of T-cell-mediated immunity makes PDT a unique dual-action therapy: both local ablative treatment and endogenous cancer vaccine. This may explain the increasing interest for such platforms in the perspective of a synergy with modern immunotherapies.

Other photosensitizers have been developed in order to associate photodynamic therapy (PDT) and light-activated immunomodulation. Thus, pyropheophorbide a coupled to a folic acid unit (patent WO2019 016397-A1, 24 January 2019) was recently developed with a view to target folic acid receptor, over-expressed in pancreatic tumour cells.[109] PDT (1 mW cm^{-2} for 1 hour, 3.6 J cm^{-2}) induced a significant reduction in cell viability, with a 95% decrease observed within 10 min and complete elimination within 24 hours in the Capan-1, Capan-2, MIA PaCa-2 and PANC-1 cell lines. In addition, it has been shown that PDT can stimulate the proliferation of human T lymphocytes, indicating an immunostimulatory effect. The PDT efficacy of the targeted PS was further evaluated in a humanised SCID mouse model of pancreatic cancer receiving a fractionated illumination of 2 h 30 in total (fractionated illumination of 1 min followed by 2 min rest, and repeated 45 times, resulting in a total of 2 h 30 illumination at 11 mW cm^{-2}, 29.7 J cm^{-2}). This approach led to a significant delay in tumour growth (Fig. 10). The results of this study indicate that this folic acid targeted PS can be a doubly effective strategy, combining direct tumour destruction and activation of the immune system.

In 2024, Qu *et al.* designed a light-activated targeted NP for imaging and PDT treatment.[37] They opted for Midkine (MDK), a growth factor highly expressed in PDAC, as a tumour-specific target. MDK was fragmented into four nanobodies (Nb) candidates for higher stability and tumour penetration, with the D4 nanobody displaying the best target selectivity. NPs were based on a light responsive semiconducting polymer (poly[2,6(4,4-bis(2-ethylhexyl)-4*H*-cyclopenta-[2,1-*b*:3,4-*b*]-dithiophene-*alt*-4,7-bis(thiophen-2-yl)benzo-2,1,3-thiadiazole]), (PCPDTTBTT) formulated with DSPE-PEG2000-MAL, providing ROS production under light activation. *In vitro*, white light irradiation of the targeted NPs induced immunogenic cell death (ICD) through ER and mitochondrial damage. Cellular internalization studies showed a peak uptake at 12 h post addition. These results were also confirmed *in vivo* when the NPs were injected to KPC and AsPC-1 pancreatic tumour bearing mice that subsequently underwent a whole-body near-infrared (NIR)-I fluorescence imaging and photoacoustic imaging, demonstrating effective tumour accumulation, highlighting the theranostic potential of the platform. *In vivo* efficacy was tested in KPC PDAC models, with mice receiving four separate NP injections (200 μL, 40 μg mL^{-1}) followed by white light excitation (80 mW cm^{-2} for 10 min) over 14 days. Significant tumour reduction and ICD induction were observed, with Damage-associated pattern (DAMPs) release enhancing immune activation.

Kim and coworkers focused on exploiting the targeting properties of the monoclonal antibody cetuximab (CTX), known to target the EGFR, a growth factor overexpressed in most PDAC cells –although often having a negligible action as anti-tumoral agent in PDAC due to KRAS mutations.[110] CTX was conjugated with a maleimidepolyethylene glycol-ce6 moiety (the resulting construct is called CMPC), enabling light triggered ROS production with CMPC (Fig. 11).

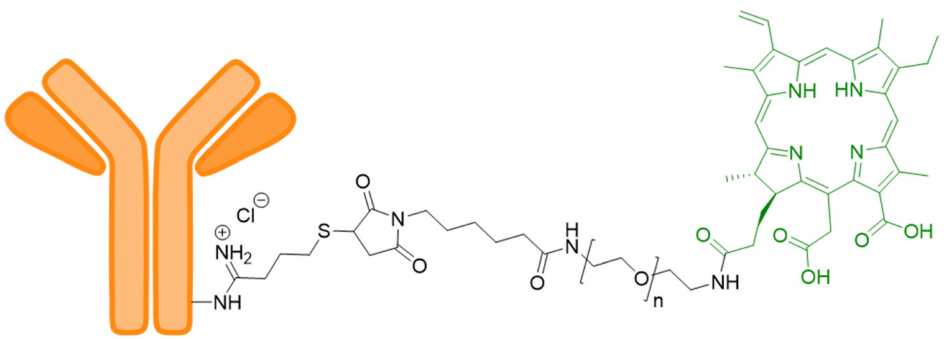

CTX-Mal-PEG-Ce6
(CMPC)

Fig. 11 Chemical structure of CMPC (monoclonal antibody cetuximad conjugated with a maleimidepolyethylene glycol-Ce6 moiety).

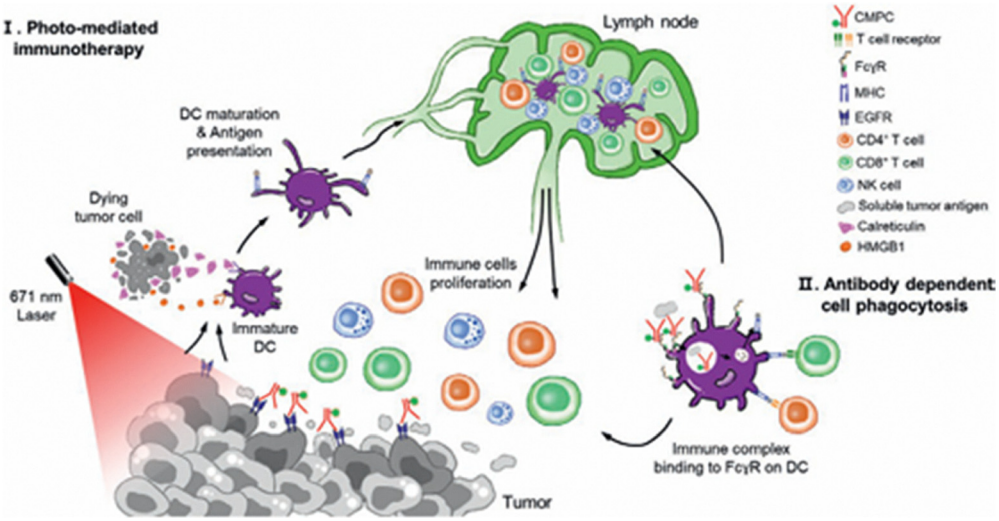

Fig. 12 Schematic illustration of antibody photosensitizer (Ce6) conjugate (CMPC) targets and anticancer responses. Reproduced from ref. 110 with permission from "John Wiley and Sons", copyright (2025).

The cytotoxicity of CMPC during light excitation was correlated *in vitro* with the expression levels of EFGR expression levels on the cell lines used, with up to 90% with AsPC-1 cells. *In vivo* PDT (671 nm, 200 mW cm^{-2} for 500 s, at t = 12 h and t = 24 h after injection) was performed on AsPC-1 tumour bearing BALB/c mice, showing a good biodistribution into the tumour and significant tumour size reduction. Furthermore, a stimulated immunogenic response was observed with activation of anti-tumoural adaptive immune cells (CD4+, $CD8^+$ T-cells) as well as innate immune cells (DCs, NK cells) (Fig. 12).

In 2024, Li *et al.* went further in their study on PDT with quantum dots (QDs) based on a cadmium selenide core with a zinc sulfide shell and a carboxylate outer coating.[38] These were conjugated with the RGD peptide sequence (arginine–glycine–aspartic acid), an integrin antagonist able to bind to integrin αvβ3 which regulates tumour growth. The resulting QDs-RGD NPs were able to selectively target tumour cells and produce ROS under light activation. Although *in vitro* testing of the NPs showed some toxicity in Panc02 cells after 3 h in the absence of light, it was well tolerated in C57BL/6 mice upon illumination at 650 nm (100 mW cm^{-2}, for 30 min with 1 min of dark every 2 min of exposure). Different immune response markers were analysed and it was found that QDs-RGD displayed a stronger immunostimulatory effect than the porphyrin YLG-1 (Fig. 13) used for comparison. Moreover, the combination of QDs-RDG PDT with CTA-4 checkpoint blockade significantly enhanced distant tumour inhibition compared to YLG-1 PDT/CTLA-4.

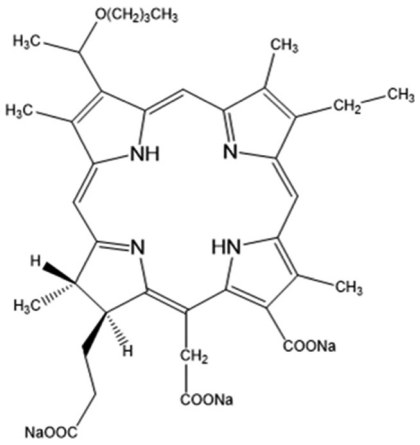

Fig. 13 Chemical structure of YLG-1.

Pancreatic cancer is characterized by severe hypoxia: when normal tissue typically contain 2–9% of O_2, the oxygenation in PDAC can be as low as 0.02%.[111] This hypoxia is a major concern for the efficacy of PDT, which depends on oxygen levels present within the irradiated zone for ROS production. Wang *et al.* proposed a solution using chemically inactive and nontoxic polyfluorocarbon, known to have a high affinity for oxygen.[112] They developed NPs based on such an amphiphilic oxygen carrying PF_{11}, loaded with the photodynamic agent $DiIC_{18}$ (DiD) and a chemo-immuno-modulary prodrug of gemcitabine (gemcitabine-thioketal-oleylamine, GTO). These NPs (PF11-DG) were compared to non-oxygen delivering poly(ε-caprolactone) *block*-poly(ethylene glycol) (PCL–PEG) NPs (PDG). Better cellular uptake, intratumoural incorporation and ROS production was found for the polyfluorinated NPs. Oxyhemoglobin saturation at 4 h after injection into 4T1 cells was better with the fluorinated NPs compared to PDG (10% *vs.* 1%) and the generated ROS enabled a more efficient thioketal cleavage to release gemcitabine (80% *vs.* 27%, for 5 min of illumination at 655 nm 2.0 W cm^{-2}). Moreover, light excitation in presence of PF_{11}-DG led to a clearly higher ICD response than free gemcitabine alone. During *in vivo* testing on 4T1 and Panc02 tumour mice model, preferential accumulation at tumour sites was observed potentially due to the small size of the NPs (30–50 nm) through the EPR effect. Mice treated with PF_{11}-DG and irradiation showed only a 1.48× tumour growth during the test, which translates to an inhibition of 94% compared to the blank group injected with PBS (Fig. 14).

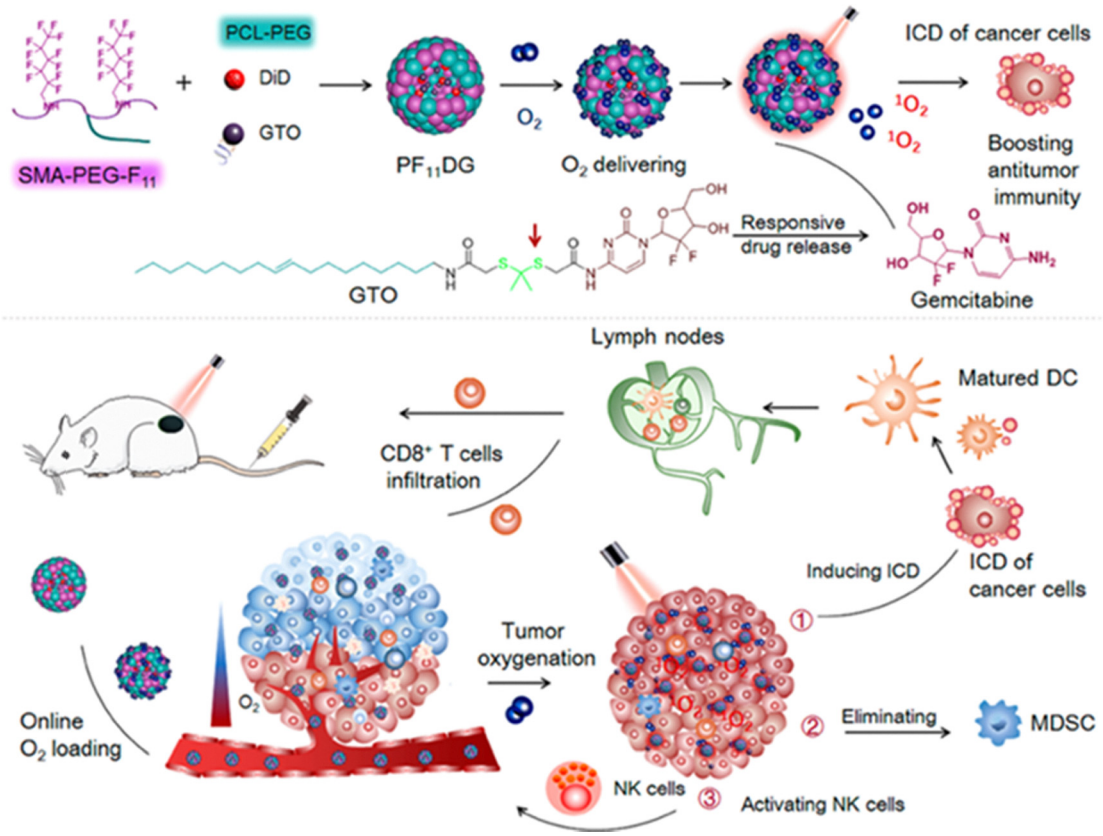

Fig. 14 Schematic illustration of NPs ($PF_{11}DG$) design and application on pancreatic cancer. Reproduced from ref. 112 with permission from American Chemical Society, copyright (2025).

In order to selectively target pancreatic cancer and induce an antitumour response by PDT, Sun *at al.* developed a NP with host–guest strategy by using hyaluronic acid polymer covalently grafted by β-cyclodextrin.[113] Two prodrugs elaborated by Adamantine conjugated with pyropheophorbide a (PPa) or with a JQ1 – a (bromodomain-containing protein 4 inhibitor (BRD4i)) respectively, were encapsulated into cyclodextrin. These supramolecular complexes (HCJSP) are able to selectively target CD44 highly expressed on the surface of pancreatic tumours. It was shown that PPa-mediated PDT improves the tumour immunogenicity through eliciting ICD cascade yet aggravation of hypoxia hampers the PDT efficacy. Meanwhile, JQ1 is able to regulate tumour glycolysis and immune evasion by inhibiting expression of c-Myc and PD-L1. Thus, tumour growth has been significantly inhibited and survival rate prolonged with HCJSP-mediated photoimmunotherapy. Moreover, association of HCJSP and laser treatment induced systemic immune response and sustained memory effect to prevent tumour recurrence and metastasis.

In 2021, De Silva *et al.* completed their study (*vide supra*) of triple-receptor-targeted photoimmuno-nanoconjugate (TR-PINs).[114] The increased potential for different binding to tumour cells was evaluated by the efficacy of PDT under red light and its associated immune-stimulatory effect. Using a complex heterogeneous 3D spheroid model containing pancreatic cancer celles and pancreatic associated fibroblast (PCAFs), they have shown that photodynamic priming (PDP), triggered during the photodynamic treatment, allowed not only uptake for nanoplatform but also induced a potent immunogenic cell death (ICD), as highlighted by the upregulation of Hsp60, Hsp70, CRT and HMGB1. ICD induced to induce immunogenic cell death by efficiently priming of CD4 + T and $CD8^+$ T cells through the upregulation of INFγ and degranulation marker CD107a. Thus, these activated T-cells recognize tumour cells and eliminate the remaining MIA PaCa-2 and PCAF cells in pancreatic cancer spheroids (Fig. 15).

One year after, the same group reported the study of systematic evaluation of PDT antibody-targeted PDT using cetuximab of a BPD *vs.* liposomal BPD (Visudyne) in 3D heterotypic coculture models of PDAC with different varying ratio of PDAFs.[115] The results showed that both liposomal BPD and PICs were effective in 3D spheroids with a low stromal content. However, when the stromal content increased above 50% in 3D spheroids, the efficacy of Visudyne-PDT was reduced by up to 10-fold, while PICs retained its efficacy. For example, PICs are 14-fold more phototoxic *versus* Visudyne, in spheroids with 90% PCAFs. This important difference of PDT treatment efficacy between Visudyne, the clinically approved PS formulation of BPD, and PICs, was attributed to the ability of PICs to penetrate more efficiently within stroma containing 3D spheroids and distribute more homogeneously.

Lim *et al.* described the feature of a human serum albumin (HAS)-coated zeolite imidazolate framework-8 (ZIF-8) containing

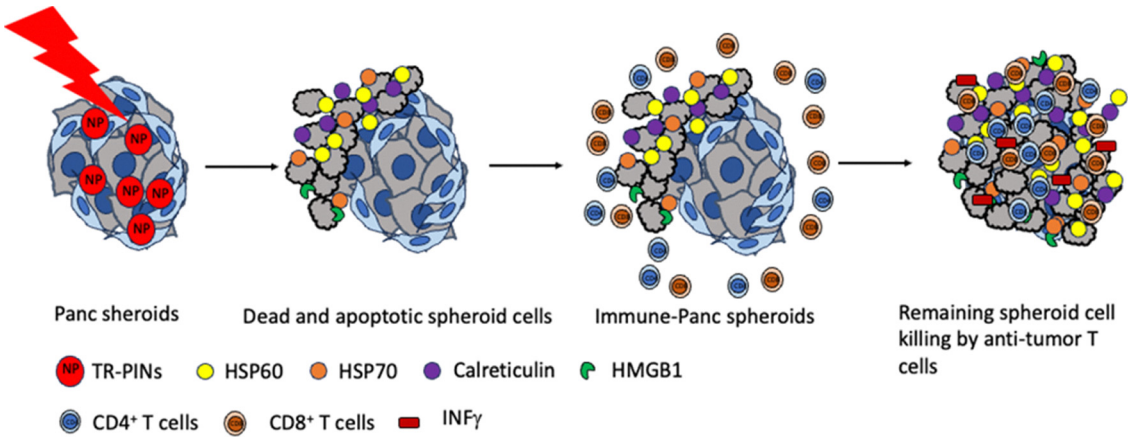

Fig. 15 Schematic concept of the study.[114]

Pheophorbide as a PS (called HPZ).[116] This complex is able after PDT treatment to optimize the effectiveness of the immune response. Under acidic conditions (microenvironment of tumours), NPs undergo a decomposition which led to rapid and simultaneous release of zinc ion and PS. *In vitro* evaluation on different cancer cell lines including PANC-1 showed uptake of HPZ and a synergic effect of higher concentration of Zn^{2+} and production of ROS underlight illumination.

Zhang *et al.* investigated the efficacy of two PSs (IR700DX-6T, IR700DX-mbc94) known to target the translocator protein (TSPO) and type 2 cannabinoid receptor (CB_2R), respectively, to investigate their PDT efficacy.[117] *In vitro* evaluation showed that after illumination (40 mW cm^{-2} for 10 min), the two PSs can inhibit the growth of pancreatic cancer cell lines (PANC-1, Panc-2, SW1990, Mia PaCa-2 and FC1245). When injected in C57BL/6 mice bearing Panc-2 cancer cell-derived xenografts, IR700DX-6T, and IR700DX-mbc94 suppressed tumour progression after illumination (50 mW cm^{-2} for 10 min). Moreover, IR700DX-6T, IR700DX-mbc94 mediated PDT significantly induced $CD8^+$ T cells, promoted maturation of dendritic cells and suppressed regulatory T cells, with a stronger effect exerted from IR700DX-6T-compared to IR700DX-mbc94. Note that the authors do not provide any information about the light sources and wavelengths used for *in vitro* and *in vivo* experiments.

Lum *et al.* described in 2020 the synthesis of IR700 (hydrophilic phthalocyanine) grafted with a humanized monoclonal antibody ARB102 which specifically binds cadherin-17, a surface marker overexpressed in gastrointestinal cancer. *In vitro* results showed that photoimmunotherapy (PIT) of gastrointestinal cancer cell lines (CDH17-positive) with IR700-ARB102 induced cell death after near-infrared illumination.[118] *In vivo* efficacy study was realized on a pancreatic adenocarcinoma AsPC-1 xenograft tumour model in nude mice. Fluorescence analysis showed that IR700-ARB102 accumulated preferentially in the tumour site. Moreover, after excitation with a laser at 680 nm, PIT significantly inhibited tumour growth (Fig. 16).

Jang *et al.* focused on exploiting tumour-derived exosomes (R-Exo) which were simultaneously used as both PSs delivery carriers and as immunostimulatory agents.[119] These R-Exo were loaded with Ce6 as a PS to form Ce6-R-Exo. *In vitro* results showed that exosomes are able to selectively target selectively MIA PaCa-2 pancreatic cancer cell lines. Ce6-R-exo can be visualized by photoacoustic imaging (7 ns pulsed laser, 700 nm) and can generate ROS inside tumour cells (671 nm, 100 mW cm^{-2} for 30 s). In addition, RAW264.7 macrophage was used to confirm whether exosomes elicit an immune response. Thus, a clear increase in TNF-α and IL-1β by macrophages was observed with R-Exo and this result indicated that

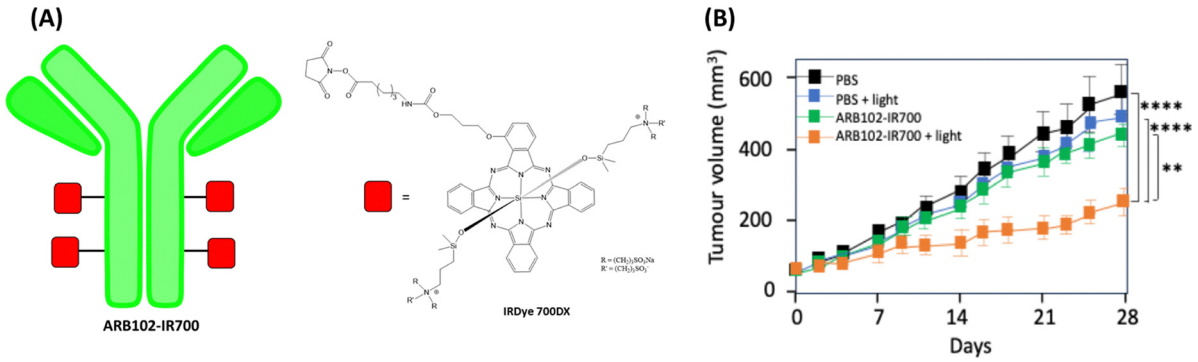

Fig. 16 (A) Chemical structure of antibody ARB102-IR700. (B) *In vivo* ARB102-IR700 PIT efficacy study in nude mice AsPC-1 xenograft models. Tumour size changes during *in vivo* PIT efficacy study.

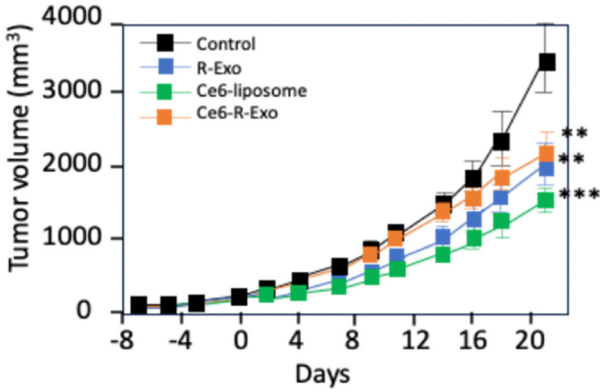

Fig. 17 *In vivo* therapeutic effect of Ce6-R-Exo upon light illumination on tumour volume in C57BL/6 N mice bearing B16F10 cell-derived xenografts.

R-exo could be used for immunotherapy (IMT). *In vivo* experiments of Ce6-R-Exo on C57BL/6 N mice bearing B16F10 cell-derived xenografts showed decreased tumour progression after laser excitation (200 mW for 1 min, 100 J cm^2). In addition, the combination of PDT and IMT (Ce6-R-Exo) achieves smaller tumour volumes than either therapy alone (Fig. 17).

Gurung *et al.* investigated the Ce6-PDT mediated antitumour abscopal effect. To this end, they used a bilateral subcutaneous melanoma (B16F10) and pancreatic tumour (Panc02) mouse model to test Ce6-PDT for the treatment of both local and distant tumours.[120] Results showed that after illumination (660 nm, 100 J cm^{-2} for 8 min 20 s), Ce6-PDT can induce potent local systemic antitumour immune response. Authors showed that the antitumour effect of PDT treatment inhibited the PD-1/PD-L1 interaction by increasing the proliferation and cytotoxic activity of $CD8^+$ T cells while decreasing CD39-expressing Treg cells in dose-dependent manner. These results showed that Ce6-PDT is a promising immunotherapy (IMT) and accelerated the abscopal antitumour effect.

Karimnia *et al.* investigated the photodegradation of non-cellular components of PDAC stroma (Photodynamic Stromal Depletion) (PSD).[121] To do so, they used *in vitro* heterocellular 3D co-culture models. They found that softening the ECM improved the transport of NPs. They showed more specifically that PSD improved delivery of NPs bearing an inhibitor of miR-21-5p, a PDAC microRNA. In parallel, PDT-induced photodestruction of stromal fibroblast was shown to further contribute to tumour suppression (Verteporfin, 690 nm, 100 mW cm^{-2}).

Chen *et al.* infected human pancreatic cancer MiaPaCa-2 cells with an oncolytic adenovirus system adv-MCK which are able to produce catalase (CAT), a single-gene encoded antioxidant enzyme.[122] CAT degraded H_2O_2 into water and produced oxygen at the same time. Thus, CAT reversed the hypoxic environment of tumours. *In vivo* experiment with human subcutaneous tumour model in Balb/C mice showed that adv-MCK reduced hypoxia by endogenous oxygen production, which is catalyzed by killerRed to generate $^1O_2$ and increase PDT efficacy. On the other hand, authors also showed that tumours treated by adv-MCK and light enhanced immune killing by increasing γδT-cell and neutrophil infiltration.

The details of all the studies published between 2020 and 2025 dealing with both active and passive targeted PDT to treat PDAC coupled to immunotherapy are collected in Table 5.

Chemotherapy. In PDAC, therapeutic strategies are highly stage-dependent. There is a growing interest in combining chemotherapy with PDT to enhance treatment efficacy, reduce drug-related toxicity, and potentially overcome tumour resistance mechanisms. For this purpose, co-delivery systems, such as NPs capable of encapsulating both PSs and anticancer agents, often offer enhanced tumour specificity, controlled drug release, and reduced systemic toxicity. The main preclinical studies of the PDT-chemotherapy combination in PDAC are summarized in Table 6.

Several preclinical studies have explored the synergistic potential of PDT when combined with standard-of-care chemotherapeutic agents. Notably, gemcitabine[126,129,136,140,145–147,150] and taxanes[133,137] have been the subject of such investigations. For instance, Pigula *et al.* reported that combining visudyne-based PDT (690 nm, 100 mW cm^{-2}, 50 J cm^{-2}) with nab-paclitaxel in MIA PaCa-2 and AsPC-1 orthotopic models led to effective local tumour control, reduction in metastases of up to 100% in early-stage models, and complete elimination of established metastases in 55% of late-stage models.[138] Similarly, Wu *et al.* engineered a nanoplatform based on disulfide-bonded paclitaxel prodrug co-loaded with gemcitabine and a porphyrin (5,10,15,20-tetrakis(4-hydroxyphenyl)21*H*-23*H* porphyrin or THPP) as a PS in DSPE-PEG micelles.[136] Upon 650 nm laser activation, this system induced potent cell death in PANC-1 cells and significantly inhibited tumour progression *in vivo*. Liu *et al.* developed nanocrystal with rare earth atoms containing protoporphyrin IX and folic acid and demonstrated that PDT with 980 nm laser (1 W cm^{-2}), even at subtherapeutic doses, could sensitize PANC-1 and pancreatic stellate cells to gemcitabine administered alone.[151] They also proved an enhancement of tumour growth inhibition from 28% in untreated recurrent tumours to 71% following PDT.

Additional studies have examined the integration of PDT with components of the FOLFIRINOX regimen.[132,142,144,148] A liposomal formulation encapsulating porphyrin–phospholipid and irinotecan demonstrated complete tumour regression in mice bearing MIA PaCa-2 xenografts or patient-derived low-passage tumour models after PDT (690 nm, 100 mW cm^{-2}, 75 J cm^{-2}), which closely recapitulate clinical PDAC features.[131] Oxaliplatin has also been evaluated *in vitro* on PANC-1 in 3D models in combination with verteporfin-based PDT (690 nm, 100 mW cm^{-2}). Since PDAC 3D nodules co-cultured with fibroblasts exhibit increased response to PDT relative to homotypic cultures, PDT appears to more effectively target ECM-invading and chemoresistant cancer cells.

Chemophototherapy strategies involving doxorubicin-loaded nanocarriers have also been developed and one of them is currently in a clinical trial (NCT05040213). Such a system, using long-circulating doxorubicin in porphyrin–phospholipid

Table 5 Reference, targeting method, PS used, light excitation conditions, *in vitro* and *in vivo* conditions for active and passive targeted PDT coupled to immunotherapy to treat PDAC

		Targeting method		PS			Biological tests – *in intro*, *in vivo*	
Ref.	Antibody or vector used	Type	Specificities	Nature	ROS produced	Light excitation conditions	Cell lines used	Animal model used
109	Folic acid	Active	Folic acid receptor	Porphyrin PS-FOL/PS2	$^1O_2$	637 nm 1 mW cm^{-2}, 1 h or 11 mW cm^{-2}, 2.5 h *in vivo*	Capan-1, Capan-2, MiapaCa-2, Panc-1	SCID mice
37	MDK Nbs	Active	Antibody NP	PCPDTTBTT	—	White light	HEK-293, Huh-1, HepG2, Hepa1-6, HuH-7, AsPC-1, Panc02	C57/B6 mice
110	Cetuximab	Active	EGFR	Polymer-conjugated CMPC containing ce6	—	671 nm 100 J cm^{-2}, 200 mW cm^{-2}	L-929, Capan-1, Panc-1, Aspc-1	KPC or AsPC-1 Nude mice BALB/c Capan-1, Aspc-1
113	JQ1	Active	CD44	NPs of HCJSP containing pyropheophorbide a (PPa)	—	671 nm	Panc02	C57BL/6 mice
115	Cetuximab	Active	EGFR	Visudyne liposomale PIC	—	690 nm, 150 mW cm^{-2}	MIA PaCa-2, PCAF	—
118	Antibody ARB102	Active	Cadherin-17 (CDH17 aka CA17)	IRdye 700DX	$^1O_2$	680 nm	SW480, AsPC-1	Female nude mice BALB/c
117	Antibody-TSPO	Active	TSPO	IR700DX-6T	—	40 mW cm^{-2}	Panc-1, Miapaca-2, FC1245, HPAF-II, SW1990, Panc-2	Female mice C57BL/6
	Antibody-CB_2R		CB_2R	IR700DX-mbc94				
119	Exosomes R-Exo	Active		Ce6-Loaded tumour-derived re-assembled exosome (Ce6-R-Exo)	—	671 nm 100 mW cm^{-2}	MIA-PaCa-2, HUVEC	BALB/c nude mice
121	pTP-TAMRA-ARAL	Active	OncomiRs (miR-21-5P)	Verteporfin-based NPs	—	690 nm 100 mW cm^{-2}	PANC-1, MRC5	—
120		Active	PD-L1.	Ce6	—	660 nm 100 J cm^{-2}	Panc02, B16F10	C57BL/6 male mice
122		Active	UTR	KillerRed (KR)	$^1O_2$	561 nm, 1.5 mW cm^{-2}	MIA PaCa-2, HEK293A, HT29, AGS, HepG2, B16-F10	Mice BALB/c
114	Trastuzumab, transferrine, cetuximab	Active	HER-2, TfR, EGFR,	TR-PINs benzoporphyrine (BPD-PC)	$^1O_2$	690 nm	MIA PaCa-2, PCAF	—
38	Peptide RDG	Active	Integrine $\alpha\nu\beta3$	Quantum dots (QDs)	$^1O_2$	650 nm *in vitro*: 20 J cm^{-2} *in vivo*: 100 mW cm^{-2}	Panc02	C57BL/6 mice
123	α-PD-L1 antibodie	Active	PD-L1	DBP encapsulated with iTPAL liposomes	$^1O_2$	690 nm, 40 J cm^{-2}, 25 mW cm^{-2}	CT1BA, MC38, BMFA3, LLC, AT84, ID8	Mice
124		Passive	EPR	NPs ZIF-8 containing HPZ	—	670 nm, 50 m cm^{-2}	MDA-MB-231, HCT 116, CT26,	Mice souris BALB/c
125		Passive	EPR	Membrane PS TBD-3C	—	White light 40 mW cm^{-2}	Panc02, KPC	Male mice C57BL/6
112		Passive	EPR	NPs $PF_{11}DG$ with DiD: DilC18(5): (1,1′-dioctadecyl-3,3,3′,3′-tetramethylindodicarbocyanine-5,5′-disulfonic acid)	$^1O_2$	655 nm, 2.0 W cm^{-2}	PANC02, 4T1	Female mice BALB/C Female mice C57 4T1 and PANC02

Table 6 Reference, targeting method, PS used, light excitation conditions, *in vitro* and *in vivo* conditions for PDT coupled to chemotherapy to treat PDAC

		Targeting method		PS			Biological tests – *in vitro*, *in vivo*	
Ref.	Chemotherapeutic agent	Type	Target	Nature	ROS produced	Light excitation conditions	Cell lines used	Animal model used
126	Gemcitabine (gem)	Both	EPR + SMAC N7 peptide,	Ce6: NPs of Ce6-*gem*-SMAC	—	660 nm, 20 mW cm^{-2}	PANC-1, 3T3-L1	Balb/c Female nude mice
127	Selumetinib (SEL) Dactolisib (BEZ235)	Active	Plectin-1 targeting peptide (PTP)	Zinc-phtalocyanine NPs Z/B-PLS (PTP peptide + low molecular weight heparin + SEL) + BEZ	—	671 nm, 90 J cm^{-2} 5 minutes	Panc-1	Nude mice
128	Chlorambucil	Active	DPP-QS Cleavage by Esterase	Diketopyrrolopyrrole (DPP)	$^1O_2$	Mia PaCa-2	Nude mice	
129	Gemcitabine	Active	UBI^{29-41} antimicrobial peptide targeting bacterias	Pyropheophorbide-a forms micelles (UPPM)	—	671 nm	Escherichia coli Nissle (EcN), Panc02	Balb/c nude mice
130	$NaYF_4$ doped with Yb^{3+} and Er^{3+} or Tm^{3+} NP $Zn_xMn_{1-x}S$ coated with a membrane derived from BxPC-3 (BUC@ZMS)	Passive		NP BUC@ZMS	$^1O_2$	100 mW cm^{-2} 980 nm, 1 W cm^{-2}	BxPC-3, 3T3, HUVECs	BALB/c nude mice
131	Irinotecan	Active	Vitamin D3 receptor (VDR)	Visudyne	$^{\bullet}OH$ —	690 nm, 100 mW	MIA-PaCa-2, AsPC-1, and MRC-5	Swiss nude Mice
132	Irinotecan, cetuximab	Active	EGFR-targeted (cetuximab)	Benzoporphyrin derivative (BDP): liposome containing irinotecan	—	75 J cm^{-2} 100 mW cm^{-2}	MIA PaCa-2 & PCAFs	Athymic Swiss Nude mice
133	Monomethyl auristatin E (MMAE)	Active	Caspase-3 cleavable peptide (KGDEVD)	Ce6: NPs of Ce6-MMAE	—	50 J cm^{-2} Visible light	KPC 960	Mice with KPC960 orthotopic model
134	Cabozantinib	Active	Recepteur MET (c-Met) (carbozantinib)	BDP: liposome containing BPD + cabozantinib	—	40 mW, 5 min 690 nm, 150 mW cm^{-2}	MRC5, AsPC-1	—
135	Cobalamin	Active	Transcobalamin receptors (TCblR)	Bodipy 650-cobalamin	—	650 nm	MIA PaCa-2 MIA PaCa-2	Athymic nude mice
52	Cetuximab	Active	EGF-receptor	BDP: multi-photoactivable inhibitor liposomes containing BDP and cetuximab	$^1O_2$ (5%)	6 MV X-ray photon radiation 690 nm 40 J cm^{-2}, 100 mW m^{-2} or 20 J cm^{-1}	MIA PaCa-2 and PCAF	Athymic Swiss Nude mice
136	Gemcitabine Paclitaxel	Passive	EPR	TPG NPs: DSPE-PEG containing THPP, PTX, Gem	—	650 nm, 0.4 W cm^{-2} 5 min	PANC-1, MCF-10A	Mice C57BL/6
137	Paclitaxel (PTX)	Passive	EPR	PCN-Fe(III)-PTX NPs	$^1O_2$	670 nm	PANC-1	Nude mice

Table 6 (*continued*)

		Targeting method		PS			Biological tests – *in vitro*, *in vivo*	
Ref.	Chemotherapeutic agent	Type	Target	Nature	ROS produced	Light excitation conditions	Cell lines used	Animal model used
138	Nab-paclitaxel (NabP)	Passive	EPR	Verteporfine	—	690 nm	—	Male nude mice suisses
	Gem					100 mW cm^{-2} 50 J cm^{-2}		
139	Simvastatine	Passive	EPR	YLG-1	—	650 nm	SW1990, Panc-1	Female nude mice BALB/c
						50 J cm^{-2}		
124	Dihydroartémisinine (DHA)	Passive	EPR	Lipid-supported manganese oxide nanozyme, MLP@DHA&Ce6	$^{\bullet}OH$ $^{1}O_2$	660 nm 25 mW cm^{-2}	BxPC-3	Nude mice BALB/c
140	Gemcitabine	Passive	EPR	Liquid crystal NPs (LCNP) containing Re(I) bisquinolinyl	—	630 nm	SW 1990, BxPC3, MRC5	—
141	Oxaliplatine	Passive	EPR	Verteporfine	—	690 nm 25 J cm^{-2}	PANC1	—
142	Irinotecan (IRI)	Passive	EPR	Liposomal formulation of irinotecan IRI-PoP containing porphyrin-phospholipid (PoP)	—	665 nm 200 mW cm^{-2}	MIA-PaCa2	Female nude mice
143	Doxorubicine (Dox)	Passive	EPR	Liposomes LC-Dox-PoP containing Porphyrin-phospholipid (PoP)	—	665 nm 150 mW cm^{-2} 800 mW	MIA PaCa-2	Female nude mice
144	Irinotecan, IRI	Passive		DBP conjugated with nanoliposomal PMIL	—	690 nm 25 J cm^{-2} 150 mW cm^{-2}	MIA PaCa-2, AsPC-1, pancreatic cancer associated fibroblasts	—
145	Gemcitabine	Passive		Hypericin combined with Gemcitabine	$^{1}O_2$	20 W/30 fluorescent tubes 3.15 mW cm^{-2}	Capan-2	—
146	Oxaliplatin gemcitabine	Passive		Verteporfin combined with gemcitabine or with oxaliplatin.	$^{1}O_2$	690 nm 5 J cm^{-2} to 20 J cm^{-2} 100 mW cm^{-2}	PSC, PANC-1, CFPAC-1, MRC5	—
147	Gemcitabine	Passive	EPR	NanoC60GEM: a NPs of [60]fullerene conjugated with gemcitabine	$^{1}O_2O^{\bullet-}{}_2$	440 nm 20 mW cm^{-2}	PANC-1, PAN02, A549, MCF-7, AsPc-1	—
148	Macrocyclic polyamine di(triazole-[12]aneN3)	Passive	EPR	1,1-Dicyano-2-phenyl-2-(4-diphenylamino) phenyl-ethylene	—	450 nm 20 mW cm^{-2} 30 min	BxPC-3 HeLa HUVECs	BALB/c nude mice
149	Olaparib	Passive	EPR	Ce6 encapsulation and self-assembly in a single potZIF-8@(Ce6 + Ola)	—	660 nm 300 mW cm^{-2}	Panc02	—

liposomes (LC-Dox-PoP), demonstrated improved outcomes with a dual-illumination protocol. A single administration of 3 mg kg^{-1} LC-Dox-PoP followed by 150 J cm^{-2} laser irradiation at 1 h and 50 J cm^{-2} at 8 hours post-injection, outperformed a single 200 J cm^{-2} dose at either time point in both MIA PaCa-2 and patient-derived subcutaneous PDAC models.[143]

Beyond conventional chemotherapeutics, the integration of PDT with targeted therapies and smart nanoplatforms has garnered increasing attention.[152] In particular, multifunctional nanocarriers that respond to tumour-specific stimuli such as pH changes or ROS have shown promise in preclinical models. Furthermore, the ubiquitous presence of KRAS mutations in PDAC has motivated the development of PDT-based combination strategies targeting KRAS-driven metabolic reprogramming and signalling.[134] Notably, Qiao *et al.* designed a ROS-responsive nanoplatform co-loading zinc phthalocyanine (ZnPc) as a PS and the dual PI3K/mTOR inhibitor BEZ235, co-loaded into PLS (Z/B-PLS NPs), while conjugating the MEK inhibitor selumetinib to low molecular weight heparin *via* a ROS-cleavable oxalate bond.[127] ZnPc-mediated PDT enhanced ROS generation and facilitated downstream KRAS pathway inhibition, creating a self-reinforcing therapeutic loop that led to complete tumour elimination *in vivo* (Fig. 18).

Liu *et al.* also developed an alternative nanoplatform, designing BUC@ZMS NPs composed of $NaYF_4$ doped with Yb^{3+} and Er^{3+} or Tm^{3+}, encapsulated within a semiconductor shell made of zinc and manganese sulfide $Zn_xMn_{1-x}S$ and coated with a BxPC-3 cell membrane.[130] These NPs are capable of absorbing NIR light and emitting UV/visible light *via* up-conversion mechanisms. The presence of the $Zn_xMn_{1-x}S$ shell enabled efficient ROS generation, resulting in significant anti-cancer effects in BxPC-3 cell models. In BxPC-3 tumour-bearing mice, these NPs selectively accumulated in tumour tissues and led to a significant reduction in tumour growth under NIR irradiation, without causing side effects or damage to healthy tissues.

Similarly, a liposome-based MnO_2 nanozyme loaded with dihydroartemisinine (DHA) and Ce6 (referred to as MLP@DHA&Ce6) demonstrated efficient $^1O_2$ and hydroxyl radical generation under illumination at 660 nm (25 mW cm^{-2}) in BxPC-3 cell.[124] Furthermore, this nanoformulation exhibited tumour-targeted accumulation in mice bearing subcutaneous BxPC-3 xenografts, resulting in nearly complete inhibition of tumour growth.

Other strategies have also explored the combination of PDT with chemical agents such as chlorambucil, a nitrogen mustard alkylating agent primarily used to treat hematologic malignancies. *In vivo* experiments demonstrated that the chlorambucil prodrug displayed tumour microenvironment-activatable properties and excellent therapeutic effects through synergistic chemo-PDT, achieving a complete inhibition of tumour growth in a subcutaneous MIA PaCa model.[153]

More surprisingly, Shen *et al.* studied simvastatin, a widely used statin for lowering cholesterol that has attracted interest in cancer research due to its potential anticancer properties beyond lipid regulation. They assessed the effect of low-dose YGL-1 PDT on PANC-1 tumours in combination with simvastatin (SIM) and observed reduced migration, invasion, metastasis and MMP-2/9 expression.[139] In the L-PDT group, liver metastases fused and occupied more than 50% of the liver surface. In contrast, in the L-PDT + SIM group, the liver metastases occupied less than 50% of the liver surface, with a significant reduction in number and size of both tumour cells compared to the L-PDT group (Fig. 19).

A 2022 study by Obaid and colleagues proposed a novel therapeutic approach using photoactivatable multi-inhibitor liposomes (TPMILs) targeting the EGFR.[52] These NPs formulation combines three treatment modalities: chemotherapy (irinotecan), phototherapy (PS BPD-PC) and molecular targeting (cetuximab). This combination enables precise and controlled release of the therapeutic payload, upon light exposure. An orthotopic desmoplastic was established using MIA PaCa-2 PDAC model co-implanted with patient-derived pancreatic cancer-associated fibroblasts (PCAFs) in Athymic male Swiss nu/nu mice. Light activation at 690 nm (40 J cm^{-2}) of TPMILs (IC_{50} = 3.5 ± 0.92 nM) was found to be 21 times more phototoxic than the non-targeted PMIL formulation (IC50 = 74 ± 25 nM). These results suggest that tumour growth could be reduced from 90% to just 8% of the equivalent human

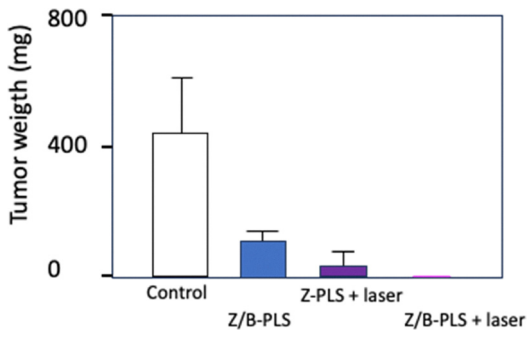

Fig. 18 Tumour weight after PDT (ZnPc 3 mg kg^{-1}, 671 nm, 90 J cm^{-2}, 5 min).

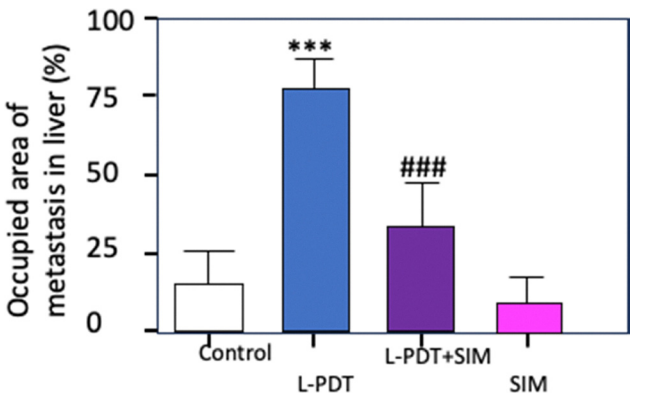

Fig. 19 Occupied area of liver pancreatic cancer metastases at 10 days post intrasplenic injection with or without SIM (n = 4). The results are expressed as the mean ± SD (n = 3–4). ***$P < 0.001$, *$P < 0.05$ *versus* the Con group; ###$P < 0.001$, ##$P < 0.01$ *versus* the L-PDT group; L-PDT: low-dose YLG-1-PDT, SIM: simvastatin.

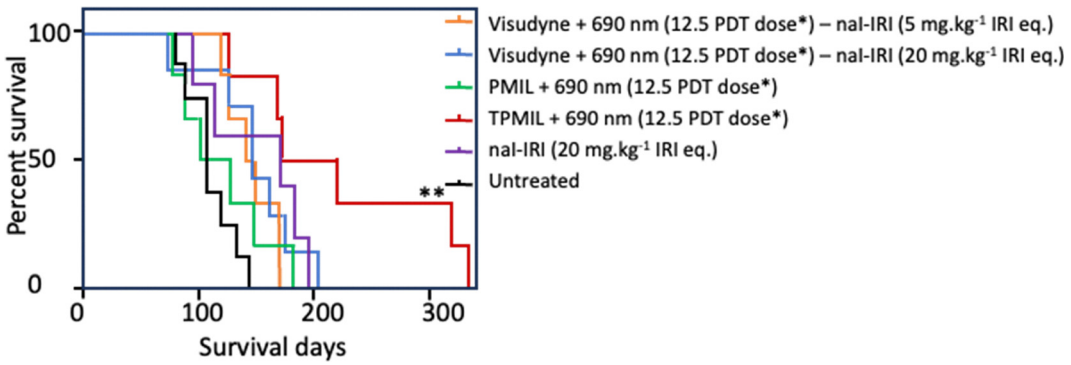

Fig. 20 690 nm-activated TPMIL constructs extended mice survival more than all other treatment groups (*PDT dose refers to the dose product of mg BPD eq kg^{-1} J cm^{-2}; n = 4–8; *$p \leq 0.05$,**$p \leq 0.005$).

liposomal irinotecan dose. Beyond cytotoxic effects, TPMILs were shown to degrade tumour collagen and decrease its density, thereby enhancing treatment penetration. Overall, a single EGFR-targeted TPMIL construct encapsulating a lipidated BPD and irinotecan chemotherapy, was capable of simultaneously controlling tumour growth (Fig. 20) alleviating desmoplasia, and doubling survival.

Lei *at al.* developed a zeolite imidazolate framework-8 (ZIF-8) with Ce6 and PARP inhibitor Olaparib (Ola), which is able to inhibit the DNA repair and genome maintenance.[149] *In vitro* evaluation realized with Panc02 pancreatic cancer cell lines showed high-level cellular uptake of ZIF-8 (FACS analysis) and good biosafety. NPs (ZIF-8)@(Ce6 + Ola) showed, after laser excitation (660 nm for 30 s, 300 mW cm^{-2}) a strong ROS production facility. Finally, the Panc02 apoptosis rate was significantly increased compared with ZIF-8@Ce6 and ZIF-8@(Ce6 + Ola). Thus, the expression of cleaved caspase-3 with ZIF-8@(Ce6 + Ola) was significantly higher than other groups. These results demonstrated that combining PARP inhibitor (Ola) with PDT *via* ZIF-8 decreased DNA damage repair and enhanced the efficacy of PDT.

These findings underscore the emerging role of PDT as a potent adjunct to chemotherapy in PDAC. Although clinical validation is still needed, combining PDT with standard or targeted chemotherapies holds great promise for improving therapeutic outcomes in this notoriously treatment-resistant malignancy.

Photothermal therapy (PTT). Combination of PDT and PTT is also an interesting strategy to improve the efficacy due to the synergistic effect and the limited side effects. PTT generates hyperthermia upon light illumination of a photothermal agent, leading to an overexpression of heat shock protein (HSPs) by cancer cells to fight thermal damage. This often leads to an insufficient killing of deep tumours. However, the hyperthermia generated by PTT can improve blood flow, thereby increasing the concentration of oxygen in tumour tissue. As discussed earlier, PDT efficacy is limited by hypoxia. Therefore, PTT could improve the effectiveness of PDT, which in turn damages the heat-resistant cells in PTT.

These strategies target three levels:

Vascular level: PTT can improve tumour oxygenation, boosting PDT effectiveness.[154] However, PTT may also exacerbate PDT-induced vascular damage, which can be exploited to increase NPs accumulation for enhanced treatment.[155]

Extracellular matrix (ECM) level: PDT and PTT affect ECM, altering tissue architecture and tumour perfusion. Combination therapies can improve drug delivery and counter desmoplasia, a key feature of tumours.[156]

Cellular level: PTT increases mitochondrial ROS, sensitizing cells to PDT, while PDT enhances sensitivity to heat *e.g.* by affecting heat-shock proteins. Both therapies can trigger immune responses, though the interaction between PDT, PTT, and immunotherapy requires further study.[157]

In conclusion, PDT and PTT combination is likely to induce synergistic effects at multiple levels, but optimal treatment conditions for maximum efficacy still need to be identified.

Jin *et al.* describe the elaboration of magnetic copper-doped iron oxide NP coated with transferrin and tLyp-1, a tumour homing peptide binding to p32 receptor as well as Fe^{3+} and IR820, an organic photothermal agent.[158] This is a triple-augmented synergy combining ferroptosis, PTT and PDT. After incorporation into BxPC-3 cells, the NPs degrade, leading to the release of Cu^{2+}, Fe^{2+}, Fe^{3+} and IR820. The metal ions trigger ferroptosis, while the dye IR820 has PDT and PTT properties, thereby favouring ferroptosis. After light illumination (1 W cm^{-2} for 5 min) the temperature of the NP increased to 48.7 °C and temperature of free IR820 to 37 °C. Moreover, higher $^1O_2$ amount was detected for the NP compared to free IR820. *In vivo* experiments on BALB/c nude mice bearing BxPC-3 tumour bearing BALB/c nude mice were performed (4.0 mg kg^{-1} IR820, 808 nm illumination 1.0 W cm^{-2}, 10 min after 24 h injection). IR820 and light led to 61% inhibition of the tumour growth, 85% for NP without IR820 and 93% for the NP after 20 days, showing the interest of synergistic triple-augmented PTT/PDT and ferroptosis (Fig. 21).

Li *et al.* developed a molecule DCTBT encapsulated in a liposome coupled to a peptide GE11 targeted EGF receptor (EGFR) (Fig. 22).[159]

CTBT was chemically modified in order to amplify its AIE properties and to improve its photophysical properties as well as type-I ROS generation and photothermal conversion upon illumination. *In vivo* experiments were performed on PANC-1 tumour (10 mg kg^{-1}, 808 nm, 0.8 W cm^{-2} for 5 min). The

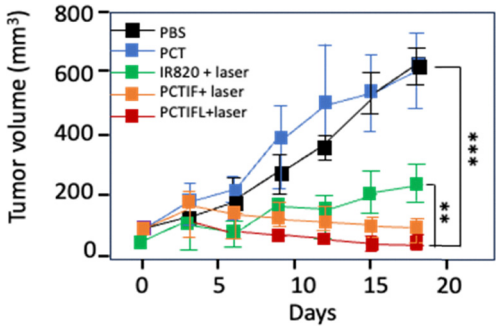

Fig. 21 Curves of tumour volume change for different NPs treated mice including PBS, PCT, free IR820, PCTIF and PCTIFL in presence/absence of 808 nm laser illumination.

temperature increased from 33 to 60 °C within 1 min. For *in vivo* tumour growth inhibition studies, 2 mg kg^{-1} were used. Tumour inhibition rate was 88% for targeted NPs compared to 73% for non-targeted NP. Targeted NP triggered the most severe necrosis or apoptosis and allowed the suppression of cancer cell proliferation.

Tao *et al.* described the development of a NP containing Brusatol, MnO_2, Ce6 as a PS and poly(ethylene glycol)-folate-modified polydopamine brusatol/silica@MnO_2/Ce6@PDA–PEG–FA (BSMCPF).[160] Brusatol is a nuclear factor erythroid 2-related factor (Nrf2 inhibitor), a regulator of redox homeostasis and MnO_2 an oxygen generator. In acidic TME due to H^+, MnO_2 collapses H_2O_2 and GSH triggers the release of Ce6, brusatol and generation of O_2. With additional O_2, ROS production will increase during PDT but Brusatol downregulates the expression of Nrf2 and avoids the activation of defence mechanisms. *In vitro* experiments were done on MIA PaCa-2 cells, with two types of illumination 660 nm (500 mW cm^{-2}) for PDT and 808 nm (1.5 W cm^{-2}) for PTT. PDT and PTT led to better efficiency than PDT or PTT alone and further increased in the presence of MnO_2. *In vivo* phototherapeutic activity of the NP was evaluated in mice bearing MIA PaCa-2 tumours. After light illumination, the temperature in the BSMCPF group increased to 52 °C in 10 min. The tumour inhibition was 87% for BSMCPF higher than BSCPF (NP without MnO_2) (53%) and SMCPF (NP without brusatol) (64%). They demonstrated that BSMCPF induced tumour cell death *via* ferroptosis through Fenton reaction $Fe^{2+} + H_2O_2 \rightarrow Fe^{3+} + OH^- + OH^\circ$.

The details of the publications dealing with PDT and chemotherapy are provided in Table 7.

X-Ray and ionizing radiations. Reaching deep seated tumours, such as PDAC, remains a significant challenge for PDT due to the limited tissue penetration of light to efficiently excite common PSs. Nearly two decades ago, Chen and Zhang introduced the concept of X-ray-induced photodynamic therapy (X-PDT), a strategy designed to overcome this limitation by activating PDT using X-ray irradiation.[162] However, as most conventional PSs exhibit low X-ray absorption cross-sections, a direct excitation using X-rays is rather inefficient. To address this, the X-PDT approach employs nanotransducers that convert high-energy X-ray photons into visible light within the tumour microenvironment, thereby enabling local activation of nearby PSs. These nanotransducers, also known as nanoscintillators, are engineered to emit intense luminescence upon X-ray irradiation, with emission spectra that overlap the absorption spectrum of the selected PS. While such spectral overlap is essential for energy transfer, it is not sufficient on its own to guarantee efficient PS activation and effective X-PDT. A growing number of experimental proof-of-concept studies have demonstrated promising results – showing significant tumour growth inhibition in various subcutaneous *in vivo* cancer models, as summarized in many reviews including.[146,163–167]

However, many key parameters underlying the optimal design of nanoscintillator/PS conjugates remain poorly understood. Likewise, the underlying mechanisms of action are still only superficially characterized, highlighting the need for deeper mechanistic insights and systematic optimization.

Recently, a novel therapeutic approach known as Cerenkov-induced PDT (CR-PDT) has been proposed.[168,169] This method leverages Cerenkov radiation—a luminescent signal emitted by charged particles coming from radionuclides decay. For Cerenkov radiation to occur, two conditions must be met: the medium must be dielectric, and the charged particle must move faster than the phase velocity of light in that medium. Under these conditions, Cerenkov photons are emitted along

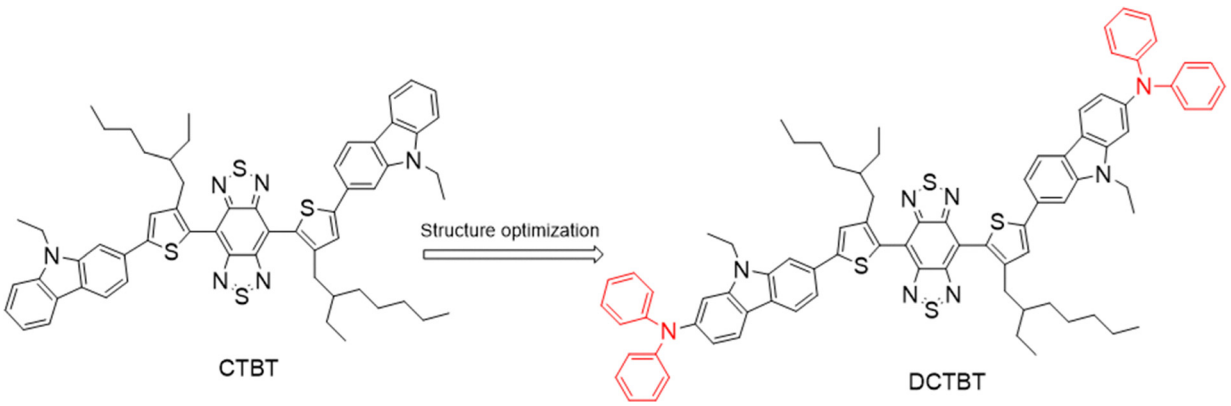

Fig. 22 Chemical structure of CTBT and DCTBT.

Table 7 Reference, targeting method, PS used, light excitation conditions, *in vitro* and *in vivo* conditions for PDT and chemotherapy to treat PDAC

Ref.	PTT responsive material	Targeting method		PS		Light excitation conditions	Biological tests – *in vitro*, *in vivo*	
		Type	Specificities	Nature	ROS produced		Cell lines used	Animal model used
158	IR820	Active	Transferrin receptor (TfR) Receptor p32	NPs PMA/CuIO-Tf@IR820/ Fe^{3+}-LyP-1	—	808 nm 1.0 W cm^{-2}	BxPC-3	BALB/c female nude mice
159	NP-DCTBT	Active	EGFR	Liposomes loaded with DCTBT conjugated with an EGFR-targeting peptide NP lip-DCTBT	Type I	808 nm 0.8 W cm^{-2} 5 min	PANC-1	Mice
160	PDA	Active	Folate receptors	Silica NP encapsulating brusatol coated with MnO_2, ce6 and PEG-FA	$^{\bullet}OH$	808 nm, 1.5 W cm^{-2}	Mia-PaCa-2	Male nude mice
					$^1O_2$	660 nm 500 mW cm^{-2}		
161	SNAP	Passive	ip-DTI/NO	DIBT	Type-I $O_2^{\bullet-}$ $ONOO^-$	808 nm 0.8 W cm^{-1} 5 min	PANC-1 NIH3T3	BALB/c nude mice PANC-1/ NIH3

the particle's path, producing constructive interference during repeated cycles of medium polarization and depolarization.

Ran *et al.* were the first to introduce CR-PDT, suggesting that its therapeutic efficacy results from the combined radiotherapeutic and phototherapeutic effects. The latter involves light-mediated activation of PSs.[170] However, the production of $^1O_2$ is significantly limited in CR-PDT, as the quantity of Cerenkov photons absorbed by the PS is insufficient. Adding a NP such as those developed for X-PDT which embed nanoscintillators greatly improved the $^1O_2$ production.[171]

To date, only a few original studies have detailed the use of CR-PDT *in vitro* and *in vivo*.[172,173] These studies collectively show that cancer cell death is enhanced when β-emitting radionuclides and PS are used together. The observed effects depend on the amount of radioactivity delivered to tumour cells, the PS concentration, and the extent of Cerenkov radiation absorption which is improved with higher PS uptake.[174] Notably, when PS and radionuclides are closely co-localized, therapeutic efficacy improves significantly. The PDT effect also appears to vary by cell line, influenced by differences in radionuclide accumulation and particle kinetic energy.[175] Additionally, cell lines show variable sensitivity to ionizing radiation and Cerenkov light, which may modulate the overall cytotoxic impact of CR-PDT. Nonetheless, the therapeutic potential of this strategy has been demonstrated *in vivo*, where it has reduced tumour growth in xenograft models and decreased levels of circulating tumour cells.[172]

Although such techniques overcome the light depth penetration issue, it has not yet been investigated for pancreatic tumour. Probably because external radiotherapy itself is still not completely validated in the clinical routine. Indeed, post-operative radiotherapy combined with chemotherapy appears to be justified in patients with resected pancreatic cancer exhibiting pT3 and pN+ mutations. However, in patients with hardly resectable pancreatic cancer, the role of radiotherapy remains to be clarified.[176]

In the period 2020–2025 only one publication deals with targeted PS to treat pancreas cancer cells with X-PDT.[177] Clement *et al.* developed poly(lactic-*co*-glycolic acid) NPs (PLGA NPs) with an average diameter of 85 ± 12 nm in which they encapsulated Verteporfin (VP) on which they grafted cell-penetrating HIV *trans*-activator of transcription (TAT) peptide. The uptake of PLGA–VP–TAT NPs was two times better than the uptake of PLGA–VP in human pancreatic cancer (PANC-1) cells. In the absence of X-ray irradiation, cell viability was around 90% for PLGA–VP–TAT NPs and > 95% for PLGA–VP NPs and PLGA NPs without VP. After X-ray irradiation (at 4 Gy, clinical 6 MV LINAC at the Genesis Cancer Care, Macquarie Hospital, Sydney, Australia) the cell viability was reduced to 75 ± 8% (p = 0.02) with PLGA–VP NPs and 62 ± 5% (p = 0.007) for PLGA–VP–

Table 8 Reference, targeting method, PS used, light excitation conditions, *in vitro* and *in vivo* conditions for PDTX to treat PDAC

Ref.	X-Ray excitation source	Targeting method		PS		X-ray irradiation conditions	Biological tests – *in vitro*, *in vivo*	
		Type	Specificities	Nature	ROS produced (QY)		Cell lines used	Animal model used
177	LINAC clinique de 6 MV	Active	Importin α and β receptors (karyopherin)	PLGA-VP-TAT (NP, VertéporfinP, and the TAT peptide)	$^1O_2$	4 Gy X-rays	PANC-1	—

TAT NPs. Using Green Fluorescent $^1O_2$ Sensor (SOSG), they could prove the formation of $^1O_2$ upon X-ray irradiation. Details are given in Table 8.

Sonodynamic therapy. In recent years, sonodynamic therapy (SDT) has emerged as a promising alternative to PDT, particularly for targeting deeply located tumours situated several centimeters beneath the skin, in anatomical regions where light penetration is limited or would necessitate invasive delivery techniques. The use of focused ultrasound (FUS) enables the concentration of ultrasonic energy within a focal zone only a few millimeters in diameter, thereby allowing precise activation of sensitizers in deep anatomical structures. This characteristic makes SDT particularly suitable for the complex treatment of tumours located in the brain[178] or in the pancreas.[179] SDT enables highly precise targeting under the guidance of magnetic resonance imaging (MRI) or ultrasound imaging, while being non-invasive and associated with minimal adverse effects.

Although the exact mechanisms of SDT remain incompletely understood, cavitation is widely recognized as a central contributor. Upon ultrasound excitation, bubbles form within tissues and can undergo oscillation, growth, and eventual collapse. At low ultrasound intensities, stable cavitation occurs, characterized by the regular oscillation of bubbles and the generation of microstreaming in the surrounding fluid. In contrast, higher intensities induce inertial cavitation, marked by rapid bubble expansion followed by violent collapse, producing shear forces and shock waves capable of mechanically damaging tumour cells.[180] It has been demonstrated that cavitation induces the generation of large quantities of ROS.[181] During bubble collapse, the release of substantial energy results in a brief emission of light,[182] known as sonoluminescence. This light can activate sensitizers, triggering the production of ROS.[183] *In vivo* studies using low-frequency ultrasound provide evidence supporting the involvement of sonoluminescence in SDT,[184] and underscore the potential of many photosensitisers to also act as effective sonosensitizers. Additionally, the administration of exogenous microbubbles has been shown to further enhance the therapeutic efficacy of SDT. For instance, the combination of oxygen-loaded microbubbles with SDT and 5-fluorouracil has shown promising results in pancreatic cancer models.[185] SDT is currently under clinical investigation for the treatment of diffuse intrinsic pontine glioma, glioblastoma, and tumours of the biliary tract.

In the period 2020–2025, a few publications were related to SDT for PDAC but none of them with PS or NP coupled to targeting units (Table 9).

The details of the publications dealing with PDT and ultrasound are given in Table 9.

Further combinations of therapies and perspectives. As explained previously, combination of PDT and PTT improve the treatment efficiency due to a potential synergistic effect.[23,189] It has also been reported that PTT and PDT elicit a systemic antitumour immune response *via* tumour-associated antigens (TAAs) from disrupted cancer cells that accompany the release of danger-associated molecular patterns (DAMPs).[190]

Table 9 Reference, targeting method, PS used, light excitation conditions, *in vitro* and *in vivo* conditions for SDT to treat PDAC

		Targeting method		PS		Irradiation conditions		Biological tests – *In vitro*, *In Vivo*	
Ref.	US responsive material	Type	Specificities	Nature	ROS produced	Light	US	Cell lines used	Animal model used
186	SONOPORE KTAC-4000	Passive	EPR	PPIX micelles (PPM) in perfluoropentane (PFP)-doped oxygen microbubbles (OPMBs)	Increase of 22% to 50% in oxygen	Xenon lamp 600–700 nm 5 min 40 mW cm^{-2}	1.03 MHz, 25% duty cycle, 0.7 W cm^{-2}	MDA-MB-231	Balb/c and C57BL/6 nude mice
187	Sonidel SP100	Passive	EPR	Rose Bengal, in oxygen microbubble		—	1 MHz, 30% duty cycle, 100 Hz pulse repetition frequency at 3.5 W cm^{-2} (about 880 kPa peak negative pressure)	PSN-1, BxPC-3	Mice
188	Mettler Sonicator 740	Passive	EPR	Tablet-like TiO_2/C nanocomposite with a metal–organic-framework-derived carbon structure	Type I and II	—	1 MHz, 0.5 W cm^{-2}	Panc02	BALB/c female nude mice

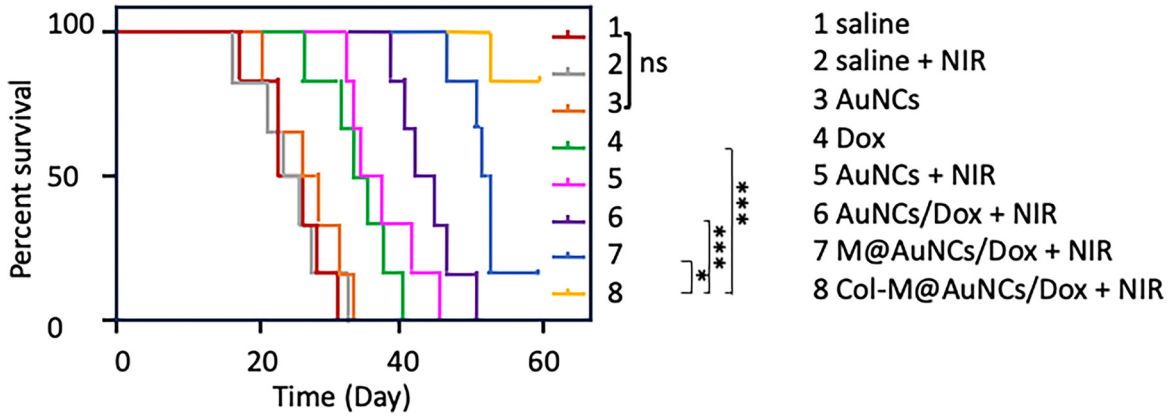

Fig. 23 Survival rate of mice bearing BxPC-3 tumour bearing mice after receiving different treatments (n = 6/group).

The increase of temperature can also lead to immunologic tumour cell death. This is why the combination of PDT, PTT and checkpoint inhibition with an anti-PD-1 antibody is a new strategy to reverse hypoxia by changing the microenvironment. It is also possible to couple these methods with chemotherapy, in which potent cytotoxic drugs are used to disrupt the way cancer cells grow and proliferate.[152]

Yang *et al.* designed a gold NP with a collagenase-functionalized biomimetic drug to degrade the matrix barrier and treat PDAC through PTT, PDT and chemotherapy.[191] Indeed, in PDAC, there is an excessive ECM deposition that impedes the diffusion of molecules or NPs into the tumour. Therefore, a nanosystem consisting of gold NPs with Doxorobucin (Dox) encapsulated, coated with PDAC tumour cell membrane and functionalized with collagenase (Col-M@AuNP/Dox) was synthesized. In solution after 10 min illumination at 808 nm (1 W cm^{-2}) a solution of PBS increased by only 2 °C whereas the gold NPs reached a temperature of 50 °C due to the PTT effect. Moreover, ROS were produced due to the PDT effect. *In vitro* studies were performed on the BxPC-3 cell line. Light illumination induced the release of dox that could enter the nucleus. To check the degradation of ECM, they elaborated a multicellular tumour spheroid (MTS) and showed that Col-M@AuNP/Dox were able to degrade collagen, the MST decreased and disappeared after several days. In BxPC-3 tumour bearing mice, it was observed that Col-M@AuNP/Dox penetrated 3.3 times deeper than M@AuNP/Dox without collagenase. At 24 h post-injection (10 mg kg^{-1}) after 808 nm illumination (1 W cm^{-2}), Dox was released in a controlled manner, and Col-M@AuNP/Dox induced a strong tumour inhibition effect (Fig. 23).

Li *et al.*[192] combined PDT/PTT with immunotherapy. Ferritin NPs were designed to load biliverdin (BV), a green pyrrolic compound formed during haem catabolism that has shown promise in PDT and PTT, and econazole (E), a known antifungal and anticancer drug (Fig. 24).

These Ferritin NP improved the water solubility and half-life of econazole. *In vitro* experiments were performed in human PANC-1 and MIA PaCa-2 cells as well as in mouse Panc02. Ferritin NPs efficiently co-deliver BV and econazole into cancer cells. Cells viability decreased with 808 nm light excitation around 20% with 0.1 mg mL^{-1} of BV. It was proven that Ferritin NPs produce ROS leading to apoptosis and autophagic cell death. *In vivo* experiments were done in mice bearing PANC-1 xenograft tumour, as well as in a syngeneic model Panc02 implanted in C57BL/6 mice (NOD.CB17-Prkdcscid/NcrC). The temperature of the tumour region reached nearly 56 °C and a remarkable growth inhibition (98%) was observed after PTT (2 mg kg^{-1} BV, 6 h incubation, 808 nm, 1 W cm^{-2} for 5 min). Moreover, intracellular econazole increased the expression of PD-L1 thereby improving the immune response rate. The synergy effects of PDT/PTT and PD-L1 checkpoint blockade

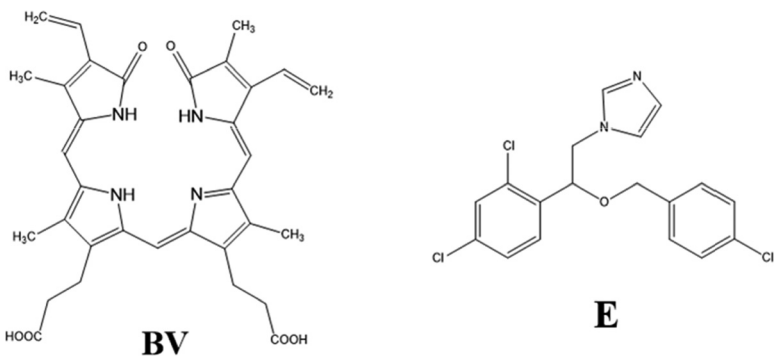

Fig. 24 Chemical structure of biliverdin (BV) and econazole (E).

Table 10 Reference, targeting method, PS used, light excitation conditions, *in vitro* and *in vivo* conditions for PDT and other therapy to treat PDAC

Ref.	Other therapy	Targeting method		PS		Light excitation conditions	Biological tests – *in vitro*, *vivo*	
		Type	Specificities	Nature	ROS produced (QY)		Cell lines used	Animal model used
192	MW-GX-808	Both	PD1	NPs FBE NPs (biliverdin)	$^{\bullet}OH$	808 nm, 1 W cm^{-2}	PANC-1, MIA-PACA-2, Pan02	Male nude mice BALB/c
	Econazole Antibodi α-PD-L1			NPs α-PDL1/FBE				
191	Doxorubicine	Active	BxPC3 cell membranes	NPs Col-M@AuNCs/Dox	$^1O_2$	808 nm, 1 W cm^{-2}	BxPC3, H22, B16, 4T1, THP-1	Female nude mice BALB/c and mice BALB/c
193	Doxorubicine	Passive	EPR	NPs of PSPP-Au_{980}-D containing phtalocyanine (SiPc)	$^1O_2$	980 nm, 1 W cm^{-2}, 680 nm	MIA PaCa-2	Mice

allow direct killing effects and immunotherapy to stop tumour growth.

The details of the publications dealing with PDT and other therapies are given in Table 10.

In the search for innovative strategies to overcome the limited penetration of visible light in tissues, several approaches have emerged that rely on secondary photon generation, including X-PDT, CR-PDT and SDT.

Proofs of concept have been established for each modality; however, their underlying mechanisms remain only partially understood. For example, it is still debated whether SDT relies primarily on sonoluminescence to locally excite the PS or whether its therapeutic effect arises mainly from ROS generated during acoustic cavitation. Similarly, X-PDT seems to not only rely on scintillation-photon to activate the PS, but additional mechanisms seem to be at play.[166] If we consider the hypothesis that X-PDT, CR-PDT and SDT act by locally producing light capable of exciting a PS and thus triggering PDT, then each approach exhibits advantages and limitations. Therefore, they appear as complementary and could be selected according to the specific situation.

Unlike CR-PDT, both X-PDT and SDT largely preserve the spatial selectivity that characterizes conventional PDT. Nanoscintillators used in X-PDT and sonosensitizers used in SDT are intrinsically non-toxic unless activated by X-rays or ultrasound, respectively. Because these physical stimuli—especially ultrasound—can be specifically focused on the tumor, the resulting cytotoxicity would be restricted to the tumor volume. In contrast, CR-PDT lacks this selectivity. Indeed, Cerenkov emission is produced wherever the radiopharmaceutical is, making the therapy's spatial profile dependent on the radioisotope's biodistribution rather than on externally applied energy. As a result, minimizing off-target toxicity—especially in clearance organs such as the kidneys and liver—requires highly precise control over radiotracer uptake and elimination. Penetration depth further differentiates these modalities. Although megavoltage X-rays used in clinical radiotherapy have essentially no limitation in tissue penetration, the photon energies most efficient for X-PDT fall in the orthovoltage range.[166] Unfortunately, orthovoltage beams penetrate tissues less effectively and can deposit clinically significant doses in bones or intervening organs when targeting deep-seated tumors. Brachytherapy may offer a solution by locally delivering X-rays of appropriate energy, but standard external-beam radiotherapy regimens---including those used for PDAC—operate with megavoltage irradiators, implying that adjustments or dedicated setups would be required for X-PDT implementation.

CR-PDT, by contrast, inherently bypasses the penetration limitation because Cerenkov light is generated directly at the site of radiopharmaceutical accumulation. If this local density is sufficiently tumor-specific, tissue depth ceases to be problematic. SDT occupies a different position: ultrasound penetration depends strongly on frequency, with lower frequencies achieving clinically relevant depths. For deep tumors such as PDAC, appropriate frequency selection, intensity and focusing strategies could, in principle, enable effective SDT, with combined sonophysical (*e.g.* permeabilisation, temperature increase) and sonoluminescent effects, though practical constraints and dosimetric considerations require further clarification.

Overall, these approaches present complementary advantages and constraints. A deeper mechanistic understanding, alongside optimized delivery strategies, is needed to determine the clinical contexts in which each modality may be most beneficial.

Photodiagnostic and development of specific light devices

Low light penetration can be a problem to treat tumours. A recent review discussed light technology for an efficient and effective PDT.[194] However, delivering light to the pancreas *via* extra-corporeal sources remains a significant yet to be overcome. Using interstitial PDT is one of the solutions, as described by Shafirstein *et al.*[195] More recently, alternative new devices have been developed.

Li *et al.* developed a novel soft robot laparoscope that can perform linear translation, in-plane bending, and axial rotation.[196] A micro camera is integrated in order to do image guidance. Calibration-based kinematics are developed to obtain robot kinematics. Differential kinematics and estimated task location are obtained on the basis of generalized forward kinematics modelling. The proposed modelling methods were

validated *in silico* by numerical simulations and *in vivo* in two mice models. The results are promising, the tumour size decreased from 15.3 and 11.8 mm^3 to 12.1 and 4.4 mm^3, respectively.

Yu *et al.* developed a dual-diffusing optical fiber probe (DDOFP), capable of uniformly illuminating the anatomical structure of the pancreatic duct for PDT in clinical settings.[197] This is the smallest clinically available optical fiber and it is officially approved by the Korea Food and Drug Administration (item approval number: 17–516).

Pogue's team studied the possibility to use UV light excitation of fresh tumour tissue of PDAC to visualize and quantify desmoplasia, in an orthotopic xenograft mouse model.[198] 2 of the 5 mice were injected with 0.5 mg kg^{-1} of Visudyne and were illuminated at 690 nm (75 J cm^{-2}, 100 mW cm^{-2}). Collagen deposition was successfully visualized in PDAC tumours and a decrease of 13% was observed. This approach also allowed to detect necrosis and perfusion.

The same team developed in 2020 a method to visualize hypoxia.[199] The idea was to use the delayed fluorescence of PPIX that is sensitive to the concentration of O_2. If the fluorescence of PPIX is around 10–16 ns, the delayed fluorescence is typically in the μs–ms. ALA was applied topically thanks to Ameluz cream or was injected in athymic nude mice implanted with BxPC3 human pancreatic tumour cells. PPIX was excited with a 635 nm light (0.25–1 mW, 0.3–1.2 mW cm^{-2}). It was shown that the developed approach could successfully image PPIX-PDT-induced hypoxia in skin as well as pre-existing hypoxia. Oxygen depletion depends on fluence rates. No depletion was found at 1.2 mW cm^{-2} while higher fluence rate (>6 mW cm^{-2}) caused fast oxygen depletion. Oxygen recovery was faster after small radiant exposure (several minutes for 2 J cm^{-2}) and longer (tens of minutes) after high radiant exposure (5 J cm^{-2}). The main advantage is that the oxygen sensitive probe is the PS itself.

Fiber-based therapeutic strategies for photodynamic therapy of pancreatic cancer

Routes for fiber insertion and clinical techniques. Three main access strategies are used for pancreatic PDT; fiber design and procedural workflow differ between them.

• Endoscopic ultrasound (EUS)–guided interstitial PDT (EUS–PDT)

EUS allows real-time ultrasound visualization and transgastric/transduodenal insertion of a small-diameter optical fiber through a standard 19G needle into pancreatic lesions. Pioneering clinical work (dose-escalation, phase I) demonstrated feasibility and measurable CT-defined necrosis in a proportion of patients with locally advanced pancreatic cancer (LAPC). EUS-PDT is currently the principal minimally invasive route in clinical investigation because of its ability to target tumors adjacent to the stomach/duodenum under ultrasound guidance.[200]

• Percutaneous image-guided interstitial PDT

CT- or ultrasound-guided percutaneous placement of interstitial fibers (through the abdominal wall) has been used in early clinical series and preclinical models. Percutaneous approaches are useful for lesions away from the GI lumen but must account for potential intervening bowel, major vessels, and respiratory motion. Bown and colleagues reported one of the early clinical series using percutaneous/interstitial PDT in PDAC with acceptable results.[201]

• Intra-operative/open surgical placement

When a patient is having open laparotomy (*e.g.*, exploratory or cytoreductive procedures), fibers can be placed under direct vision—this allows multiple fibers and larger diffusers to be positioned, and optical dosimetry probes placed—but this route is limited to operable patients or those whose surgical exploration is already planned. Early clinical interstitial PDT work used laparotomy placement in some cases.[201]

Fiber and diffuser designs. In order to achieve illumination, usually cylindrical diffusing fibers are used. These fibers feature a light-scattering region along their distal length, typically 1–5 cm, providing 360-degree radial light emission.[202]

Beyond cylindrical diffusers, various fiber tip modifications have been developed to optimize light delivery patterns for specific anatomical situations. Standard flat-cleaved fibers emit light in a forward-directed cone, suitable for surface illumination or when fibers are positioned at the tumor periphery. The divergence angle depends on the numerical aperture of the fiber, typically ranging from 10–25 degrees. However, Baran *et al.* demonstrated that for the same number of fibers, cylindrical diffusers allow for a shorter treatment duration compared to flat cleaved fibers.[203]

Fibers with microfabricated lenses at the tip can provide collimated or focused beams, enabling precise energy delivery to specific regions within the tumor. These fibers show promise when using an endovenous route for illumination of the pancreatic cancer.[204]

At last, multiple fibers can be arranged in parallel to treat larger tumor volumes. Chamberlain *et al.* have proposed a flexible silicone mesh applicator with multiple cylindrically diffusing optical fibers.[205]

Light sources. The demanding requirements of clinical PDT—reliable power output, precise wavelength control, stable operation, and compatibility with fiber delivery favor diode laser systems over solid state, gas lasers or broadband sources. Semiconductor diode lasers offer compact form factors, electrical efficiency, and wavelengths spanning the clinically relevant range. For PDT applications, wavelengths between 630 and 850 nm are most relevant, matching the absorption spectra of clinical photosensitizers while providing adequate tissue penetration. Modern diode laser systems for PDT typically provide 1–5 W of fiber-coupled output with wavelength stability within ±2 nm. The relatively broad spectral bandwidth (2–5 nm FWHM) is acceptable for most photosensitizer activation. Air or water cooling maintains stable operation during extended treatment sessions lasting 30–90 minutes. It is important to mention that PDT lasers must meet regulatory requirements in their respective jurisdictions before clinical use. In the USA, the Food and Drug Administration (FDA) regulates medical lasers. PDT laser systems typically receive 510(k) clearance as Class II medical devices. Specific PDT treatments require separate

approval of the photosensitizer-laser wavelength combination. In the European Union, medical lasers must meet Medical Device Regulation (MDR) requirements and bear CE marking.[206]

Clinical applications of PDT to treat pancreatic cancer

The first clinical studied of PDT to treat locally advanced pancreatic tumours was conducted in 2002 by Bown *et al.*, using *m*THPC in 16 patients. Since then, few clinical studies have been performed and are well described by Lee and Kim.[207] Their review describes methodologies and outcomes of various endoscopic strategies for pancreatobiliary malignancies, including the management of complications, local palliative therapy, endoscopically assisted interventions, and pain control using endoscopic retrograde cholangiopancreatography (ERCP) or endoscopic ultrasound (EUS). In this section, we will focus on studies published after 2020.

In 2020, Tseimakh *et al.* describe the results of a complex treatment with or without PDT of patients with pancreatobiliary malignancies complicated by obstructive jaundice made in Russia.[208] 187 patients were recruited, 22 patients received complex palliative treatment with PDT, 165 without PDT. Among the 22 patients, 21 were treated with PDT and photoditazine (OOO ''VETA-GRAND'', Russia), 1 mg kg^{-1} of body weight and 1 patient with Radachlorin (OOO) ''RADA-PHARMA'', Russia, 1 mg kg^{-1} of body weight. First, a systemic PDT was performed and blood was illuminated (662–665 nm, 1200–1400 J cm^{-2}, 0.22 W cm^{-2}) then after 3–5 hours, local PDT was performed (662 nm, 220 J cm^{-2}, 0.7 W, 0.22 W cm^{-2}). In both groups mechanical jaundice stopped. There was a significant decrease in the size of malignant neoplasm of the head of the pancreas after PDT (39.50 mm to 25.50 mm). The overall survival in the group with PDT was higher than the group without PDT ($p < 0.05$).

The results of a pilot study were published in 2021.[209] In this clinical trial (NCT03033225, VERTPAC-02) PDT was performed with Verteporfin. 8 adults with locally advanced pancreatic cancer with adequate biliary drainage were prospectively enrolled. 4 mg kg^{-1} was infused 60 to 90 minutes before EUS, during which the tumour was illuminated at 50 J cm^{-1} for 333 seconds. The mean pre-trial tumour diameter was 33.3 ± 13.4 mm. At the second-day scan, 5 patients showed an area of necrosis measuring a mean diameter of 15.7 ± 5.5 mm; 3 cases did not develop necrosis. No adverse events occurred during or after the procedure (days 1–3), and patient-reported outcomes remained unchanged, confirming the feasibility and tolerability of PDT in this setting.

Pogue's team study the way to obtain more information from clinical image data; in particular, the use of texture analysis is interesting to predict survival outcomes or stratifying cystic lesions. In 2020, they published a paper concerning the use of texture analysis to examine CT scans before and after PDT treatment of 7 patients with pancreatic cancer.[210] Patients received a pre-treatment CT scan one week before PDT to identify the tumour site. Visudyne was injected (0.4 mg kg^{-1} body weight during 10 min) and 1 hour after, light treatment was performed at 690 nm (40 J cm^{-1}). A post-treatment CT scan was performed 48 h after PDT treatment. No significant change in size could be observed. Nevertheless, regions that responded well were less dense, present a lower average CT number and were more uniform. They could also visualize the microscopic-level effects of PDP and proved that the best PDT results occurred in areas of lower tumour density and higher homogeneity.

Two clinicals, registered on ClinicalTrials.gov are now in progress: the first clinical study titled ''Photoradiation with Verteporfin to Facilitate Immunologic Activity of Pembrolizumab in Unresectable, Locally Advanced or Metastatic Pancreatic Cancer'' (ClinicalTrials.gov Identifier: NCT06381154) is a Phase II, single-arm, open-label trial sponsored by the Mayo Clinic. It aims to evaluate the efficacy and safety of combining PDP using verteporfin with pembrolizumab immunotherapy and standard chemotherapy (mFOLFIRINOX) in patients with unresectable, locally advanced, or metastatic pancreatic ductal adenocarcinoma who have failed first-line treatment. The study plans to enrol approximately 25 patients. The treatment protocol involves intravenous administration of verteporfin followed by intratumoural photoradiation guided by endoscopic ultrasound or computed tomography on day 0, pembrolizumab infusion on day 1, and mFOLFIRINOX chemotherapy on days 3, 15, and 29 of cycle 1, then on days 1, 15, and 29 of subsequent 42-day cycles, for up to 6 months. The primary objective is to assess the overall response rate (ORR) per immune-mediated RECIST (iRECIST) criteria. Secondary objectives include evaluating duration of response (DOR), progression-free survival (PFS), overall survival (OS), and toxicity profile per CTCAE v5.0. Additional exploratory objectives involve assessing local and systemic immune responses, biomarker analysis, and quality of life measurements. The trial started in October 2024, with estimated completion in 2029. The trial started in October 2024, with estimated completion in 2029 (NCT06381154).

The second study titled ''Padeliporfin VTP Treatment for Unresectable Pancreatic Adenocarcinoma'' (ClinicalTrials.gov Identifier: NCT05919238) is a Phase 1, multicenter, open-label, non-randomized trial designed to evaluate the safety and preliminary efficacy of padeliporfin Vascular Targeted Photodynamic (VTP) therapy in patients with Stage III, locally advanced, unresectable pancreatic ductal adenocarcinoma. The study involves endovascular application of padeliporfin *via* a fiber-optic catheter inserted into the superior mesenteric artery (SMA), with intravenous administration of padeliporfin at a fixed dose of 4 mg kg^{-1}, followed by 10 min illumination at 753 nm. The trial is structured in two parts: part A employs a 3 + 3 dose-escalation schema to determine the maximum tolerated light dose (MTD) and/or recommended Phase 2 dose (RP2D), testing light intensities of 200, 400, and 600 mW cm^{-1}. Part B is a dose-expansion phase at the MTD/RP2D to further assess safety, tolerability, and preliminary efficacy. Primary outcomes include safety assessments using CTCAE v5.0 and determination of MTD/RP2D, while secondary outcomes focus on tumour response and resectability rates based on RECIST 1.1 criteria. The study aims to enrol approximately 30 participants across

sites in California, with an estimated completion date in October 2026 (NCT05919238).

Conclusion and perspectives

PDAC remains one of the most intractable malignancies, with patient survival widely unchanged over the past five decades. Conventional radiotherapy plays a limited role in PDAC due to intrinsic radioresistance and the proximity of radiosensitive gastrointestinal organs. Stereotactic body radiation therapy has recently emerged as an option for locally advanced disease, with local control rates of approximately 75%. However, these encouraging results have not translated into improved overall survival, and gastrointestinal toxicities $\geq$grade 3 can affect up to 22% of patients in the acute setting and 44% in the long term. Moreover, the absence of standardized guidelines for treatment and management currently limits its widespread use.[211] This therapeutic context underscores the urgent need for alternative strategies.

PDT has emerged as a credible option, particularly through the use of targeted PSs and NPs, and in combination with established modalities such as chemotherapy, immunotherapy, or PTT. Additional innovations, including ultrasound or X-ray activation of PSs and the refinement of endoscopic devices for local delivery, further broaden the translational potential of PDT in PDAC. Nevertheless, major barriers remain. From a biological standpoint, tumour hypoxia, dense and heterogeneous stroma, and limited light penetration continue to restrict PDT efficacy. Preclinical development is also hindered by the absence of standardized, clinically relevant models. On the clinical side, selective targeting, long-term safety, cost, and the slow pace of translation must be addressed before PDT can be widely adopted.

Opportunities are, however, considerable. Among the most compelling is the ability of PDT to elicit ICD, providing a mechanistic basis for its integration with immunotherapy. Advances in nanotechnology may improve PS delivery, overcome hypoxia, and enable multifunctional theranostics. Imaging-guided approaches hold promise for more precise and adaptive treatments. In the longer term, tailoring PDT regimens to molecularly defined PDAC subtypes could help overcome tumour heterogeneity and improve therapeutic outcomes.

Altogether, PDT should be regarded not as a marginal alternative but as a versatile platform capable of complementing and enhancing current standards of care. By addressing existing limitations and capitalising on technological advances, PDT could evolve into a clinically relevant component of multimodal strategies for PDAC, with the potential to improve both survival and quality of life.

Conflicts of interest

There are no conflicts to declare.

Data availability

No primary research results, software or code have been included and no new data were generated or analysed as part of this review.

Acknowledgements

This work was supported by a French government grant managed by the Agence Nationale de la Recherche under the France 2030 program, reference ANR-23-EXLU-0002 (PEPR LUMA). We would like to thank Nidia Maldonado Carmona for her help in designing the graphical abstract.

References

1 R. R. Allison and C. H. Sibata, Oncologic photodynamic therapy photosensitizers: a clinical review, *Photodiagn. Photodyn. Ther.*, 2010, **7**(2), 61–75.
2 P. S. Maharjan and H. K. Bhattarai, Singlet Oxygen, Photodynamic Therapy, and Mechanisms of Cancer Cell Death, *J. Oncol.*, 2022, 7211485.
3 J. Kleeff, M. Korc, M. Apte, C. La Vecchia, C. D. Johnson and A. V. Biankin, *et al.*, Pancreatic cancer, *Nat. Rev. Dis Primers*, 2016, **2**, 16022.
4 A. J. Aguirre, Integrated Genomic Characterization of Pancreatic Ductal Adenocarcinoma, *Cancer Cell*, 2017, **32**, 185–203.
5 M. Hilmi, F. Delecourt, J. Raffenne, T. Bourega, N. Dusetti and J. Iovanna, *et al.*, Redefining phenotypic intratumor heterogeneity of pancreatic ductal adenocarcinoma: a bottom-up approach, *J. Pathol.*, 2025, **265**(4), 448–461.
6 C. A. Iacobuzio-Donahue, Highly expressed genes in pancreatic ductal adenocarcinomas: a comprehensive characterization and comparison of the transcription profiles obtained from three major technologies, *Cancer Res.*, 2003, **63**, 8614–8622.
7 T. Conroy, P. Hammel, M. Hebbar, M. Ben Abdelghani, A. C. Wei and J. L. Raoul, *et al.*, FOLFIRINOX or Gemcitabine as Adjuvant Therapy for Pancreatic Cancer, *N. Engl. J. Med.*, 2018, **379**(25), 2395–2406.
8 J. E. Murphy, J. Y. Wo, D. P. Ryan, W. Jiang, B. Y. Yeap and L. C. Drapek, *et al.*, Total Neoadjuvant Therapy With FOLFIRINOX Followed by Individualized Chemoradiotherapy for Borderline Resectable Pancreatic Adenocarcinoma: A Phase 2 Clinical Trial, *JAMA Oncol.*, 2018, **4**(7), 963–969.
9 P. P. D. Ghaneh, S. Cicconi, R. Jackson, C. M. Halloran and C. Rawcliffe, Immediate surgery compared with short-course neoadjuvant gemcitabine plus capecitabine, FOLFIRINOX, or chemoradiotherapy in patients with borderline resectable pancreatic cancer (ESPAC5): a four-arm, multicentre, randomised, phase 2 trial, *Lancet Gastroenterol. Hepatol.*, 2023, **8**, 157–168.
10 L. Schwarz, J. B. Bachet, A. Meurisse, O. Bouche, E. Assenat and G. Piessen, *et al.*, Neoadjuvant FOLF(IRIN)OX Chemotherapy for Resectable Pancreatic Adenocarcinoma: A Multicenter Randomized Noncomparative Phase II Trial (PANACHE01 FRENCH08 PRODIGE48 study), *J. Clin. Oncol.*, 2025, **43**(17), 1984–1996.
11 K. J. Labori, S. O. Bratlie, B. Andersson, J. H. Angelsen, C. Biorserud and B. Bjornsson, *et al.*, Neoadjuvant FOLFIRINOX versus upfront surgery for resectable pancreatic head cancer (NORPACT-1): a multicentre, randomised, phase 2 trial, *Lancet Gastroenterol. Hepatol.*, 2024, **9**(3), 205–217.
12 R. G. M. Fietkau, R. Grützmann, U. A. Wittel, L. Jacobasch and W. Uhl, Randomized phase III trial of induction chemotherapy followed by chemoradiotherapy or chemotherapy alone for nonresectable locally advanced pancreatic cancer: first results of the CONKO-007 trial, *J. Clin. Oncol.*, 2022, **40**, 1681–1692.
13 X. Liu, J. Jiang and H. Meng, Transcytosis – An effective targeting strategy that is complementary to "EPR effect" for pancreatic cancer nano drug delivery, *Theranostics*, 2019, **9**(26), 8018–8025.
14 A. Wang-Gillam, C. P. Li, G. Bodoky, A. Dean, Y. S. Shan and G. Jameson, *et al.*, Nanoliposomal irinotecan with fluorouracil and

folinic acid in metastatic pancreatic cancer after previous gemcitabine-based therapy (NAPOLI-1): a global, randomised, open-label, phase 3 trial, *Lancet*, 2016, **387**(10018), 545–557.
15 Z. A. Wainberg, H. S. Hochster, E. J. Kim, B. George, A. Kaylan and E. G. Chiorean, *et al.*, Open-label, Phase I Study of Nivolumab Combined with nab-Paclitaxel Plus Gemcitabine in Advanced Pancreatic Cancer, *Clin. Cancer Res.*, 2020, **26**(18), 4814–4822.
16 Z. I. Hu and E. M. O'Reilly, Therapeutic developments in pancreatic cancer, *Nat. Rev. Gastroenterol. Hepatol.*, 2024, **21**(1), 7–24.
17 O. Olajubutu, O. D. Ogundipe, A. Adebayo and S. K. Adesina, Drug Delivery Strategies for the Treatment of Pancreatic Cancer, *Pharmaceutics*, 2023, **15**(5), 1318.
18 P. S. Harne, V. Harne, C. Wray and N. Thosani, Endoscopic innovations in diagnosis and management of pancreatic cancer: a narrative review and future directions, *Therap. Adv. Gastroenterol.*, 2024, **17**, 17562848241297434.
19 Y. Liu, W. Wu, Y. Wang, S. Han, Y. Yuan and J. Huang, *et al.*, Recent development of gene therapy for pancreatic cancer using non-viral nanovectors, *Biomater. Sci.*, 2021, **9**(20), 6673–6690.
20 Y. Wang, Y. Sun, X. Li, X. Yu, K. Zhang and J. Liu, *et al.*, Progress in the treatment of malignant ascites, *Crit. Rev. Oncol. Hematol.*, 2024, **194**, 104237.
21 T. Yano and K. K. Wang, Photodynamic Therapy for Gastrointestinal Cancer, *Photochem. Photobiol.*, 2020, **96**(3), 517–523.
22 Y. Cai, T. Chai, W. Nguyen, J. Liu, E. Xiao and X. Ran, *et al.*, Phototherapy in cancer treatment: strategies and challenges, *Signal Transduction Targeted Ther.*, 2025, **10**(1), 115.
23 M. Overchuk, R. A. Weersink, B. C. Wilson and G. Zheng, Photodynamic and Photothermal Therapies: Synergy Opportunities for Nanomedicine, *ACS Nano*, 2023, **17**(9), 7979–8003.
24 M. Sasaki, M. Tanaka, Y. Kojima, H. Nishie, T. Shimura and E. Kubota, *et al.*, Anti-tumor immunity enhancement by photodynamic therapy with talaporfin sodium and anti-programmed death 1 antibody, *Mol. Ther.: Oncol.*, 2023, **28**, 118–131.
25 N. M. Carigga Gutierrez, L. Garden, T. Le Clainche, M. Kadri Dakir, F. Johnson-Corrales and S. Bohic, *et al.*, Photochemical internalization with verteporfin-liposomes enhances oxaliplatin retention and efficacy in models of pancreatic cancer, *J. Controlled Release*, 2025, **387**, 114201.
26 N. D. Cosgrove, A. M. Al-Osaimi, H. K. Sanoff, M. M. Morris, P. W. Read and D. G. Cox, *et al.*, Photodynamic Therapy Provides Local Control of Cholangiocarcinoma in Patients Awaiting Liver Transplantation, *Am. J. Transplant.*, 2014, **14**(2), 466–471.
27 N. W. Nkune and H. Abrahamse, The Combination of Active-Targeted Photodynamic Therapy and Photoactivated Chemotherapy for Enhanced Cancer Treatment, *J. Biophotonics*, 2025, **18**(6), e70005.
28 A. M. Rezvan Yazdian-Robati, P. Asadi, M. Mogharabi-Manzari and M. Chamanara, Photodynamic therapy for pancreatic cancer, *Recent Adv. Nanocarriers Pancreatic Cancer Ther.*, 2024, 401–418.
29 Y. Wang, H. Wang, L. Zhou, J. Lu, B. Jiang and C. Liu, *et al.*, Photodynamic therapy of pancreatic cancer: Where have we come from and where are we going?, *Photodiagn. Photodyn. Ther.*, 2020, **31**, 101876.
30 S. G. Bown, Photodynamic therapy for cancer of the pancreas – The story so far, *Photonics Lasers Med.*, 2016, **5**(2), 91–100.
31 V. Karimnia, F. J. Slack and J. P. Celli, Photodynamic Therapy for Pancreatic Ductal Adenocarcinoma, *Cancers*, 2021, **13**(17), 4354.
32 S. G. Bown AZR, D. E. Whitelaw, W. R. Lees, L. B. Lovat, P. Ripley, L. Jones, P. Wyld, A. Gillams and A. W. R. Hatfield, Photodynamic therapy for cancer of the pancreas, *Gut*, 2002, 549–557.
33 G. Obaid, Z. Mai and T. Hasan, Orthotopic Models of Pancreatic Cancer to Study PDT, *Methods Mol. Biol.*, 2022, **2451**, 163–173.
34 N. Lintern, A. M. Smith, D. G. Jayne and Y. S. Khaled, Photodynamic Stromal Depletion in Pancreatic Ductal Adenocarcinoma, *Cancers*, 2023, **15**(16), 4135.
35 K. Sato, K. Ando, S. Okuyama, S. Moriguchi, T. Ogura and S. Totoki, *et al.*, Photoinduced Ligand Release from a Silicon Phthalocyanine Dye Conjugated with Monoclonal Antibodies: A Mechanism of Cancer Cell Cytotoxicity after Near-Infrared Photoimmunotherapy, *ACS Cent. Sci.*, 2018, **4**(11), 1559–1569.
36 K. N. Takuya Kato, T. Ohara, H. Kashima, Y. Katsura, H. Sato, S. Komoto, R. Katsube, T. Ninomiya, H. Tazawa, Y. Shirakawa and T. Fujiwara, Cancer-Associated Fibroblasts Affect Intratumoral $CD8^+$ and FoxP3+ T Cells Via IL6 in the Tumor Microenvironment, *Clin. Cancer Res.*, 2018, **24**, 4820–4833.
37 C. Qu, H. Yuan, M. Tian, X. Zhang, P. Xia and G. Shi, *et al.*, Precise Photodynamic Therapy by Midkine Nanobody-Engineered Nanoparticles Remodels the Microenvironment of Pancreatic Ductal Adenocarcinoma and Potentiates the Immunotherapy, *ACS Nano*, 2024, **18**(5), 4019–4037.
38 M. M. Li, Y. Zhang, F. Sun, M. X. Huai, F. Y. Zhang and J. X. Pan, *et al.*, Photodynamic Therapy Using RGD-Functionalized Quantum Dots Elicit a Potent Immune Response in a Syngeneic Mouse Model of Pancreatic Cancer, *Int. J. Nanomed.*, 2024, **19**, 9487–9502.
39 B. Chen, B. W. Pogue, P. J. Hoopes and T. Hasan, Vascular and cellular targeting for photodynamic therapy, *Crit. Rev. Eukaryotic Gene Expression*, 2006, **16**(4), 279–305.
40 H. Deng, K. Xie, L. Hu, X. Liu, Q. Li and D. Xie, *et al.*, Polyamine Derived Photosensitizer: A Novel Approach for Photodynamic Therapy of Cancer, *Molecules*, 2024, **29**(17), 4277.
41 M. M. Esther, D. N. D. Smeets, G. M. Franssen, M. S. van Essen, C. Frielink, M. W. J. Stommel, M. Trajkovic-Arsic, P. F. Cheung, J. T. Siveke, I. Wilson, A. Mascioni, E. H. J. G. Aarntzen and S. A. M. van Lith., Fibroblast Activation Protein-Targeting Minibody-IRDye700DX for Ablation of the Cancer-Associated Fibroblast with Photodynamic Therapy, *Cells*, 2023, **12**, 1420.
42 S. Bano, G. Obaid, J. W. R. Swain, M. Yamada, B. W. Pogue and K. Wang, *et al.*, NIR Photodynamic Destruction of PDAC and HNSCC Nodules Using Triple-Receptor-Targeted Photoimmuno-Nanoconjugates: Targeting Heterogeneity in Cancer, *J. Clin. Med.*, 2020, **9**(8), 2390.
43 A. Ferino, G. Nicoletto, F. D'Este, S. Zorzet, S. Lago and S. N. Richter, *et al.*, Photodynamic Therapy for ras-Driven Cancers: Targeting G-Quadruplex RNA Structures with Bifunctional Alkyl-Modified Porphyrins, *J. Med. Chem.*, 2020, **63**(3), 1245–1260.
44 A. Garcia-Sampedro, A. Prieto-Castaneda, A. R. Agarrabeitia, J. Banuelos, I. Garcia-Moreno and A. Villanueva, *et al.*, A highly fluorescent and readily accessible all-organic photosensitizer model for advancing image-guided cancer PDT, *J. Mater. Chem. B*, 2024, **12**(31), 7618–7625.
45 L. Zhu, X. Wang, T. Tian, Y. Chen, W. Du and W. Wei, *et al.*, A Lambda-Ir(III)-phenylquinazolinone complex enhances ferroptosis by selectively inhibiting metallothionein-1, *Chem. Sci.*, 2024, **15**(27), 10499–10507.
46 Y. Kuroda, T. Oda, O. Shimomura, S. Hashimoto, Y. Akashi and Y. Miyazaki, *et al.*, Lectin-based phototherapy targeting cell surface glycans for pancreatic cancer, *Int. J. Cancer*, 2023, **152**(7), 1425–1437.
47 Y. Luo, Z. Zeng, T. Shan, X. Xu, J. Chen and Y. He, *et al.*, Fibroblast activation protein alpha activatable theranostic prophotosensitizer for accurate tumor imaging and highly-specific photodynamic therapy, *Theranostics*, 2022, **12**(8), 3610–3627.
48 J. Yang, B. Ren, X. Yin, L. Xiang, Y. Hua and X. Huang, *et al.*, Expanded ROS Generation and Hypoxia Reversal: Excipient-free Self-assembled Nanotheranostics for Enhanced Cancer Photodynamic Immunotherapy, *Adv. Mater.*, 2024, **36**(30), e2402720.
49 D. N. Dorst, E. M. M. Smeets, C. Klein, C. Frielink, D. Geijs and M. Trajkovic-Arsic, *et al.*, Fibroblast Activation Protein-Targeted Photodynamic Therapy of Cancer-Associated Fibroblasts in Murine Models for Pancreatic Ductal Adenocarcinoma, *Mol. Pharm.*, 2023, **20**(8), 4319–4330.
50 O. Shapoval, D. Vetvicka, V. Patsula, H. Engstova, O. Kockova and M. Konefal, *et al.*, Temoporfin-Conjugated Upconversion Nanoparticles for NIR-Induced Photodynamic Therapy: Studies with Pancreatic Adenocarcinoma Cells In Vitro and In Vivo, *Pharmaceutics*, 2023, **15**(12), 2694.
51 Y. Sakamaki, J. Ozdemir, Z. Heidrick, A. Azzun, O. Watson and M. Tsuji, *et al.*, A Bio-Conjugated Chlorin-Based Metal-Organic Framework for Targeted Photodynamic Therapy of Triple Negative Breast and Pancreatic Cancers, *ACS Appl. Bio Mater.*, 2021, **4**(2), 1432–1440.
52 S. B. Girgis Obaid, H. Thomsen, S. Callaghan, N. Shah, J. W. R. Swain, W. Jin, X. Ding, C. G. Cameron, S. A. McFarland, J. Wu, M. Vangel, S. Stoilova-McPhie, J. Zhao, M. Mino-Kenudson, C. Lin and T. Hasan, Remediating Desmoplasia with EGFR-Targeted Photoactivable Multi-Inhibitor Liposomes Doubles Overall Survival in Pancreatic Cancer, *Adv. Sci.*, 2022, **9**(24), e2104594.

53 S. Gavas, S. Quazi and T. M. Karpinski, Nanoparticles for Cancer Therapy: Current Progress and Challenges, *Nanoscale Res. Lett.*, 2021, **16**(1), 173.
54 M. J. Saadh, H. Baher, Y. Li, M. Chaitanya, J. L. Arias-Gonzales and O. Q. B. Allela, *et al.*, The bioengineered and multifunctional nanoparticles in pancreatic cancer therapy: bioresponsive nanostructures, phototherapy and targeted drug delivery, *Environ. Res.*, 2023, **233**, 116490.
55 A. A. Yetisgin, S. Cetinel, M. Zuvin, A. Kosar and O. Kutlu, Therapeutic Nanoparticles and Their Targeted Delivery Applications, *Molecules*, 2020, **25**, 2193.
56 W. P. Li, C. J. Yen, B. S. Wu and T. W. Wong, Recent Advances in Photodynamic Therapy for Deep-Seated Tumors with the Aid of Nanomedicine, *Biomedicines.*, 2021, **9**(1), 69.
57 R. Shrestha, H. J. Lee, J. Lim, P. Gurung, T. B. Thapa Magar and Y. T. Kim, *et al.*, Effect of Photodynamic Therapy with Chlorin e6 on Canine Tumors, *Life*, 2022, **12**(12), 2102.
58 L. Shi, C. Nguyen, M. Daurat, N. Richy, C. Gauthier, E. Rebecq, M. Gary-Bobo, S. Cammas-Marion, O. Mongin, C. O. Paul-Roth and F. Paul., Encapsulation of Hydrophobic Porphyrins into Biocompatible Nanoparticles: An Easy Way to Benefit of Their Two-Photon Phototherapeutic Effect without Hydrophilic Functionalization, *Cancers*, 2022, **14**, 2358.
59 S. Thavornpradit, S. M. Usama, G. K. Park, J. Dinh, H. S. Choi and K. Burgess, QuatCy-I(2) and MHI-I(2) in Photodynamic Therapy, *ACS Med. Chem. Lett.*, 2022, **13**(3), 470–474.
60 J. Chen, X. Jin, Z. Shen, Y. Mei, J. Zhu and X. Zhang, *et al.*, H(2)O(2) enhances the anticancer activity of TMPyP4 by ROS-mediated mitochondrial dysfunction and DNA damage, *Med. Oncol.*, 2021, **38**(6), 59.
61 S. Wen, W. Wang, R. Liu and P. He, Amylase-Protected Ag Nanodots for in vivo Fluorescence Imaging and Photodynamic Therapy of Tumors, *Int. J. Nanomed.*, 2020, **15**, 3405–3414.
62 W. Zhou, A. Lim, O. H. M. Elmadbouh, M. Edderkaoui, A. Osipov and A. J. Mathison, *et al.*, Verteporfin induces lipid peroxidation and ferroptosis in pancreatic cancer cells, *Free Radical Biol. Med.*, 2024, **212**, 493–504.
63 A. Srivatsan, P. Pera, P. Joshi, A. J. Marko, F. Durrani and J. R. Missert, *et al.*, Highlights on the imaging (nuclear/fluorescence) and phototherapeutic potential of a tri-functional chlorophyll-a analog with no significant toxicity in mice and rats, *J. Photochem. Photobiol., B*, 2020, **211**, 111998.
64 L. Li, Z. Yang, W. Fan, L. He, C. Cui and J. Zou, *et al.*, In Situ Polymerized Hollow Mesoporous Organosilica Biocatalysis Nanoreactor for Enhancing ROS-Mediated Anticancer Therapy, *Adv. Funct. Mater.*, 2020, **30**(4), 1907716.
65 Y. Wang, H. Shen, Z. Li, S. Liao, B. Yin and R. Yue, *et al.*, Enhancing Fractionated Cancer Therapy: A Triple-Anthracene Photosensitizer Unleashes Long-Persistent Photodynamic and Luminous Efficacy, *J. Am. Chem. Soc.*, 2024, **146**(9), 6252–6265.
66 T. B. Thapa Magar, J. Lee, J. H. Lee, J. Jeon, P. Gurung and J. Lim, *et al.*, Novel Chlorin e6-Curcumin Derivatives as a Potential Photosensitizer: Synthesis, Characterization, and Anticancer Activity, *Pharmaceutics*, 2023, **15**(6), 1577.
67 K. Chen, B. Yin, Q. Luo, Y. Liu, Y. Wang and Y. Liao, *et al.*, Endoscopically guided interventional photodynamic therapy for orthotopic pancreatic ductal adenocarcinoma based on NIR-II fluorescent nanoparticles, *Theranostics*, 2023, **13**(13), 4469–4481.
68 K. Y. Pham, L. C. Wang, C. C. Hsieh, Y. P. Hsu, L. C. Chang and W. P. Su, *et al.*, 1550 nm excitation-responsive upconversion nanoparticles to establish dual-photodynamic therapy against pancreatic tumors, *J. Mater. Chem. B*, 2021, **9**(3), 694–709.
69 N. Chauhan, M. Koli, R. Ghosh, A. G. Majumdar, A. Ghosh and T. K. Ghanty, *et al.*, A BODIPY-Naphtholimine-BF(2) Dyad for Precision Photodynamic Therapy, Targeting, and Dual Imaging of Endoplasmic Reticulum and Lipid Droplets in Cancer, *JACS Au*, 2024, **4**(8), 2838–2852.
70 O. Shapoval, V. Patsula, D. Vetvicka, H. Engstova, V. Oleksa and M. Kabesova, *et al.*, Temoporfin-Conjugated PEGylated Poly(*N*,*N*-dimethylacrylamide)-Coated Upconversion Colloid for NIR-Induced Photodynamic Therapy of Pancreatic Cancer, *Biomacromolecules*, 2024, **25**(9), 5771–5785.
71 N. Shah, S. R. Soma, M. B. Quaye, D. Mahmoud, S. Ahmed and A. Malkoochi, *et al.*, A Physiochemical, In Vitro, and In Vivo Comparative Analysis of Verteporfin-Lipid Conjugate Formulations: Solid Lipid Nanoparticles and Liposomes, *ACS Appl. Bio Mater.*, 2024, **7**(7), 4427–4441.
72 R. McMorrow, H. S. de Bruijn, I. Que, D. C. Stuurman, C. M. A. de Ridder and M. Doukas, *et al.*, Rapid Assessment of Bio-distribution and Antitumor Activity of the Photosensitizer Bremachlorin in a Murine PDAC Model: Detection of PDT-induced Tumor Necrosis by IRDye(R) 800CW Carboxylate, Using Whole-Body Fluorescent Imaging, *Mol. Imaging Biol.*, 2024, **26**(4), 616–627.
73 S. Y. Kim, E. A. Cho, S. M. Bae, S. Y. Kim and D. H. Park, The effect of a newly developed mini-light-emitting diode catheter for interstitial photodynamic therapy in pancreatic cancer xenografts, *J. Transl. Med.*, 2021, **19**(1), 248.
74 J. Yang, C. H. Ma, J. A. Quinlan, K. McNaughton, T. Lee and P. Shin, *et al.*, Light-activatable minimally invasive ethyl cellulose ethanol ablation: biodistribution and potential applications, *Bioeng. Transl. Med.*, 2024, **9**(6), e10696.
75 E. Di Giorgio, A. Ferino, H. Choudhary, P. M. G. Loffler, F. D'Este and V. Rapozzi, *et al.*, Photosensitization of pancreatic cancer cells by cationic alkyl-porphyrins in free form or engrafted into POPC liposomes: the relationship between delivery mode and mechanism of cell death, *J. Photochem. Photobiol., B*, 2022, **231**, 112449.
76 Y. Liu, S. K. Mensah, S. Farias, S. Khan, T. Hasan and J. P. Celli, Efficacy of photodynamic therapy using 5-aminolevulinic acid-induced photosensitization is enhanced in pancreatic cancer cells with acquired drug resistance, *Photodiagn. Photodyn. Ther.*, 2024, **50**, 104362.
77 D. L. D'Antonio, S. Marchetti, P. Pignatelli, S. Umme, D. De Bellis and P. Lanuti, *et al.*, Effect of 5-Aminolevulinic Acid (5-ALA) in "ALADENT" Gel Formulation and Photodynamic Therapy (PDT) against Human Oral and Pancreatic Cancers, *Biomedicines.*, 2024, **12**(6), 1316.
78 H. Fu, Q. Lu, Y. Zhang, P. Wan, H. Xu and C. Liao, *et al.*, Multi-target responsive nanoprobe with cellular-level accuracy for spatiotemporally selective photodynamic therapy, *Mikrochim. Acta*, 2023, **190**(11), 448.
79 D. R. Q. de Almeida, A. F. Dos Santos, R. A. M. Wailemann, L. F. Terra, V. M. Gomes and G. S. Arini, *et al.*, Necroptosis activation is associated with greater methylene blue-photodynamic therapy-induced cytotoxicity in human pancreatic ductal adenocarcinoma cells, *Photochem. Photobiol. Sci.*, 2023, **22**(4), 729–744.
80 H. Yang, R. Liu, Y. Xu, L. Qian and Z. Dai, Photosensitizer Nanoparticles Boost Photodynamic Therapy for Pancreatic Cancer Treatment, *Nanomicro Lett.*, 2021, **13**(1), 35.
81 B. Dhaini, B. Kenzhebayeva, A. Ben-Mihoub, M. Gries, S. Acherar and F. Baros, *et al.*, Peptide-conjugated nanoparticles for targeted photodynamic therapy, *Nanophotonics*, 2021, **10**(12), 3089–3134.
82 B. Sun, H. Yang, Y. Li, J. F. Scheerstra, M. van Stevendaal and S. Li, *et al.*, Targeted pH-Activated Peptide-Based Nanomaterials for Combined Photodynamic Therapy with Immunotherapy, *Biomacromolecules*, 2024, **25**(5), 3044–3054.
83 J. Yan, T. Gao, Z. Lu, J. Yin, Y. Zhang and R. Pei, Aptamer-Targeted Photodynamic Platforms for Tumor Therapy, *ACS Appl. Mater. Interfaces*, 2021, **13**(24), 27749–27773.
84 K. Huang, Y. Niu, G. Yuan, M. Yan, J. Xue and J. Chen, EGFR-targeted photosensitizer for enhanced photodynamic therapy and imaging therapeutic effect by monitoring GSH decline, *Sens. Actuators, B*, 2022, 355.
85 A. A. Obalola, H. Abrahamse and S. S. Dhilip Kumar, Enhanced therapeutic precision using dual drug-loaded nanomaterials for targeted cancer photodynamic therapy, *Biomed. Pharmacother.*, 2025, **184**, 117909.
86 Y. Cheng, H. Cheng, C. Jiang, X. Qiu, K. Wang and W. Huan, *et al.*, Perfluorocarbon nanoparticles enhance reactive oxygen levels and tumour growth inhibition in photodynamic therapy, *Nat. Commun.*, 2015, **6**, 8785.
87 R. A. Day and E. M. Sletten, Perfluorocarbon nanomaterials for photodynamic therapy, *Curr. Opin. Colloid Interface Sci.*, 2021, **54**, 101454.
88 M. Xavierselvan, J. Cook, J. Duong, N. Diaz, K. Homan and S. Mallidi, Photoacoustic nanodroplets for oxygen enhanced photodynamic therapy of cancer, *Photoacoustics*, 2022, **25**, 100306.
89 Y. Zheng, Z. Li, H. Chen and Y. Gao, Nanoparticle-based drug delivery systems for controllable photodynamic cancer therapy, *Eur. J. Pharm. Sci.*, 2020, **144**, 105213.

90 S. S. Hafiz, M. Xavierselvan, S. Gokalp, D. Labadini, S. Barros and J. Duong, *et al.*, Eutectic Gallium-Indium Nanoparticles for Photodynamic Therapy of Pancreatic Cancer, *ACS Appl. Nano Mater.*, 2022, **5**(5), 6125–6139.
91 H. Zhao, R. Naganawa, Y. Yamada, Y. Osakada, M. Fujitsuka and H. Mitomo, *et al.*, π-extended porphyrin-based near-infrared photosensitizers for mitochondria-targeted photodynamic therapy, *J. Photochem. Photobiol., A*, 2024, **449**, 115397.
92 Y. Tao, C. Yan, D. Li, J. Dai, Y. Cheng and H. Li, *et al.*, Sequence-Activated Fluorescent Nanotheranostics for Real-Time Profiling Pancreatic Cancer, *JACS Au*, 2022, **2**(1), 246–257.
93 L. Yan, Y. Jiang, J. Qian, J. Bai, C. Meng and Z. Xu, *et al.*, Octreotide modified self-assembly Chlorin e6 nanoparticles with redox responsivity and active targeting for highly selective pancreatic neuroendocrine neoplasms photodynamic therapy, *Microchem. J.*, 2025, **208**, 112303.
94 W. Dai, X. Zhou, J. Zhao, L. Lei, Y. Huang and F. Jia, *et al.*, Tumor microenvironment-modulated nanoparticles with cascade energy transfer as internal light sources for photodynamic therapy of deep-seated tumors, *Biomaterials*, 2025, **312**, 122743.
95 O. Yurt, Radiolabeling, In Vitro Cell Uptake, and In Vivo Photodynamic Therapy Potential of Targeted Mesoporous Silica Nanoparticles Containing Zinc Phthalocyanine, *Mol. Pharmaceutics*, 2020, **17**(7), 2648–2659.
96 Q. Wu, L. You, E. Nepovimova, Z. Heger, W. Wu and K. Kuca, *et al.*, Hypoxia-inducible factors: master regulators of hypoxic tumor immune escape, *J. Hematol. Oncol.*, 2022, **15**(1), 77.
97 J. Tao, G. Yang, W. Zhou, J. Qiu, G. Chen and W. Luo, *et al.*, Targeting hypoxic tumor microenvironment in pancreatic cancer, *J. Hematol. Oncol.*, 2021, **14**(1), 14.
98 J. Wei, M. Hu and H. Du, Improving Cancer Immunotherapy: Exploring and Targeting Metabolism in Hypoxia Microenvironment, *Front. Immunol.*, 2022, **13**, 845923.
99 O. R. Colegio, N.-Q. Chu, A. L. Szabo, T. Chu, A. M. Rhebergen and V. Jairam, *et al.*, Functional polarization of tumour-associated macrophages by tumour-derived lactic acid, *Nature*, 2014, **513**(7519), 559–563.
100 M. Z. Noman, M. Hasmim, Y. Messai, S. Terry, C. Kieda and B. Janji, *et al.*, Hypoxia: a key player in antitumor immune response. A Review in the Theme: Cellular Responses to Hypoxia, *Am. J. Physiol.: Cell Physiol.*, 2015, **309**(9), C569–C579.
101 J.-J. Zhang, C. Shao, Y.-X. Yin, Q. Sun, Y.-N. Li and Y.-W. Zha, *et al.*, Hypoxia-Related Signature Is a Prognostic Biomarker of Pancreatic Cancer, *Dis. Markers*, 2022, **2022**(1), 6449997.
102 V. Papa, F. Furci, P. L. Minciullo, M. Casciaro, A. Allegra and S. Gangemi, Photodynamic Therapy in Cancer: Insights into Cellular and Molecular Pathways, *Curr. Issues Mol. Biol.*, 2025, **47**(2), 69.
103 M. Wang, M. Wu, X. Liu, S. Shao, J. Huang and B. Liu, *et al.*, Pyroptosis Remodeling Tumor Microenvironment to Enhance Pancreatic Cancer Immunotherapy Driven by Membrane Anchoring Photosensitizer, *Adv. Sci.*, 2022, **9**(29), 2202914.
104 G. Yang, S.-B. Lu, C. Li, F. Chen, J.-S. Ni and M. Zha, *et al.*, Type I macrophage activator photosensitizer against hypoxic tumors, *Chem. Sci.*, 2021, **12**(44), 14773–14780.
105 S. Xu, X. Xie, P. He, S. Zhu, X. Li and Q. Chen, *et al.*, Nitric Oxide-Producing Multiple Functional Nanoparticle Remodeling Tumor Microenvironment for Synergistic Photodynamic Immunotherapy against Hypoxic Tumor, *ACS Nano*, 2025, **19**(6), 6371–6387.
106 M. Zhou, L. Xu, J. Hu, W. Chen, J. Hong and M. Wang, *et al.*, Metabolic reprogramming through PIM3 inhibition reverses hypoxia-induced CAR-T cell dysfunction in solid tumors, *J. Transl. Med.*, 2025, **23**(1), 1230.
107 W. Chou, T. Sun, N. Peng, Z. Wang, D. Chen and H. Qiu, *et al.*, Photodynamic Therapy-Induced Anti-Tumor Immunity: Influence Factors and Synergistic Enhancement Strategies, *Pharmaceutics*, 2023, **15**(11), 2617.
108 Y. Zhao, X. Liu, X. Liu, J. Yu, X. Bai and X. Wu, *et al.*, Combination of phototherapy with immune checkpoint blockade: theory and practice in cancer, *Front. Immunol.*, 2022, **13**, 955920.
109 A. Quilbe, O. Morales, M. Baydoun, A. Kumar, R. Mustapha and T. Murakami, *et al.*, An Efficient Photodynamic Therapy Treatment for Human Pancreatic Adenocarcinoma, *J. Clin. Med.*, 2020, **9**(1), 192.
110 D. Kim, S. Lee and K. Na, Immune Stimulating Antibody-Photosensitizer Conjugates via Fc-Mediated Dendritic Cell Phagocytosis and Phototriggered Immunogenic Cell Death for KRAS-Mutated Pancreatic Cancer Treatment, *Small*, 2021, **17**(10), e2006650.
111 J. S. Bertout and M. Celeste Simon, The impact of O_2 availability on human cancer, *Nat. Rev. Cancer*, 2008, **8**(12), 967–975.
112 Z. Wang, X. Gong, J. Li, H. Wang, X. Xu and Y. Li, *et al.*, Oxygen-Delivering Polyfluorocarbon Nanovehicles Improve Tumor Oxygenation and Potentiate Photodynamic-Mediated Antitumor Immunity, *ACS Nano*, 2021, **15**(3), 5405–5419.
113 F. Sun, Q. Zhu, T. Li, M. Saeed, Z. Xu and F. Zhong, *et al.*, Regulating Glucose Metabolism with Prodrug Nanoparticles for Promoting Photoimmunotherapy of Pancreatic Cancer, *Adv. Sci.*, 2021, **8**(4), 2002746.
114 S. B. Pushpamali De Silva, B. W. Pogue, K. K. Wang, E. V. Maytin and T. Hasan, Photodynamic priming with triple-receptor targeted nanoconjugates that trigger T cell-mediated immune responses in a 3D in vitro heterocellular model of pancreatic cancer, *Nanophotonics*, 2021, **12**, 3199–3214.
115 M. A. Saad, W. Zhung, M. E. Stanley, S. Formica, S. Grimaldo-Garcia and G. Obaid, *et al.*, Photoimmunotherapy Retains Its Anti-Tumor Efficacy with Increasing Stromal Content in Heterotypic Pancreatic Cancer Spheroids, *Mol. Pharm.*, 2022, **19**(7), 2549–2563.
116 B. Lim, K. S. Kim and K. Na, pH-Responsive Zinc Ion Regulating Immunomodulatory Nanoparticles for Effective Cancer Immunotherapy, *Biomacromolecules*, 2023, **24**(9), 4263–4273.
117 D. Zhang, Q. Xie, Y. Liu, Z. Li, H. Li and S. Li, *et al.*, Photosensitizer IR700DX-6T- and IR700DX-mbc94-mediated photodynamic therapy markedly elicits anticancer immune responses during treatment of pancreatic cancer, *Pharmacol. Res.*, 2021, **172**, 105811.
118 Y. L. Lum, J. M. Luk, D. E. Staunton, D. K. P. Ng and W. P. Fong, Cadherin-17 Targeted Near-Infrared Photoimmunotherapy for Treatment of Gastrointestinal Cancer, *Mol. Pharm.*, 2020, **17**(10), 3941–3951.
119 Y. Jang, H. Kim, S. Yoon, H. Lee, J. Hwang and J. Jung, *et al.*, Exosome-based photoacoustic imaging guided photodynamic and immunotherapy for the treatment of pancreatic cancer, *J. Controlled Release*, 2021, **330**, 293–304.
120 P. Gurung, J. Lim, R. Shrestha and Y. W. Kim, Chlorin e6-associated photodynamic therapy enhances abscopal antitumor effects via inhibition of PD-1/PD-L1 immune checkpoint, *Sci. Rep.*, 2023, **13**(1), 4647.
121 V. Karimnia, M. E. Stanley, C. T. Fitzgerald, I. Rizvi, F. J. Slack and J. P. Celli, Photodynamic Stromal Depletion Enhances Therapeutic Nanoparticle Delivery in 3D Pancreatic Ductal Adenocarcinoma Tumor Models, *Photochem. Photobiol.*, 2023, **99**(1), 120–131.
122 Y. Chen, J. Wang, Y. Huang, J. Wu, Y. Wang and A. Chen, *et al.*, An oncolytic system produces oxygen selectively in pancreatic tumor cells to alleviate hypoxia and improve immune activation, *Pharmacol. Res.*, 2024, **199**, 107053.
123 C. Bhandari, A. Moffat, N. Shah, A. Khan, M. Quaye and J. Fakhry, *et al.*, PD-L1 Immune Checkpoint Targeted Photoactivable Liposomes (iTPALs) Prime the Stroma of Pancreatic Tumors and Promote Self-Delivery, *Adv. Healthcare Mater.*, 2024, **13**(19), e2304340.
124 G. Liu, M. Liu, X. Li, X. Ye, K. Cao and Y. Liu, *et al.*, Peroxide-Simulating and GSH-Depleting Nanozyme for Enhanced Chemodynamic/Photodynamic Therapy via Induction of Multisource ROS, *ACS Appl. Mater. Interfaces*, 2023, **15**(41), 47955–47968.
125 M. Wang, M. Wu, X. Liu, S. Shao, J. Huang and B. Liu, *et al.*, Pyroptosis Remodeling Tumor Microenvironment to Enhance Pancreatic Cancer Immunotherapy Driven by Membrane Anchoring Photosensitizer, *Adv. Sci.*, 2022, **9**(29), e2202914.
126 L. Zhu, S. Lin, W. Cui, Y. Xu, L. Wang and Z. Wang, *et al.*, A nanomedicine enables synergistic chemo/photodynamic therapy for pancreatic cancer treatment, *Biomater. Sci.*, 2022, **10**(13), 3624–3636.
127 J. Qiao, S. Liu, Y. Huang, X. Zhu, C. Xue and Y. Wang, *et al.*, Glycolysis-non-canonical glutamine dual-metabolism regulation nanodrug enhanced the phototherapy effect for pancreatic ductal adenocarcinoma treatment, *J. Colloid Interface Sci.*, 2024, **665**, 477–490.
128 K. Y. Xixin Gu, S. Li, J. Mei, X.-P. He and W. Chen, and Jianli Hua An esterase-activated diketopyrrolopyrrole-based theranostic

prodrug for precise pyroptosis and synergistic chemo-photodynamic therapy of pancreatic cancer, *Mater. Chem. Front.*, 2024, (8), 1993–2001.
129 R. Liu, H. Yang, S. Qu, P. Yang, X. Zhi and Y. Xu, *et al.*, Photodynamic eradication of intratumoral microbiota with bacteria-targeted micelles overcomes gemcitabine resistance of pancreatic cancer, *Aggregate*, 2023, **5**(1), e423.
130 X. Liu, Z. Chu, B. Chen, Y. Ma, L. Xu and H. Qian, *et al.*, Cancer cell membrane-coated upconversion nanoparticles/$Zn_{(x)}Mn_{(1-x)}S$ core–shell nanoparticles for targeted photodynamic and chemodynamic therapy of pancreatic cancer, *Mater. Today Bio*, 2023, **22**, 100765.
131 S. Anbil, M. Pigula, H. C. Huang, S. Mallidi, M. Broekgaarden and Y. Baglo, *et al.*, Vitamin D Receptor Activation and Photodynamic Priming Enables Durable Low-dose Chemotherapy, *Mol. Cancer Ther.*, 2020, **19**(6), 1308–1319.
132 G. Obaid, M. Eroy, J. Zhao, S. Bano, M. Mino-Kenudson and T. Hasan, Immunofluorescence profiling of collagen subtypes is a predictor of treatment outcomes in pancreatic cancer, *J. Photochem. Photobiol., B*, 2024, **250**, 112811.
133 I. K. Cho, M. K. Shim, W. Um, J. H. Kim and K. Kim, Light-Activated Monomethyl Auristatin E Prodrug Nanoparticles for Combinational Photo-Chemotherapy of Pancreatic Cancer, *Molecules*, 2022, **27**(8), 2529.
134 M. Broekgaarden, A. Alkhateeb, S. Bano, A. L. Bulin, G. Obaid and I. Rizvi, *et al.*, Cabozantinib Inhibits Photodynamic Therapy-Induced Auto- and Paracrine MET Signaling in Heterotypic Pancreatic Microtumors, *Cancers*, 2020, **12**(6), 1401.
135 L. N. Gendron, D. C. Zites, E. P. M. LaRochelle, J. R. Gunn, B. W. Pogue and T. A. Shell, *et al.*, Tumor targeting vitamin B12 derivatives for X-ray induced treatment of pancreatic adenocarcinoma, *Photodiagn. Photodyn. Ther.*, 2020, **30**, 101637.
136 Q. Wu, X. Ma, W. Zhou, R. Yu, J. M. Rosenholm and W. Tian, *et al.*, Co-Delivery of Paclitaxel Prodrug, Gemcitabine and Porphine by Micelles for Pancreatic Cancer Treatment via Chemo-Photodynamic Combination Therapy, *Pharmaceutics*, 2022, **14**(11), 2280.
137 T. Zhang, Z. Jiang, L. Chen, C. Pan, S. Sun and C. Liu, *et al.*, PCN-Fe(III)-PTX nanoparticles for MRI guided high efficiency chemo-photodynamic therapy in pancreatic cancer through alleviating tumor hypoxia, *Nano Res.*, 2020, **13**(1), 273–281.
138 M. Pigula, Z. Mai, S. Anbil, M. G. Choi, K. Wang and E. Maytin, *et al.*, Dramatic Reduction of Distant Pancreatic Metastases Using Local Light Activation of Verteporfin with Nab-Paclitaxel, *Cancers*, 2021, **13**(22), 5781.
139 Y. Shen, M. Li, F. Sun, Y. Zhang, C. Qu and M. Zhou, *et al.*, Low-dose photodynamic therapy-induced increase in the metastatic potential of pancreatic tumor cells and its blockade by simvastatin, *J. Photochem. Photobiol., B*, 2020, **207**, 111889.
140 H. S. Liew, C. W. Mai, M. Zulkefeli, T. Madheswaran, L. V. Kiew and L. J. W. Pua, *et al.*, Novel Gemcitabine-Re(I) Bisquinolinyl Complex Combinations and Formulations With Liquid Crystalline Nanoparticles for Pancreatic Cancer Photodynamic Therapy, *Front. Pharmacol.*, 2022, **13**, 903210.
141 R. Jafari, G. M. Cramer and J. P. Celli, Modulation of Extracellular Matrix Rigidity Via Riboflavin-mediated Photocrosslinking Regulates Invasive Motility and Treatment Response in a 3D Pancreatic Tumor Model, *Photochem. Photobiol.*, 2020, **96**(2), 365–372.
142 S. Ghosh, B. Sun, D. Jahagirdar, D. Luo, J. Ortega and R. M. Straubinger, *et al.*, Single-treatment tumor ablation with photodynamic liposomal irinotecan sucrosulfate, *Transl. Oncol.*, 2022, **19**, 101390.
143 S. Ghosh and J. F. Lovell, Two Laser Treatments Can Improve Tumor Ablation Efficiency of Chemophototherapy, *Pharmaceutics*, 2021, **13**(12), 2183.
144 S. Bano, J. Q. Alburquerque, H. J. Roberts, S. Pang, H. C. Huang and T. Hasan, Minocycline and photodynamic priming significantly improve chemotherapy efficacy in heterotypic spheroids of pancreatic ductal adenocarcinoma, *J. Photochem. Photobiol., B*, 2024, **255**, 112910.
145 L. Sun, H. Shang, Y. Wu and X. Xin, Hypericin-mediated photodynamic therapy enhances gemcitabine induced Capan-2 cell apoptosis via inhibiting NADPH level, *J. Pharm. Pharmacol.*, 2022, **74**(4), 596–604.
146 V. Karimnia, I. Rizvi, F. J. Slack and J. P. Celli, Photodestruction of Stromal Fibroblasts Enhances Tumor Response to PDT in 3D Pancreatic Cancer Coculture Models, *Photochem. Photobiol.*, 2021, **97**(2), 416–426.
147 P. Nalepa, R. Gawecki, G. Szewczyk, K. Balin, M. Dulski and M. Sajewicz, *et al.*, A [60]fullerene nanoconjugate with gemcitabine: synthesis, biophysical properties and biological evaluation for treating pancreatic cancer, *Cancer Nanotechnol.*, 2020, **11**, 2.
148 J. B. Yang, D. Z. Xu, Z. H. Zhang, X. Zhang, Z. X. Ren and Z. L. Lu, *et al.*, Multifunctional System with Camptothecin and [12]aneN(3) Units for Effective In Vivo Anti Pancreatic Cancer through Synergistic Chemotherapy, Gene Therapy, and Photodynamic Therapy, *ACS Appl. Mater. Interfaces*, 2024, **16**(49), 67203–67215.
149 S. Lei, F. Ge, M. Lin, X. Wang, J. Shen and Y. Yang, *et al.*, PARP inhibitors diminish DNA damage repair for the enhancement of tumor photodynamic therapy, *Photodiagn. Photodyn. Ther.*, 2022, **40**, 103058.
150 Y. Q. Zhang, Q. H. Liu, L. Liu, P. Y. Guo, R. Z. Wang and Z. C. Ba, Verteporfin fluorescence in antineoplastic-treated pancreatic cancer cells found concentrated in mitochondria, *World J. Gastrointest. Oncol.*, 2024, **16**(3), 968–978.
151 Y. Liu, X. Wu, F. Chen, H. Li, T. Wang and N. Liu, *et al.*, Modulating cancer-stroma crosstalk by a nanoparticle-based photodynamic method to pave the way for subsequent therapies, *Biomaterials*, 2022, **289**, 121813.
152 L. Menilli, C. Milani, E. Reddi and F. Moret, Overview of Nanoparticle-Based Approaches for the Combination of Photodynamic Therapy (PDT) and Chemotherapy at the Preclinical Stage, *Cancers*, 2022, **14**(18), 4462.
153 G. Y. K. Liu, S. Li, J. Mei, X.-P. He and W. Chen, An esterase-activated diketopyrrolopyrrole-based theranostic prodrug for precise pyroptosis and synergistic chemo-photodynamic therapy of pancreatic cancer, *Mater. Chem. Front.*, 2024, 1993–2001.
154 B. W. Henderson, S. M. Waldow, W. R. Potter and T. J. Dougherty, Interaction of photodynamic therapy and hyperthermia: tumour response and cell survival studies after treatment of mice in vivo, *Cancer Res.*, 1985, **45**, 6071–6077.
155 B. Chen, B. W. Pogue, J. M. Luna, R. L. Hardman, P. J. Hoopes and T. Hasan, Tumor vascular permeabilization by vascular-targeting photosensitization: effects, mechanism, and therapeutic implications, *Clin. Cancer Res.*, 2006, **12**(3 Pt 1), 917–923.
156 Q. Hu, Z. Huang, Y. Duan, Z. Fu and L. Bin, Reprogramming Tumor Microenvironment with Photothermal Therapy, *Bioconjugate Chem.*, 2020, **31**(5), 1268–1278.
157 S. Anand, T. A. Chan, T. Hasan and E. V. Maytin, Current Prospects for Treatment of Solid Tumors via Photodynamic, Photothermal, or Ionizing Radiation Therapies Combined with Immune Checkpoint Inhibition (A Review), *Pharmaceuticals*, 2021, **14**(5), 447.
158 Y. Jin, J. Huang, Y. Tang, Z. Li, A. Zhang and Z. Yang, *et al.*, Boosting ferroptosis by intervention of redox balance and synergetic with photothermal/photodynamic therapy for suppression of pancreatic cancer, *Chem. Eng. J.*, 2024, **497**, 154569.
159 D. Li, X. Chen, D. Wang, H. Wu, H. Wen and L. Wang, *et al.*, Synchronously boosting type-I photodynamic and photothermal efficacies via molecular manipulation for pancreatic cancer theranostics in the NIR-II window, *Biomaterials*, 2022, **283**, 121476.
160 W. Tao, N. Wang, J. Ruan, X. Cheng, L. Fan and P. Zhang, *et al.*, Enhanced ROS-Boosted Phototherapy against Pancreatic Cancer via Nrf2-Mediated Stress-Defense Pathway Suppression and Ferroptosis Induction, *ACS Appl. Mater. Interfaces*, 2022, **14**(5), 6404–6416.
161 D. Li, X. Chen, W. Dai, Q. Jin, D. Wang and J. Ji, *et al.*, Photo-Triggered Cascade Therapy: A NIR-II AIE Luminogen Collaborating with Nitric Oxide Facilitates Efficient Collagen Depletion for Boosting Pancreatic Cancer Phototheranostics, *Adv. Mater.*, 2024, **36**(13), e2306476.
162 W. Chen and J. Zhang, Using nanoparticles to enable simultaneous radiation and photodynamic therapies for cancer treatment, *J. Nanosci. Nanotechnol.*, 2006, **6**(4), 1159–1166.
163 H. Z. Tianzi Zhang, F. Zhang, C. Chu, T. Liao, L. Xie, G. Liu and W. Cai, Rare-earth scintillating nanoparticles for X-ray induced photodynamic therapy, *J. Lumin.*, 2023, **261**, 119862.
164 J. S. Klein, C. Sun and G. Pratx, Radioluminescence in biomedicine: physics, applications, and models, *Phys. Med. Biol.*, 2019, **64**(4), 04TR1.

165 B. Yao, X. Liu, W. Zhang and H. Lu, X-ray excited luminescent nanoparticles for deep photodynamic therapy, *RSC Adv.*, 2023, **13**(43), 30133–30150.
166 K. Bedregal-Portugal, A. Mercier, S. Stelse-Masson, C. Aubrun, H. Elleaume and C. Verry, *et al.*, Nanoscintillators as Next-Generation Radiotherapeutics: Bridging Physics, Chemistry, and Oncology, *Bioconjugate Chem.*, 2025, **36**(9), 1919–1932.
167 A. B. Christophe Dujardin, A.-L. Bulin, F. Chaput and B. Mahler, Inorganic Nanoscintillators: Current Trends and Future Perspectives, *Adv. Opt. Mater.*, 2025, **13**(12), 2402739.
168 R. S. Dothager, R. J. Goiffon, E. Jackson, S. Harpstrite and D. Piwnica-Worms, Cerenkov radiation energy transfer (CRET) imaging: a novel method for optical imaging of PET isotopes in biological systems, *PLoS One*, 2010, **5**(10), e13300.
169 H. Liu, X. Zhang, B. Xing, P. Han, S. S. Gambhir and Z. Cheng, Radiation-luminescence-excited quantum dots for in vivo multiplexed optical imaging, *Small*, 2010, **6**(10), 1087–1091.
170 C. Ran, Z. Zhang, J. Hooker and A. Moore, In vivo photoactivation without ''light'': use of Cherenkov radiation to overcome the penetration limit of light, *Mol. Imaging Biol.*, 2012, **14**(2), 156–162.
171 P. Schneller, C. Collet, Q. Been, P. Rocchi, F. Lux and O. Tillement, *et al.*, Added Value of Scintillating Element in Cerenkov-Induced Photodynamic Therapy, *Pharmaceuticals*, 2023, **16**(2), 143.
172 N. Kotagiri, M. L. Cooper, M. Rettig, C. Egbulefu, J. Prior and G. Cui, *et al.*, Radionuclides transform chemotherapeutics into phototherapeutics for precise treatment of disseminated cancer, *Nat. Commun.*, 2018, **9**(1), 275.
173 N. Kotagiri, G. P. Sudlow, W. J. Akers and S. Achilefu, Breaking the depth dependency of phototherapy with Cerenkov radiation and low-radiance-responsive nanophotosensitizers, *Nat. Nanotechnol.*, 2015, **10**(4), 370–379.
174 A. Brad, H. H. Hartl, L. Marcu and S. R. Cherry, Activating Photodynamic Therapy in vitro with Cerenkov Radiation Generated from Yttrium-90, *J. Environ. Pathol. Toxicol. Oncol.*, 2016, **35**, 185–192.
175 Y. Nakamura, T. Nagaya, K. Sato, S. Okuyama, F. Ogata and K. Wong, *et al.*, Cerenkov Radiation-Induced Photoimmunotherapy with (18)F-FDG, *J. Nucl. Med.*, 2017, **58**(9), 1395–1400.
176 M. Falco, B. Masojc and T. Sulikowski, Radiotherapy in Pancreatic Cancer: To Whom, When, and How?, *Cancers*, 2023, **15**(13), 3382.
177 S. Clement, A. G. Anwer, L. Pires, J. Campbell, B. C. Wilson and E. M. Goldys, Radiodynamic Therapy Using TAT Peptide-Targeted Verteporfin-Encapsulated PLGA Nanoparticles, *Int. J. Mol. Sci.*, 2021, **22**(12), 6425.
178 A. E. A. Prada, Sonodynamic Therapy Using 5-Aminolevulinic Acid for Malignant Gliomas: A Review, *Life*, 2025, **15**, 718.
179 S. M. Peng Cheng, W. Cao, J. Wu, Q. Tian, J. Zhu and W. Wei, Recent advances in sonodynamic therapy strategies for pancreatic cancer, *Wiley Interdiscip. Rev.: Nanomed. Nanobiotechnol.*, 2024, **16**(1), e1945.
180 Z. L. Jide He, X. Zhu, H. Xia, H. Gao and J. Lu, Ultrasonic Microbubble Cavitation Enhanced Tissue Permeability and Drug Diffusion in Solid Tumor Therapy, *Pharmaceutics*, 2022, **14**(8), 1642.
181 X. J. Yifei Yin and L. Sun, Hongyan Li Continuous inertial cavitation evokes massive ROS for reinforcing sonodynamic therapy and immunogenic cell death against breast carcinoma, *Nanotoday*, 2021, **36**, 101009.
182 H. Yin, N. Chang, S. Xu and M. Wan, Sonoluminescence characterization of inertial cavitation inside a BSA phantom treated by pulsed HIFU, *Ultrason. Sonochem.*, 2016, **32**, 158–164.
183 J. Cheng, X. Sun, S. Guo, W. Cao, H. Chen, Y. Jin, B. Li, Q. Li, H. Wang, Z. Wang, Q. Zhou, P. Wang, Z. Zhang, W. Cao and Y. Tian, Effects of 5-aminolevulinic acid-mediated sonodynamic therapy on macrophages, *Int. J. Nanomed.*, 2013, **8**, 669–676.
184 D. X. Yonghong He, S. Tan and Y. Tang, and Ken-ichi Ueda. In vivo sonoluminescence imaging with the assistance of FCLA, *Phys. Med. Biol.*, 2002, **47**(9), 1535–1541.
185 S. K. Conor McEwan, J. Owen, H. Nesbitt, B. Callan, M. Borden, N. Nomikou, R. A. Hamoudi, M. A. Taylor, E. Stride, A. P. McHale and J. F. Callan, Combined sonodynamic and antimetabolite therapy for the improved treatment of pancreatic cancer using oxygen loaded microbubbles as a delivery vehicle, *Biomaterials*, 2016, **80**, 20–32.
186 Y. Xu, R. Liu, H. Yang, S. Qu, L. Qian and Z. Dai, Enhancing Photodynamic Therapy Efficacy Against Cancer Metastasis by Ultrasound-Mediated Oxygen Microbubble Destruction to Boost Tumor-Targeted Delivery of Oxygen and Renal-Clearable Photosensitizer Micelles, *ACS Appl. Mater. Interfaces*, 2022, **14**(22), 25197–25208.
187 R. J. Browning, S. Able, J. L. Ruan, L. Bau, P. D. Allen and V. Kersemans, *et al.*, Combining sonodynamic therapy with chemoradiation for the treatment of pancreatic cancer, *J. Controlled Release*, 2021, **337**, 371–377.
188 J. Cao, Y. Sun, C. Zhang, X. Wang, Y. Zeng and T. Zhang, *et al.*, Tablet-like TiO(2)/C nanocomposites for repeated type I sonodynamic therapy of pancreatic cancer, *Acta Biomater.*, 2021, **129**, 269–279.
189 S. S. Shabnum, R. Siranjeevi, C. K. Raj, A. Saravanan, A. S. Vickram and H. Chopra, *et al.*, Advancements in nanotechnology-driven photodynamic and photothermal therapies: mechanistic insights and synergistic approaches for cancer treatment, *RSC Adv.*, 2024, **14**(52), 38952–38995.
190 Y. Sun, X. Feng, C. Wan, J. F. Lovell, H. Jin and J. Ding, Role of nanoparticle-mediated immunogenic cell death in cancer immunotherapy, *Asian J. Pharm. Sci.*, 2021, **16**(2), 129–132.
191 X. Y. Yang, J. G. Zhang, Q. M. Zhou, J. N. Yu, Y. F. Lu and X. J. Wang, *et al.*, Extracellular matrix modulating enzyme functionalized biomimetic Au nanoplatform-mediated enhanced tumor penetration and synergistic antitumor therapy for pancreatic cancer, *J. Nanobiotechnol.*, 2022, **20**(1), 524.
192 Q. Li, S. Quin, H. Tian, R. Liu, L. Qiao, S. Liu, B. Li, M. Yang, J. Shi, E. C. Nice, J. Li, T. Lang and C. Huang, Nano-Econazole Enhanced PD-L1 Checkpoint Blockade for Synergistic Antitumor Immunotherapy against Pancreatic Ductal Adenocarcinoma, *Small*, 2023, **19**(23), e2207201.
193 S. Zhang, Z. Li, Q. Wang, Q. Liu, W. Yuan and W. Feng, *et al.*, An NIR-II Photothermally Triggered ''Oxygen Bomb'' for Hypoxic Tumor Programmed Cascade Therapy, *Adv. Mater.*, 2022, **34**(29), e2201978.
194 M. Algorri JFO, P. Roldan-Varona, L. Rodriguez-Cobo and J. M. Lopez-Higuera, Light Technology for Efficient and Effective Photodynamic Therapy: A Critical Review, *Cancers*, 2021, **13**(14), 3484.
195 G. Shafirstein, D. Bellnier, E. Oakley, S. Hamilton, M. Potasek, K. Beeson and E. Parilov, Interstitial Photodynamic Therapy-A Focused Review, *Cancers*, 2017, **9**(2), 12.
196 Y. Li, Y. Liu, K. Yamazaki, M. Bai and Y. Chen, Development of a Soft Robot Based Photodynamic Therapy for Pancreatic Cancer, *IEEE/ASME Trans. Mech.*, 2021, **26**(6), 2977–2985.
197 H. Yu, S. Chan Lee, G. Park, J. Kim, H. Kim, S. Ho Choi and B. Jung, Development of a Customized Endoscopic Dual-Diffusing Optical Fiber Probe for Pancreatic Cancer Therapy: Toward Clinical Use, *Photobiomodulation, Photomed., Laser Surg.*, 2022, **40**(4), 280–286.
198 P. Vincent, P. Bruza, S. M. Palisoul, J. R. Gunn, K. S. Samkoe and P. J. Hoopes, *et al.*, Visualization and quantification of pancreatic tumor stroma in fresh tissue via ultraviolet surface excitation, *J. Biomed. Opt.*, 2021, **26**(1), 016002.
199 M. Scholz, A. F. Petusseau, J. R. Gunn, M. Shane Chapman and B. W. Pogue, Imaging of hypoxia, oxygen consumption and recovery in vivo during ALA-photodynamic therapy using delayed fluorescence of Protoporphyrin IX, *Photodiagn. Photodyn. Ther.*, 2020, **30**, 101790.
200 J. M. DeWitt, K. Sandrasegaran, B. O'Neil, M. G. House, N. J. Zyromski and A. Sehdev, *et al.*, Phase 1 study of EUS-guided photodynamic therapy for locally advanced pancreatic cancer, *Gastrointest. Endosc.*, 2019, **89**(2), 390–398.
201 S. G. Bown, A. Z. Rogowska, D. E. Whitelaw, W. R. Lees, L. B. Lovat and P. Ripley, *et al.*, Photodynamic therapy for cancer of the pancreas, *Gut*, 2002, **50**(4), 549.
202 H. Yu, S. C. Lee, G. Park, J. Kim, H. Kim and S. H. Choi, *et al.*, Development of a Customized Endoscopic Dual-Diffusing Optical Fiber Probe for Pancreatic Cancer Therapy: Toward Clinical Use, *Photobiomodulation, Photomed., Laser Surg.*, 2022, **40**(4), 280–286.
203 T. M. Baran and T. H. Foster, Comparison of flat cleaved and cylindrical diffusing fibers as treatment sources for interstitial photodynamic therapy, *Med. Phys.*, 2014, **41**(2), 022701.

204 J. Zou, W. Li, N. Meng, J. Jiang, C. Wu and T. C. Lei, *et al.*, Evaluation of lensed fibers used in photodynamic therapy (PDT), *Photodiagn. Photodyn. Ther.*, 2020, **31**, 101924.
205 S. Chamberlain, D. Bellnier, S. Yendamuri, J. Lindenmann, T. Demmy and C. Nwogu, *et al.*, An Optical Surface Applicator for Intraoperative Photodynamic Therapy, *Lasers Surg. Med.*, 2020, **52**(6), 523–529.
206 M. M. Kim and A. Darafsheh, Light Sources and Dosimetry Techniques for Photodynamic Therapy, *Photochem. Photobiol.*, 2020, **96**(2), 280–294.
207 D. W. Lee and E. Y. Kim, Endoscopic Management of Pancreatobiliary Malignancies, *Dig. Dis. Sci.*, 2022, **67**(5), 1635–1648.
208 A. E. Tseimakh, A. F. Lazarev, E. L. Sekerzhinskaya, V. A. Kurtukov, A. N. Mitshenko and V. N. Teplukhin, *et al.*, Palliative treatment with the use of photodynamic therapy of patients with malignant tumors of pancreatobiliary zone complicated by obstructive jaundice, *Biomed. Photonics*, 2020, **9**(1), 4–12.
209 Y. Hanada, S. P. Pereira, B. Pogue, E. V. Maytin, T. Hasan and B. Linn, *et al.*, EUS-guided verteporfin photodynamic therapy for pancreatic cancer, *Gastrointest. Endosc.*, 2021, **94**(1), 179–186.
210 P. Vincent, M. E. Maeder, B. Hunt, B. Linn, T. Mangels-Dick and T. Hasan, *et al.*, CT radiomic features of photodynamic priming in clinical pancreatic adenocarcinoma treatment, *Phys. Med. Biol.*, 2021, **66**(17), 175006.
211 M. Tonneau, T. Lacornerie, X. Mirabel and D. Pasquier, [Stereotactic body radiotherapy for locally advanced pancreatic cancer: a systemic review], *Cancer Radiother.*, 2021, **25**(3), 283–295.